Detection and mapping of Earth body resonances with cGPS

Mensur Omerbashich
editor@geophysicsjournal.com

I recently showed that Mw5.6+ earthquakes occur due to (as the lithosphere rides on) vast waves of the Moon-driven and gravitationally aided 1–72h long-periodic Earth body resonance (EBR). Here I report a methodologically independent proof: observation of actual EBR waves in solid matter using continuous GPS (cGPS). Superharmonic resonance periods from the EBR's 55'–15 days (0.303 mHz–0.771605 μHz) band are thus recoverable in spectra of ITRF2014 positional components solved kinematically from 30-s cGPS samplings. The signal is so pure, strong, and stable that even daylong components are always and only periodic with Earth resonance periods constantly 99%-significant and of very high fidelity ($\phi>>12$); very low fidelity ($\phi<<12$) characterizes overtones and undertones. The examined cGPS stations have diurnal EBR fingerprints: unique sets of ~13-18 EBR periods, most clearly formed during ~M6+ quiescence, enabling depiction of EBR orientation for real-time EBR mapping. Furthermore, weeklong component time series reveal complete EBR and unavoidable undertone series (with very high fidelity, too) as the signature of an EBR's companion sympathetic resonance. Also, I demonstrate the concept of EBR mapping using the Mexico City–Los Angeles–San Francisco cGPS profile alongside a tectonic plate boundary, successfully depicting the preparation phase of the 2020 Puerto Rico Mw6.4–Mw6.6 sequence. I finish by showing that the EBR has triggered the 2019 Ridgecrest Mw6.4–Mw7.1, sequence too. EBR maps can now be produced — for seismic prediction and to unobscure (decouple EBR from) geophysical observables such as stress/strain. Applications of EBR include geophysical prospecting and detection at all scales and at any time.

Key words: resonance detection, resonance mapping, seismic forecast and prediction, seismogenesis, exploration.

Key points: Moon-driven mechanical resonance causes seismotectonics.

Introduction

Earlier, I had demonstrated a physical phenomenon of Earth body resonance (EBR) as the seismogenic mechanism by successfully recovering all 72 Moon-driven superharmonic resonance periods in the 55'–15 days band of interest (0.303 mHz–0.771605 μHz) from spectra of time-series of 2015-2019 global M_w5.6+ strong earthquakes. Thus seismicity time-series capture events as they occur due to the lithosphere riding on waves of incessant Earth resonances as recovered in the longest part of the Earth-Moon tidal system's energy band. Subsequently, I made a spatiotemporally independent proof of (universality of) EBR from moonquakes.

Previously, I had presented empirical proof (a pattern in occurrences of M6.2+), as well as theoretical proof (a mathematical generalization of EBR to scales of unspecified energies and times) further proportionating the Newtonian gravitational proportion and therefore gravity too via speed-of-light at macroscopic and quantum scales — as Einstein hinted for our Solar system in his rare geophysics work. (Omerbashich, 2020a, 2020b)

Here I report a methodologically and temporally independent proof of EBR. Recovered was the complete superharmonic resonance in the original band (*ibid*.) from spectra of ITRF2014 positional components, solved kinematically from daylong and weeklong 1Hz recordings by the continuous GPS (cGPS). The US National Geodetic Service (NGS) commonly decimates the data to a 30-s rate. Continuously Operating Reference Stations (CORS) with Global Navigation Satellite Systems (GNSS) installations always include at least the Global Positioning System (GPS). GPS is the longest operating GNSS, so I use the cGPS to investigate the possibility of EBR detection and mapping. I picked California as a testbed due to its high seismicity levels as well as longest and arguably best cGPS coverage anywhere on Earth (Bock and Melgar, 2016).

Data

Due to a relatively dense spatiotemporal distribution of M6+ strong seismicity on our Planet, I use daylong and weeklong cGPS recordings, likely optimal for the bend of interest. Thus, examined data sets consisted of measurements taken continuously during the first week of January, at various epochs: 2020, 2015, 2010, and 2005. When testing daylong data, I choose 01 January. January is the month with likely the least geophysical background noise during a climatically averaged year. This choice should minimize any regional and global seasonal effect as key for spectral analyses. Also, the data are newer and presumably of higher quality with time due to processing and model improvements. The data used here are also temporally independent from the data used by Omerbashich (2020a) and temporally surround them — thereby enabling genuine assessments of EBR-caused variations in the Earth's energy budget.

Month-long time series at 1Hz sampling (decimated or not) and 30 s solution rates should provide enough fidelity to distinguish between EBR and any other long-periodic components in the band of interest. As a borderline between moderate- and high-rate, the 1Hz sampling rate appeared as the optimal choice given its relative richness in systematic information and undemanding computing requirements. Finally, seismic quiescence in terms of ~M_w6+ regional and ~M_w6.5+ global earthquakes characterized the January 2020 samples, while the said preceding three epochs were seismically active in the same sense. This setup should shed light on the effects of seismicity on EBR recovery.

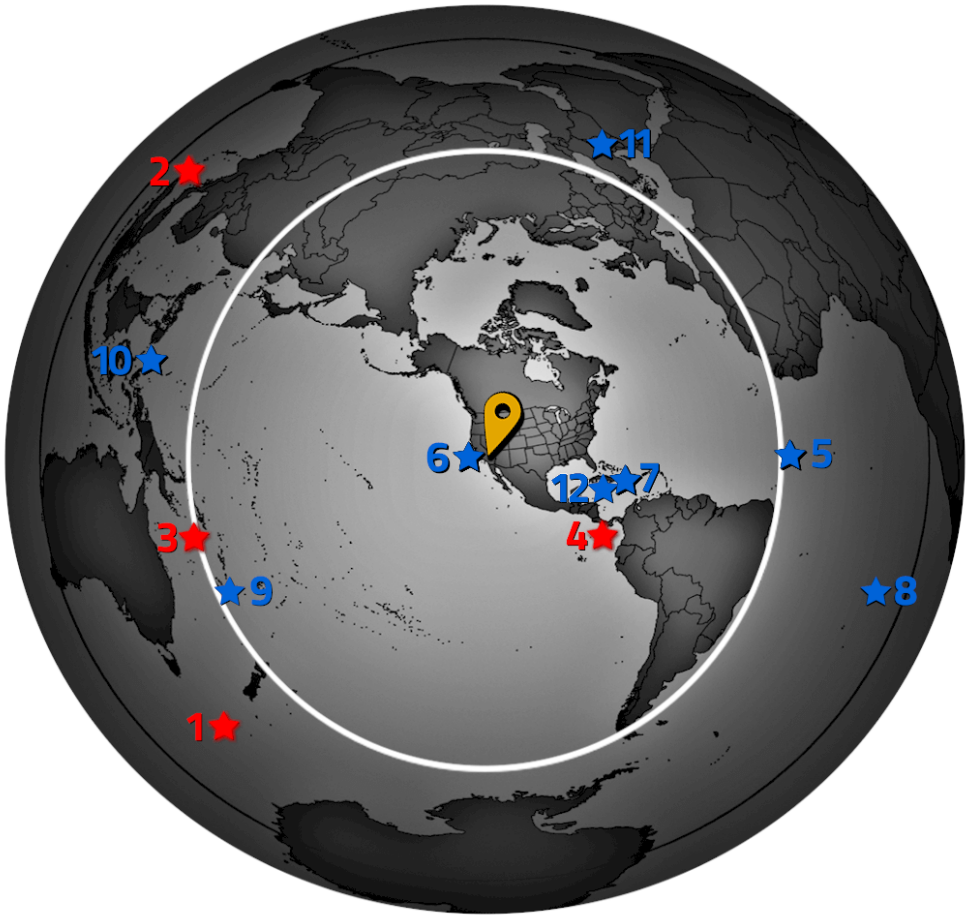

Figure 1. Geographic locations of the earthquakes that co-occurred with the sampled record –2 weeks. Earthquakes that destroyed or damaged EBR waves at Los Angeles shown in red, earthquakes that did not in blue. Distances calculations given in Table 1. Azimuthal equidistant mapping projection, centered on Los Angeles. Light circle: 10000 km. Dark circle: 15000 km.

Locale	M_w	Time rounded to nearest day	Median sample time rounded to nearest day	Timing to sample middle [days]	Timing to sample start [days]	Latitude	Longitude	Distance [km]	Notes
ZLA1						**+34° 36' 12.6648"**	**-118° 05' 02.0214"**		**Los Angeles County**
EQE01	8.1	2004-12-24	2005-01-04	-11	-8	-49° 18' 43.1994"	-161° 20' 41.9994"	12217	Macquarie Isle off New Zealand
EQE02	9.1	2004-12-26	2005-01-04	-9	-6	+03° 17' 41.9994"	+095° 58' 55.1994"	14512	Sumatra, Indonesia
EQE03	7.1	2010-01-03	2010-01-04	-1	2	-08° 46' 58.7994"	+157° 21' 14.4000"	10069	Solomon Isles
EQE04	6.5	2015-01-07	2015-01-04	3	6	+05° 54' 18.0000"	-082° 39' 28.8000"	4830	Off coast Panama
EQE05	6.8	2005-01-12	2005-01-04	8	11	+00° 52' 40.7994"	-021° 11' 38.3994"	10700	Mid-Atlantic Ridge
EQE06	6.5	2010-01-10	2010-01-04	6	9	+40° 39' 07.2000"	-124° 41' 34.7994"	889	Off coast North California
EQE07	7.0	2010-01-13	2010-01-04	9	12	+18° 26' 34.8000"	-072° 34' 15.5994"	7817	Haiti
EQE08	6.8	2010-01-05	2010-01-04	1	4	-58° 10' 22.8000"	-014° 41' 42.0000"	13958	Sandwich Isles
EQE09	6.8	2015-01-23	2015-01-04	19	22	-17° 01' 51.5994"	-168° 31' 12.0000"	9627	Vanuatu
EQE10	6.8	2019-12-15	2020-01-04	-20	-17	+06° 41' 49.2000"	125° 10' 26.4000"	11973	Philippines
EQE11	6.7	2020-01-25	2020-01-04	21	24	+38° 25' 51.5994"	039° 03' 39.5994"	11583	Turkey
EQE12	7.7	2020-01-29	2020-01-04	25	28	+19° 25' 08.4000"	-078° 45' 21.6000"	4216	Off coast Jamaica

Table 1. Ellipsoidal distances, computed by the method of Vincenty (1975), between the cGPS station ZLA1 (Los Angeles) and locations of earthquakes that co-occurred with the sampled record up to –2 weeks, Figure 1. Rows with earthquakes that destroyed or damaged EBR waves at Los Angeles are highlighted. As seen above and from Figure 1, the EBE recovery depended critically on event timing relative to the sampled cGPS data (either co-occurring or a few days within the sample) and the event's size so that M_w8+ mega quakes possibly affected the EBR recovery too. Events from the year weeks 2, 3, and 4 were included in this consideration due to possible effects of resonance's preparation phase, starting around –3 days relative to an ~M_w6+ event, as here EBR is tacitly assumed to cause all ~M_w6+ seismicity (Omerbashich, 2020a). The Puerto Rico global event of 07 January 2020, used in the following sections, is not included since the Harvard Catalog lists it by the lower (<M_w6.5) magnitude. Note, however, that inclusion of this event in the above considerations would not affect the conclusions.

To examine the effects of seismic waves on EBR waves, I use observations from the cGPS station ZLA1 (Los Angeles) and the 7.5º elevation cutoff angle/mask. To examine how multipath as the largest source of cGPS errors affects the detection of EBR from GPS, I use observations from the ZOA2 (Oakland) cGPS station. The US Federal Aviation Administration (FAA) operates these 1-Hz stations since 12/04/2003 and 03/07/2002, respectively. The stations sit at 763.1 m and -4 m above the ellipsoid — and are on different tectonic plates: the North American and the Pacific plate, respectively. ZLA1 is located at the Los Angeles Air Route Traffic Control Center near the Palmdale Regional Airport, north of Los Angeles. ZOA2 is at the Oakland Air Route Traffic Control Center, east of San Francisco. The FAA includes the two stations in neither the Primary nor Secondary Airport Control (ngs.noaa.gov/cgi-bin/airports.prl?TYPE=PACSAC).

Later on, I use the first of the two stations to examine the effects of data span on EBR recovery. To gain insight into the possible mapping of EBR, I draw the first EBR profile and do so approximately alongside a tectonic plate boundary to study the cGPS sensitivity (for EBR mapping) under extreme resonance conditions: the Mexico City—Los Angeles—San Francisco. If found plausible, the drawing of EBR profiles should enable EBR mapping on global scales. The FAA operates the MMX1 station located at the Mexico Air Traffic Control within the Mexico City International Airport. MMX1 sits on the North American tectonic plate.

This study's claims (without elaboration) on any effects of low-rate sampling and multipath are in large part based on data from the KSU1, a 15-s-sampling cGPS station maintained by UNAVCO and located at the Kansas State University. The KSU1 sits deep inland within a plateau remotest from North American seismically active zones and large water bodies (the Atlantic and Pacific oceans and the Gulf of Mexico) as EBR's natural attenuators that forbid EBR waves with destructive angular deflection to roll deep inland.

Statistical fidelity values from spectral analyses in this study ranged between 160000–9000 for the longest to 12–11 for the shortest resonance periods. Since fidelities of ϕ>12 are considered reflective of a physical process (Omerbashich, 2006), the trains of resonance periods presented herein describe a real and the Earth-driving physical process.

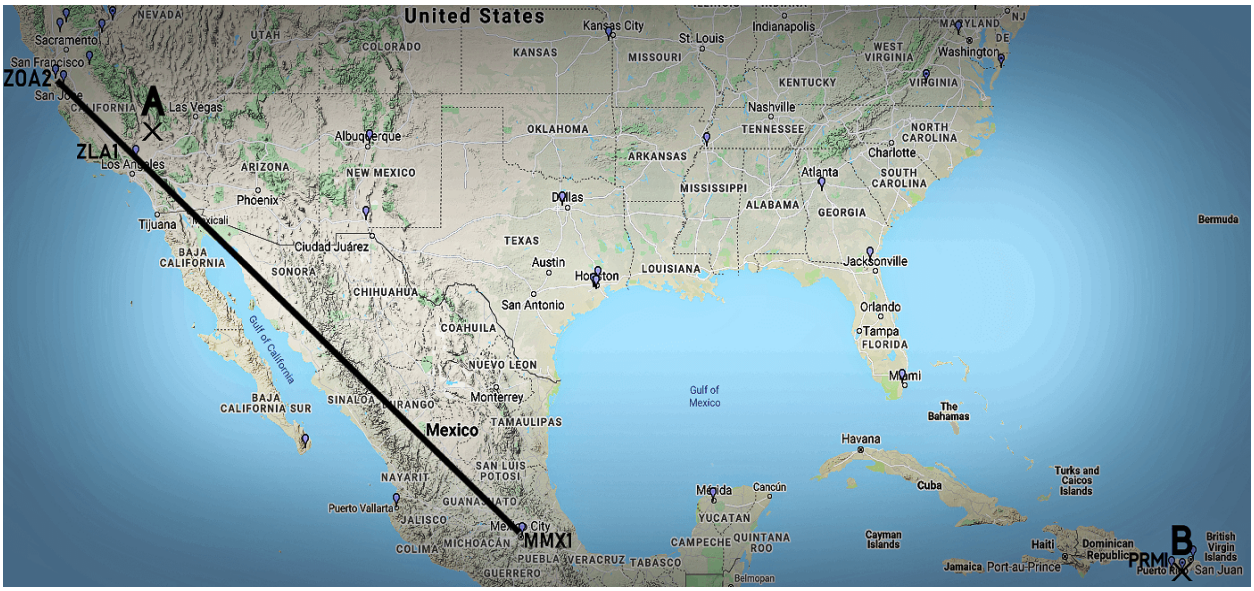

Figure 2. Locations of the 1Hz cGPS stations tracing an EBR mapping profile, roughly alongside a tectonic plate boundary. A–Ridgecrest event epicenter, B–Puerto Rico event epicenter; see Table 1. A mockup projection, not to scale.

Methodology

I used GIPSY 6.4 APPS scientific software and solutions by the Jet Propulsion Laboratory to obtain time-series of (antenna) coordinates in kinematic post-processing of dual-frequency measurements with precise pseudo-random code at the 30-s interval. The declared typical user range error was ε_{RMS} <3 cm, which should suffice for detecting resonance waves that are primarily horizontal movements on the order of decimetres-to-metres. In the real world, any Earth resonance waves most of the time can be expected to diverge from the ideal case of transverse orientation (as due to obliquity of the Earth and the Moon) and turn towards (though rarely align with) a cardinal coordinate plane. Therefore, instead of spectrally analyzing either the 2D or the 3D positional vectors, I consider positional component-series (**X**, **Y**, **Z**) independently and analyze them separately to study the most realistic mapping parameters for the depiction of EBR uniquely. Post-processed time series turned out to be up to 1% gapped.

Therefore, to examine the periodicity in cGPS data, I use the Gauss–Vaníček method of spectral analysis (GVSA) by Vaníček (1969, 1971), as a technique unaffected by gaps in data. The GVSA belongs to the least-squares class of spectral analysis techniques, has many advantages over the Fourier class of spectral analysis techniques (Press et al., 2007), has proven itself in analyzing long and gapped records (Omerbashich, 2006, 2007a), and provides total accuracy in extracting periods from sets of natural data — down to the prescribed accuracy of analyzed data themselves (Omerbashich, 2007b; 2020a; 2020b).

To examine the effects of regional and global seismicity as the Earth's largest rapid mass redistribution besides tides and EBR, and therefore the greatest terrestrial challenge for EBR recovery due to ability to damage or destroy EBR waves, I compare the aptness of the ZLA1 for recovering the EBR, at different epochs: 2005, 2010, 2015, and 2020. At the same time, all these epochs are temporally independent of considerations by Omerbashich (2020a).

Note that periods often claimed as responsible for the tidal triggering of earthquakes, such as the diurnal 12-h cycle, will not be enforced (removed) here, as that would mean taking out of the context of examining physical processes related to Earth resonances. So if the 12-h cycle turns out to be one of the earthquake-triggering periods, that can only be due to the EBR to which that period belongs – not individually (as tidal forces are insufficient for that) but as a part of the compound EBR train.

In this study, I apply neither preprocessing of data to boost the highest spectral peaks (by feeding data some extra variance) nor post-processing to enhance computed spectra. In this way, what follows represents the strictest possible verification of the EBR from both the statistics and physics points of view. Demonstrating the EBR measurable using a GNSS (here by detecting actual EBR waves as they physically disturb the masses under cGPS stations) would pave the way for new directions in basic research, including physics-based earthquake prediction, but also the development of new EBR-based techniques in geophysical applications such as reservoir detection and prospecting. In what follows then, I use the terms EBR period and EBR waves interchangeably. I depict whole EBR wave trains whenever possible.

Detection

Global resonance waves exhibit a more pronounced natural delay in the z component due to it having no degrees of freedom. Therefore one cannot expect performance improvement (either sporadically or in overall matching to theoretical EBR periods) from spectrally analyzing 2D and 3D vector series instead of individual position components' time-series. Besides, component spectra provide deeper insights into the orientation of a resonance train and groups of waves in general. Therefore, I look into position component time-series, including dynamical coordinate-component pairs xy, xz, or yz forming regular formations and thus capturing the directional orientation and position of resonance waves at a particular time and place accurately.

Of all sources of GPS errors, EBR detection is likely to suffer the most from the receiver-antenna multipath, so it may be necessary to vary the elevation cutoff angle (the mask) to find the optimal elevation mask. As studies have shown for precision GPS considerations, receiver-antenna multipath effects are very site-specific (Genrich and Bock, 2006). Therefore, the procedure for analyses here is necessarily empirical and iterative: repeat a spectral analysis of station data with different elevation masks, and the elevation mask (if any) that results in the clearest formation of resonance at that station is the optimal mask.

E B R		cGPS / CORS station ZLA1 (Los Angeles County)																					
		2005 - Jan - 1						2010 - Jan - 1						2015 - Jan - 1						2020 - Jan - 1					
P_{theor}	P_{EQE}	P_X	Δ_X	P_Y	Δ_Y	P_Z	Δ_Z	P_X	Δ_X	P_Y	Δ_Y	P_Z	Δ_Z	P_X	Δ_X	P_Y	Δ_Y	P_Z	Δ_Z	P_X	Δ_X	P_Y	Δ_Y	P_Z	Δ_Z
72.0000	75.0591																								
36.0000	33.3241			44.6753	24.1%																				
24.0000	23.2132					25.8251	7.6%	21.0811	-12.2%									21.5766	-10.1%					22.6407	-5.7%
18.0000	17.9995											18.5284	2.9%	20.1555	12.0%										
14.4000	14.4466									14.0059	-2.7%														
12.0000	12.6545																			12.6545	5.5%	12.1520	1.3%		
10.2857	10.0282	10.6076	3.1%	10.0282	-2.5%	10.0282	-2.5%	10.8585	5.6%					9.7101	-5.6%	9.9199	-3.6%							9.6084	-6.6%
9.0000	8.8661																	9.3159	3.5%						
8.0000	7.8772																								
7.2000	7.1419							7.5532	4.9%													7.0324	-2.3%		
6.5455	6.5321													6.2647	-4.3%	6.5789	0.5%			6.7730	3.5%				
6.0000	6.0183					5.9791	-0.3%											6.1803	3.0%					5.9404	-1.0%
5.5385	5.6132	5.7542	3.9%							5.4148	-2.2%	5.4795	-1.1%												
5.1429	5.1709													4.9747	-3.3%					5.0018	-2.7%	5.0849	-1.1%		
4.8000	4.7434							4.7929	-0.1%									4.6949	-2.2%						
4.5000	4.6008															4.3812	-2.6%							4.5326	0.7%
4.2353	4.2008																								
4.0000	3.9650			3.9650	-0.9%									3.9479	-1.3%					3.9310	-1.7%	3.9822	-0.4%		
3.7895	3.7696	3.8486	1.6%																						
3.6000	3.5236					3.5647	-1.0%	3.5926	-0.2%															3.6209	0.6%
3.4286	3.4443									3.3809	-1.4%	3.4443	0.5%			3.4443	0.5%	3.3934	-1.0%						
3.2727	3.2842	3.3198	1.4%											3.2378	-1.1%					3.2960	0.7%	3.2493	-0.7%		
3.1304	3.1275																								
3.0000	2.9949			2.9468	-1.8%	2.9468	-1.8%																	2.9949	-0.2%
2.8800	2.8821	2.8552	-0.9%													2.8821	0.1%								
2.7692	2.7691									2.7279	-1.5%	2.7442	-0.9%							2.7607	-0.3%	2.7442	-0.9%		
2.6667	2.6569																	2.6569	-0.4%						
2.5714	2.5821			2.5749	0.1%	2.5894	0.7%	2.6115	1.6%															2.5677	-0.1%
2.4828	2.4911	2.4979	0.6%																						
2.4000	2.4317											2.3812	-0.8%	2.4382	1.6%	2.3874	-0.5%			2.3812	-0.8%	2.3812	-0.8%		
2.3226	2.3269	2.3094	-0.6%	2.2978	-1.1%	2.3094	-0.6%			2.2864	-1.6%														
2.2500	2.2580																							2.2417	-0.4%
2.1818	2.1524													2.1574	-1.1%										
2.1176	2.1274							2.1176	0.0%							2.1176	0.0%	2.1373	0.9%			2.0887	-1.4%		
2.0571	2.0514	2.0652	0.4%	2.0560	-0.1%	2.0468	-0.5%													2.0840	1.3%				
2.0000	1.9763																							1.9891	-0.5%
1.9459	1.9636											1.9387	-0.4%												
1.8947	1.8831							1.9026	0.4%	1.8908	-0.2%			1.9105	0.8%	1.8792	-0.8%					1.8715	-1.2%		
1.8462	1.8305																	1.8564	0.6%	1.8639	1.0%				
1.8000	1.8160			1.8053	0.3%																			1.7877	-0.7%
1.7561	1.7536	1.7773	1.2%			1.7705	0.8%																		
1.7143	1.7016							1.7272	0.8%	1.7047	-0.6%	1.7207	0.4%	1.7239	0.6%					1.6953	-1.1%	1.6984	-0.9%		
1.6744	1.6646																								
1.6364	1.6351																							1.6262	-0.6%
1.6000	1.5869			1.6120	0.8%																				
1.5652	1.5573							1.5733	0.5%	1.5706	0.3%									1.5494	-1.0%				
1.5319	1.5416	1.5339	0.1%	1.5211	-0.7%	1.5287	-0.2%									1.5287	-0.2%	1.5390	0.5%			1.5468	1.0%		
1.5000	1.5062													1.5136	0.9%									1.4891	-0.7%
1.4694	1.4676																								
1.4400	1.4468									1.4537	1.0%	1.4355	-0.3%							1.4288	-0.8%	1.4266	-0.9%		
1.4118	1.4091													1.4244	0.9%										
1.3846	1.3941	1.3733	-0.8%					1.3774	-0.5%							1.3815	-0.2%							1.3774	-0.5%
1.3585	1.3590									1.3530	-0.4%							1.3712	0.9%						
1.3333	1.3412					1.3392	0.4%																		
1.3091	1.2939	1.3012	-0.6%																	1.3199	0.8%	1.3180	0.7%		
1.2857	1.2741			1.2957	0.8%									1.2759	-0.8%	1.2831	-0.2%							1.2795	-0.5%
1.2632	1.2636																	1.2706	0.6%						
1.2414	1.2381																								
1.2203	1.2103			1.2119	-0.7%															1.2265	0.5%	1.2265	0.5%		
1.2000	1.2008	1.1915	-0.7%			1.2008	0.1%	1.1977	-0.2%	1.2040	0.3%	1.2056	0.5%			1.1961	-0.3%							1.1915	-0.7%
1.1803	1.1762																								
1.1613	1.1628																								
1.1429	1.1425													1.1511	0.7%					1.1468	0.3%	1.1483	0.5%		
1.1250	1.1299											1.1313	0.6%					1.1257	0.1%					1.1175	-0.7%
1.1077	1.1107																								
1.0909	1.0909	1.0988	0.7%	1.0871	-0.3%	1.0884	-0.2%																		
1.0746	1.0693							1.0819	0.7%	1.0819	0.7%	1.0794	0.4%							1.0769	0.2%	1.0769	0.2%		
1.0588	1.0546													1.0644	0.5%	1.0534	-0.5%	1.0522	-0.6%						
1.0435	1.0438																							1.0510	0.7%
1.0286	1.0321					1.0356	0.7%	1.0217	-0.7%	1.0240	-0.4%	1.0240	-0.4%												
1.0141	1.0195																			1.0172	0.3%	1.0183	0.4%		
1.0000	0.9984	0.9877	-1.2%			0.9730	-2.7%	0.9845	-1.6%	0.9421	-5.8%	0.9459	-5.4%	0.9845	-1.6%	0.9973	-0.3%	1.0017	0.2%	0.9608	-3.9%	0.9618	-3.8%	0.9930	-0.7%
	∑	15	9	13	9	15	11	15	10	14	8	13	10	16	7	14	12	14	10	18	11	18	12	18	16
Formations xy, yz, xz		5		7		8		7		9		5		6		5		2		14		1		1	
Formations in %		33%		54%		53%		47%		64%		38%		38%		36%		14%		78%		6%		6%	

LEGEND:					
≥ 99%	matched EBR_{GNSS} with $EBR_{theor.}$	Formation:		Matches:	
99%	confidence & ϕ >>12		absent		recovered EBR periods
95%	confidence & ϕ >>12		xy		
89%	confidence & ϕ >>12		yz		
67%	confidence & ϕ >>12		xz		

Table 2. Detection of Earth body resonance (EBR) from daylong cGPS data at ZLA1, Los Angeles. The matching was against theoretical EBR (leftmost column, highlighted blue). P_{theor} marks the theoretical EBR periods, while P_{EQE} marks the seismic EBR periods, as obtained from global strong seismicity (Omerbashich, 2020a).

As expected from the nature of the GPS-sampled physical process of mechanical resonance and its magnification, which are most energetic in the longest-periodic bend(s), this distinction should get somewhat but not drastically blurred towards the low-frequency end — here for periods that are longer than ~5 h. This situation means that the entirety of an unperturbed EBR train, i.e., the physical phenomenon of EBR as such, ought to be recoverable in its original transverse formation well (i.e., without any systematic sub-band stratification) and that it be generally recoverable with cGPS fully, i.e., regardless if recovered EBR periods form component pairs or not. We cannot expect this to hold during epochs of seismic activity, so in the following, I compute component spectra also in the corresponding (always the 01 January) epochs: 2020, 2015, 2010, and 2005, in an attempt to recover significant periods of both perturbed and unperturbed states of the Earth's resonances, but primarily the EBR as the strongest.

The EBR detection from daylong cGPS data — as recorded at ZLA1 (Los Angeles) and decimated at 30 s by the NGS — is shown in Table 2 and Figures 3 & 4. Owing primarily to a mutually excluding orientation and plane disparity of seismic v. EBR waves, earthquakes did not affect the EBR recovery, except for those that had co-occurred between the 6th–12th day of a monthlong sample (here: January of 2005; 2010; 2015) — not even if mega quakes (of M_w8+) occurring far away, Table 1. Namely, only then could seismic waves be seen as destroying EBR waves. The wave destruction can be either complete — causing the affected period to vanish, or partial — resulting in a lower confidence level of that period.

The EBR formation is well-preserved at quiescence (the first three weeks of January 2020). Over the four examined epochs, recovered were 62 (or 86%) of the total of 72 EBR periods. Of those, we can safely assume that only the 13 component pairs *P*xy with supplementary lagging *P*z isolates are the best EBR representation for the epoch at this station and the Los Angeles area. A relative imprecision in the longest periods is due to their immense power and relatively short data-span. The used elevation mask was 7.5º, and the EBR band was 55'-15 days (Omerbashich, 2020). The locations of the earthquakes that had destroyed EBR waves are in Figure 3. As seen from Table 2 and Figure 1, the EBR is such an immense and overwhelming phenomenon that the Earth's crust gives in to it entirely: as an EBR wave gets destroyed, another companion-resonance wave replaces it to try to restore the total $\sum$ (energy equilibrium). Note the Δ-values, also shown in Figure 4, as the differences between computed and corresponding theoretical EBR periods for the 2020 epoch: of the 54 matched EBR periods in total, 39 (Δ-values highlighted in orange) or 72% came to within 1% of the corresponding theoretical EBR periods. At the same time, even the two shortest theoretical EBR periods differed by more than 1%. Besides, no Δ-value has exceeded the differences between the corresponding and to it adjacent two theoretical EBR periods. Therefore, the recovered train of periods is a genuine representative of the theoretical EBR, while a regular formation reflects real (original) — largely transverse — planar modulation unperturbed by strong seismicity; see Table 1 & Figure 1.

Stacked on Figure 3 are EBR spectral peaks from the ZLA1 (Los Angeles) station's daylong data of 01 January 2005, 2010, and 2015, preceded by a seismically active week in terms of M_w6+ (see Figure 1 and Table 1), v. the same from 2020 preceded by a seismically quiescent week in the same sense. The plot reveals how seismic waves damage Earth resonance waves — either partially (lowering the confidence levels to a level between 67%–99%) or completely (vanishing, i.e., dropping below the 67% significance), Table 2.

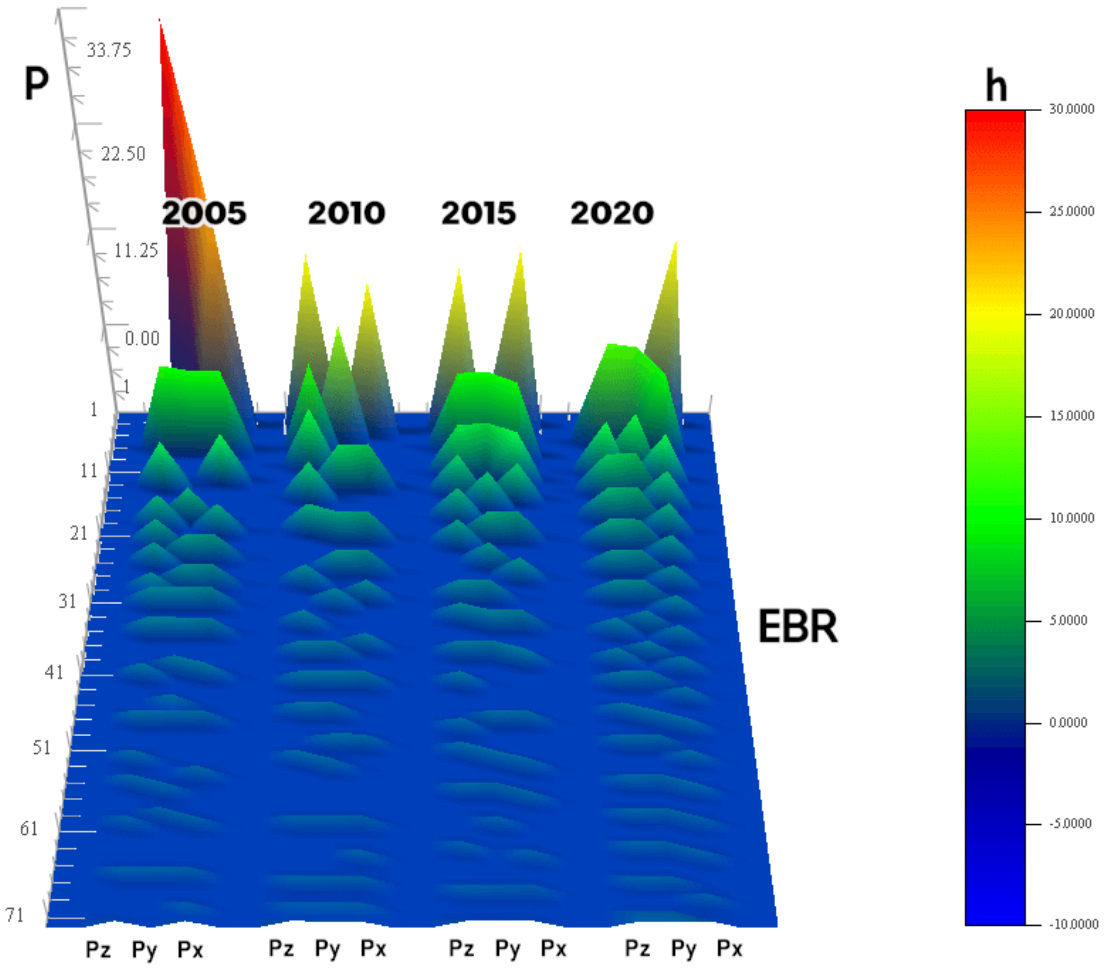

Figure 3. The effects of seismicity on the ability of daylong cGPS data at ZLA1 (Los Angeles) to reveal the EBR.

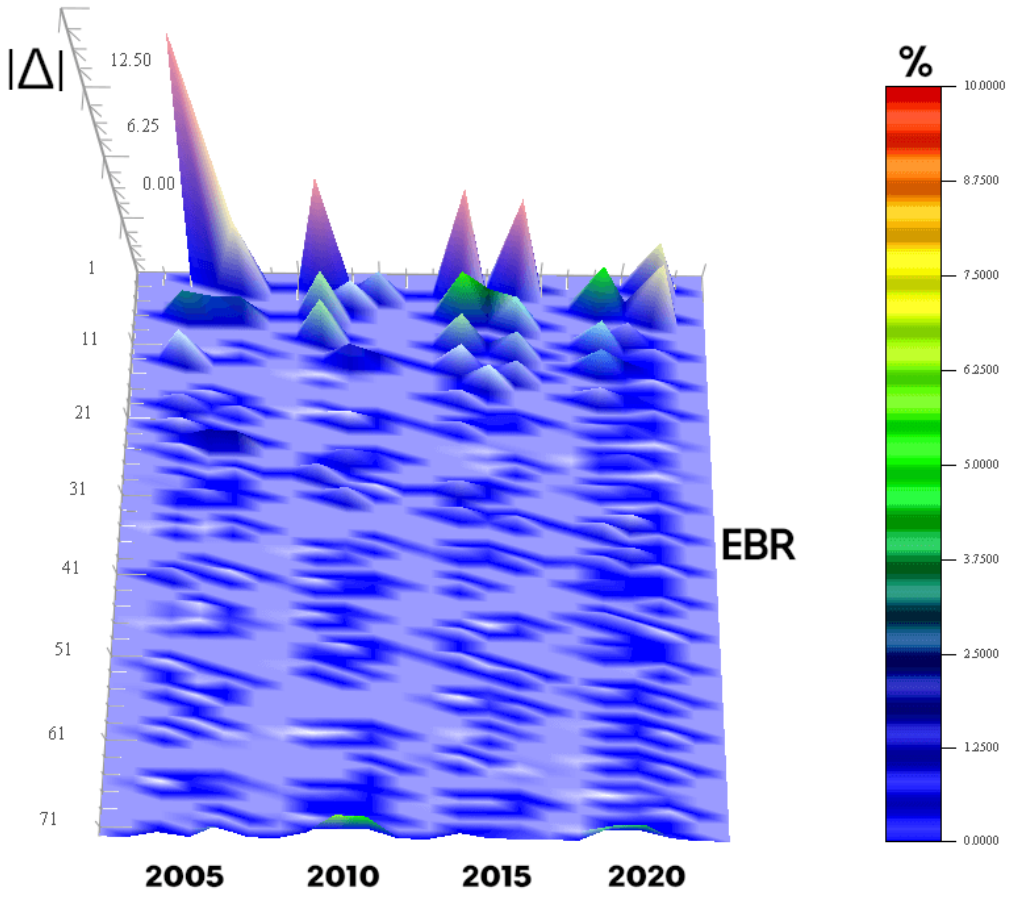

Figure 4. Δ-surface of EBR change with seismicity, where a Δ-value is the difference between a computed and its corresponding theoretical EBR period, in % to the former, Figure 3, and throughout. The plot indicates the uniform reliability of EBR spectral computations at ZLA1 (Los Angeles). Spectra computed for 01 January 2005, 2010, 2015, and 2020. The here plotted Δ-values correspond to the Figure-3 values of spectral peaks *P*x, *P*y, and *P*z, Table 2.

Although EBR is on the order of dm-to-m, it is unlikely for an observer to feel EBR waves at a cGPS site since the effects of a specific EBR wave can propagate dynamically across km-lengths and longer — across the entire region where the station is situated, while many EBR waves can envelope whole tectonic plates and continents.

As preliminary investigations have shown, using other GNSS for EBR recovery did not appear to be particularly beneficial over using just GPS. Finding the optimal mask to alleviate station errors for processing their daylong records seemed more laborious and less successful when using more GNSS. Most likely, this is due to additional and previously unaccounted sources of errors, such as satellite-antenna multipath. Unfortunately, even the differencing is unable to correct for this type of multipath, and the result is a position uncertainty on the order of a few cm (Young et al., 1985). While numerous approaches to modeling receiver-antenna multipath exist, GPS architectures ignore the problem of satellite-antenna multipath (Bock and Melgar, 2016). Besides, various sources of error could introduce pseudo-periodicities and impede the detection of real periodicities in position time-series (He et al., 2017).

This situation could mean that EBR detection from GPS (and especially GNSS) daily records is subject to the cumulative effect of different types of satellite-antenna multipath due to different space-vehicle architectures, orbits, satellite-antenna types, and so on. Such a cumulative error from combined effects – itself composed of errors of various types including systematic, random, and nonlinear (due to varying delays of signal groups) – while somewhat negligible for positioning purposes thanks to modern modeling solutions, here still could introduce pseudo-periodicities and hinder the extraction of real periodicities in month-long GPS position time-series too. However, should such effects become significant for a cGPS station, they would probably be noticeable also. Namely, the number of recovered EBR periods would drop significantly below 13 since the Earth would not be restoring pseudo-periods as it restores real EBR periods when physically destroyed by seismic waves, Table 2, or any other subtypes of kinetic waves. The significance level of a recovered EBR wave (period) thus measures the level of destruction of that period as damaged by seismic waves or other kinetic disturbances.

Mapping

That the revealed depiction genuinely represents resonance waves has become clear from the find that the X and Y components on 01 January 2020 always described the same period simultaneously, Table 2. Besides, the Z component has described another EBR period that, in most cases, lagged one to two EBR periods behind the respective horizontal *P*xy period pair. The constant lag accurately depicts the remaining degree of freedom necessary to visualize and map a resonance train – the spatial orientation of an EBR wave and overall (of the train as a whole). In other words, the single-station kinematic cGPS is a method by which it is possible to measure point-dynamics of solid Earth under a resonance wave at a given time.

It is safe to assume that the geometrically (numerically) most regular EBR formation for an epoch is also the best daily-EBR representation for that station at that time. Then of all examined ZLA1 epochs, the 13 component pairs *P*xy (and their supplementary lagging *P*z isolates) recovered from 2020 data constitute the best available such representation.

Some of the main reasons why EBR waves are difficult to model and why EBR mapping is crucial for understanding this phenomenon are:

- they are incessant and long-periodic, which makes their decoupling difficult, so it is easy to mistake them for something else – across various bands at that;
- maximum angular deflection is elusive in incessant multiple resonances of closed physical systems, making the destructive ability of EBR difficult to express uniquely;
- they spread across time intervals of an hour to many days, vast distances from townships to continents, while their amplitudes are on the (varying) order of dm to m, making it very difficult to assess timings and amplitudes, which becomes even more involved when considering different scales;
- they travel separately, making it difficult to trace or even settle just on their spatiotemporal origin(s);
- most of their motion is horizontal, so they can easily pass for (also vertical) seismic noise;
- they run counter-intuitively due to rotation and obliquity of the Earth and the Moon (conditions under which initiated), thus typically traversing coordinate systems instead of running along axes. This dispersion makes it hard to grasp the actual attack angle uniquely at a given moment;
- the input periods range themselves, and modeling of resonance down-transfer from the lithosphere to the mantle (flows) is not as simple as estimating parameters such as Reynolds and Strouhal numbers anymore because the transferred flow tend to turbulence rapidly (as fast as days to weeks) and thus parameters become very high;
- their recovery from daylong cGPS data (most useful for real-time EBR recovery and earthquake prediction) is affected by our choice of the cutoff angle mask, which means that the receiver- and satellite-antenna multipath as well as other error sources affect EBR recovery. Empirically, extreme elevation masks, such as 0º and 30º, produce the worst EBR recovery, but it is unknown what mask

in between those extremal values is the right one (recovers diurnal EBR correctly). For some stations, and provided that the cGPS coverage density is overall sufficient for EBR recovery, this problem necessitates post-mapping multi-station analyses to identify EBR waves recovered simultaneously (at the same epoch) in a series of multiple adjacent stations, which, in turn, with the help of null distribution analysis would densify EBR mapping;
- they are destroyed by (to an EBR epoch) co-temporal M6+ seismicity, but it is unknown what other phenomena can destroy EBR waves. This problem requires methodological approaches, like examining fingerprint stability at a cGPS station over time.

As seen from Table 3 and Figures 5 & 6, the EBR resolution increases with data size so that weeklong data sets already can resolve the entire EBR train, unlike daily data sets that are of a lowered resolution (13-18 periods). Seen are the 99%-significant EBR periods with a very high statistical fidelity ($\phi >> 12$) and their matchings against theoretical EBR periods. (The only three periods significant at below 99%, but at 67% level or above, were omitted for clarity.) The weeklong records enabled not only the complete recovery (of all 72 superharmonic resonance periods) of EBR but also a virtually total recovery of an undertone series (or overtone, depending on how one looks at it) as due to an Earth's inevitable sympathetic resonance accompanying the EBR at the time and place of data analyzed. Undertones are normal (weaker) companions of mechanical resonances.

The total recovery of the theoretical EBR train and its (virtually entire) companion sympathetic resonance from just one week of cGPS data at ZLA1 (Los Angeles) is the most concrete proof of EBR as such, i.e., that the solid Earth does resonate in the EBR band. Note that the Δ-values (also in Figure 6), as the differences between the computed and theoretical EBR, have revealed that no Δ-value has exceeded the differences between the corresponding period and its adjacent two theoretical-EBR periods. Therefore, the recovered EBR trains genuinely and consistently represent the theoretical EBR even when data size is varied, while the remaining train recovered from weeklong cGPS data is the undertone series. For the most part, the undertone train is linearly offset from the EBR train along the z-axis by about –5% (disregarding the longest outlier). The minus sign (meaning a companion wave is longer than the corresponding, i.e., nearest EBR wave) reveals in all components the nature of the companion resonance-train as an undertone rather than overtone series. The constant intensity of negative differences in the z-direction, and the best match to the theoretical EBR, reflect the fact that the largest bodies of mass receptive to EBR (and that thereby re-transmit it as an undertone series) sit below the EBR-carrying crust, most likely in the upper mantle.

E B R		99% significant EBR periods at cGPS station: ZLA1 (Los Angeles County) - January 2020																							
		01-02 Jan						01-03 Jan						01-07 Jan											
P_{theor}	P_{EQE}	Px	Δx	Py	Δy	Pz	Δz	Px	Δx	Py	Δy	Pz	Δz	Px	Px'	Δx	Δx'	Py	Py'	Δy	Δy'	Pz	Pz'	Δz	Δz'
72.0000	75.0591									55.4728	23.0%	79.4864	-10.4%	63.0978		12.4%		79.4864	49.4919	-10.4%	31.3%	59.0401		18.0%	
36.0000	33.3241	40.713	-13.1%	34.5793	3.9%			52.312		30.0517	16.5%			32.1569	42.6022	10.7%	-18.3%	37.3963	30.0517	-3.9%	16.5%	34.5793		3.9%	
24.0000	23.2132					23.2132	3.3%	22.0958	7.9%			23.2132	3.3%	24.4496		-1.9%		24.4496	20.6079	-1.9%	14.1%	23.2132	28.2052	3.3%	-17.5%
18.0000	17.9995	20.6079	-14.5%											17.4707	20.1555	2.9%	-12.0%	18.1619	16.5272	-0.9%	8.2%	17.1444	19.7225	4.8%	-9.6%
14.4000	14.4466											15.9528	-10.8%	14.2228	15.6803	1.2%	-8.9%	14.9161	13.3929	-3.6%	7.0%	14.0059	15.4170	2.7%	-7.1%
12.0000	12.6545	12.8314	-6.9%					12.8314	-6.9%					11.8386	12.8314	1.3%	-6.9%	12.3150	11.3977	-2.6%	5.0%	11.8386	13.0132	1.3%	-8.4%
10.2857	10.0282	9.91988	3.6%	10.9885	-6.8%	10.9885	-6.8%			10.8585	-5.6%	10.8585	-5.6%	10.0282	10.8585	2.5%	-5.6%	10.4864	9.7101	-2.0%	5.6%	10.1390	10.9885	1.4%	-6.8%
9.0000	8.8661											9.13064	-1.5%	8.7813	9.4114	2.4%	-4.6%	9.0407		-0.5%		8.8661	9.5089	1.5%	-5.7%
8.0000	7.8772													8.1571	7.6158	-2.0%	4.8%	7.8102	8.4577	2.4%	-5.7%	7.9454	8.3805	0.7%	-4.8%
7.2000	7.1419			7.03245	2.3%	7.14186	0.8%			7.08673	1.6%	7.19785	0.0%	7.1419		0.8%		7.3712	6.9790	-2.4%	3.1%	7.1419	7.5532	0.8%	-4.9%
6.5455	6.5321	6.5321	0.2%					6.5321	0.2%					6.4405	6.7730	1.6%	-3.5%	6.6746		-2.0%		6.5321	6.8234	0.2%	-4.2%
6.0000	6.0183											5.94038	1.0%	5.8645	6.1390	2.3%	-2.3%	6.3513		-5.9%		5.9791	6.2647	0.3%	-4.4%
5.5385	5.6132					5.75422	-3.9%			5.3207	3.9%	5.44697	1.7%	5.5794	5.3517	-0.7%	3.4%	5.4470	5.6830	1.7%	-2.6%	5.5457	5.7542	-0.1%	-3.9%
5.1429	5.1709	5.20015	-1.1%	5.17086	-0.5%			5.3207	-3.5%	5.17086	-0.5%			5.1419		0.0%		5.0569	5.2597	1.7%	-2.3%	5.1419	5.3207	0.0%	-3.5%
4.8000	4.7434													4.7680	4.9479	0.7%	-3.1%	4.7190	4.8952	1.7%	-2.0%	4.8181	4.9747	-0.4%	-3.6%
4.5000	4.6008					4.48832	0.3%					4.64736	-3.3%	4.4022	4.6474	2.2%	-3.3%	4.4449	4.5778	1.2%	-1.7%	4.5104	4.6710	-0.2%	-3.8%
4.2353	4.2008	4.16271	1.7%									4.36042	-3.0%	4.2593	4.1253	-0.6%	2.6%	4.2008	4.3194	0.8%	-2.0%	4.2593	4.3812	-0.6%	-3.4%
4.0000	3.9650			4.03466	-0.9%					4.05247	-1.3%			3.9995		0.0%		3.9650	4.0886	0.9%	-2.2%	4.0170	4.1253	-0.4%	-3.1%
3.7895	3.7696			3.80081	-0.3%					3.83255	-1.1%	3.81662	-0.7%	3.8166	3.6938	-0.7%	2.5%	3.7696	3.8648	0.5%	-2.0%	3.8166	3.9142	-0.7%	-3.3%
3.6000	3.5236					3.66429	-1.8%					3.62093	-0.6%	3.5926		0.2%		3.6643	3.5236	-1.8%	2.1%	3.6209	3.7237	-0.6%	-3.4%
3.4286	3.4443													3.3934	3.4835	1.0%	-1.6%	3.4315		-0.1%		3.4573	3.5372	-0.8%	-3.2%
3.2727	3.2842	3.26083	0.4%	3.24929	0.7%			3.26083	0.4%	3.26083	0.4%	3.27245	0.0%	3.3078	3.2265	-1.1%	1.4%	3.2725	3.3440	0.0%	-2.2%	3.2960	3.3809	-0.7%	-3.3%
3.1304	3.1275											3.08549	1.4%	3.1490	3.0752	-0.6%	1.8%	3.1169	3.1928	0.4%	-2.0%	3.1598	3.2265	-0.9%	-3.1%
3.0000	2.9949											2.95633	1.5%	2.9949		0.2%		3.0446	2.9468	-1.5%	1.8%	3.0245	3.0959	-0.8%	-3.2%
2.8800	2.8821					2.92804	-1.7%	2.82011	2.1%			2.87306	0.2%	2.8552	2.9187	0.9%	-1.3%	2.8912	2.8288	-0.4%	1.8%	2.9095	2.9659	-1.0%	-3.0%
2.7692	2.7691	2.81147	-1.5%	2.76075	0.3%					2.75247	0.6%			2.7442	2.7944	0.9%	-0.9%	2.7691	2.7199	0.0%	1.8%	2.7944	2.8463	-0.9%	-2.8%
2.6667	2.6569													2.6880	2.6416	-0.8%	0.9%	2.6646	2.6190	0.1%	1.8%	2.6492	2.7442	0.7%	-2.9%
2.5714	2.5821					2.54635	1.0%					2.5323	1.5%	2.5534	2.6041	0.7%	-1.3%	2.5749	2.5323	-0.1%	1.5%	2.5534	2.6959	0.7%	-4.8%
2.4828	2.4911													2.4710	2.5115	0.5%	-1.2%	2.4911	2.4512	-0.3%	1.3%	2.4643	2.5968	0.7%	-4.6%
2.4000	2.4317	2.42527	-1.1%	2.37508	1.0%			2.4317	-1.3%	2.36895	1.3%			2.3874	2.4253	0.5%	-1.1%	2.4062	2.3690	-0.3%	1.3%	2.4253	2.5115	-1.1%	-4.6%
2.3226	2.3269	2.2978	1.1%					2.30357	0.8%					2.3094	2.3448	0.6%	-1.0%	2.3269	2.2921	-0.2%	1.3%	2.3152	2.3874	0.3%	-2.8%
2.2500	2.2580					2.26381	-0.6%					2.25824	-0.4%	2.2694	2.2254	-0.9%	1.1%	2.2527		-0.1%		2.2417	2.3508	0.4%	-4.5%
2.1818	2.1524													2.1831		-0.1%		2.1676	2.1987	0.7%	-0.8%	2.1727	2.2750	0.4%	-4.3%
2.1176	2.1274											2.1225	-0.2%	2.1127	2.1473	0.2%	-1.4%	2.1324	2.0982	-0.7%	0.9%	2.1127	2.2040	0.2%	-4.1%
2.0571	2.0514	2.07454	-0.8%	2.08396	-1.3%			2.07924	-1.1%	2.08396	-1.3%			2.0514	2.0792	0.3%	-1.1%	2.0652	2.0377	-0.4%	0.9%	2.0560	2.1423	0.1%	-4.1%
2.0000	1.9763					2.00653	-0.3%					2.01092	-0.5%	1.9848	2.0153	0.8%	-0.8%	2.0065		-0.3%		1.9978	2.0840	0.1%	-4.2%
1.9459	1.9636					1.94696	-0.1%					1.93873	0.4%	1.9511	1.9225	-0.3%	1.2%	1.9346	1.9636	0.6%	-0.9%	1.9428	2.0242	0.2%	-4.0%
1.8947	1.8831	1.89472	0.0%	1.89472	0.0%			1.89472	0.0%	1.88693	0.4%	1.87155	1.2%	1.8908		0.2%		1.8831	1.9065	0.6%	-0.6%	1.8947	1.9720	0.0%	-4.1%
1.8462	1.8305													1.8415	1.8677	0.3%	-1.2%	1.8564	1.8342	-0.6%	0.7%	1.8452	1.9185	0.1%	-3.9%
1.8000	1.8160													1.7808		1.1%		1.7912	1.8124	0.5%	-0.7%	1.8018	1.8715	-0.1%	-4.0%
1.7561	1.7536					1.77734	-1.2%					1.77734	-1.2%	1.7603	1.7403	-0.2%	0.9%	1.7502	1.7705	0.3%	-0.8%	1.7569	1.8232	0.0%	-3.8%
1.7143	1.7016													1.7207	1.6984	-0.4%	0.9%	1.7079	1.7304	0.4%	-0.9%	1.7175	1.7808	-0.2%	-3.9%
1.6744	1.6646			1.67366	0.0%			1.65555	1.1%	1.67672	-0.1%			1.6767	1.6556	-0.1%	1.1%	1.6676	1.6891	0.4%	-0.9%	1.6767	1.7370	-0.1%	-3.7%
1.6364	1.6351	1.65257	-1.0%			1.63492	0.1%					1.63492	0.1%	1.6349		0.1%		1.6291	1.6466	0.4%	-0.6%	1.6408	1.6984	-0.3%	-3.8%
1.6000	1.5869													1.5924	1.6148	0.5%	-0.9%	1.6007		0.0%		1.6035	1.6585	-0.2%	-3.7%
1.5652	1.5573	1.56257	0.2%	1.54938	1.0%			1.56523	0.0%	1.54938	1.0%			1.5733	1.5546	-0.5%	0.7%	1.5626	1.5814	0.2%	-1.0%	1.5706	1.6205	-0.3%	-3.5%
1.5319	1.5416											1.52367	0.5%	1.5364	1.5186	-0.3%	0.9%	1.5287	1.5468	0.2%	-1.0%	1.5364	1.5869	-0.3%	-3.6%
1.5000	1.5062					1.51362	-0.9%							1.4939		0.4%		1.4988	1.5136	0.1%	-0.9%	1.5062	1.5546	-0.4%	-3.6%
1.4694	1.4676					1.46064	0.6%					1.46064	0.6%	1.4771	1.4606	-0.5%	0.6%	1.4700	1.4843	0.0%	-1.0%	1.4747	1.5211	-0.4%	-3.5%
1.4400	1.4468	1.44912	-0.6%	1.44002	0.0%			1.44912	-0.6%	1.43777	0.2%			1.4468	1.4310	-0.5%	0.6%	1.4400	1.4537	0.0%	-1.0%	1.4468	1.4891	-0.5%	-3.4%
1.4118	1.4091													1.4156	1.4026	-0.3%	0.6%	1.4112	1.4244	0.0%	-0.9%	1.4178	1.4606	-0.4%	-3.5%
1.3846	1.3941													1.3794	1.3920	0.4%	-0.5%	1.3857	1.3984	-0.1%	-1.0%	1.3920	1.4310	-0.5%	-3.4%
1.3585	1.3590					1.36916	-0.8%					1.36916	-0.8%	1.3550		0.3%		1.3610	1.3733	-0.2%	-1.1%	1.3530	1.4048	0.4%	-3.4%
1.3333	1.3412													1.3295	1.3431	0.3%	-0.7%	1.3353	1.3490	-0.2%	-1.2%	1.3392	1.3774	-0.4%	-3.3%
1.3091	1.2939	1.30494	0.3%	1.30866	0.0%			1.30494	0.3%	1.31052	-0.1%			1.3049	1.3162	0.3%	-0.5%	1.3105	1.3238	-0.1%	-1.1%	1.3049	1.3651	0.3%	-4.3%
1.2857	1.2741					1.28845	-0.2%					1.28845	-0.2%	1.2795	1.2921	0.5%	-0.5%	1.2866	1.2994	-0.1%	-1.1%	1.2813	1.3276	0.3%	-3.3%
1.2632	1.2636													1.2654		-0.2%		1.2567	1.2759	0.5%	-1.0%	1.2602	1.3162	0.2%	-4.2%
1.2414	1.2381											1.23974	0.1%	1.2397	1.2516	0.1%	-0.8%	1.2448	1.2347	-0.3%	0.5%	1.2482	1.2939	-0.5%	-4.2%
1.2203	1.2103	1.22813	-0.6%	1.22813	-0.6%			1.22813	-0.6%	1.22813	-0.6%	1.21674	0.3%	1.2167	1.2281	0.3%	-0.6%	1.2232	1.2119	-0.2%	0.7%	1.2281	1.2706	-0.6%	-4.1%
1.2000	1.2008													1.2040	1.1915	-0.3%	0.7%	1.2024		-0.2%		1.2087	1.2381	-0.7%	-3.2%
1.1803	1.1762					1.1747	0.5%					1.1747	0.5%	1.1807		0.0%		1.1762	1.1853	0.3%	-0.4%	1.1792	1.2183	0.1%	-3.2%
1.1613	1.1628	1.16427	-0.3%	1.15694	0.4%			1.1628	-0.1%	1.15694	0.4%			1.1599	1.1702	0.1%	-0.8%	1.1658	1.1555	-0.4%	0.5%	1.1599	1.1977	0.1%	-3.1%
1.1429	1.1425													1.1411	1.1511	0.2%	-0.7%	1.1468	1.1383	-0.3%	0.4%	1.1425	1.1884	0.0%	-4.0%
1.1250	1.1299	1.12023	0.4%											1.1243	1.1327	0.1%	-0.7%	1.1202	1.1299	0.4%	-0.4%	1.1243	1.1687	0.1%	-3.9%
1.1077	1.1107			1.07059	3.3%	1.11209	-0.4%	1.11751	-0.9%			1.11344	-0.5%	1.1041	1.1134	0.3%	-0.5%	1.1041	1.1121	0.3%	-0.4%	1.1081	1.1511	0.0%	-3.9%
1.0909	1.0909													1.0935	1.0845	-0.2%	0.6%	1.0884	1.0975	0.2%	-0.6%	1.0909	1.1341	0.0%	-4.0%
1.0746	1.0693	1.07184	0.3%					1.0731	0.1%	1.07059	0.4%			1.0756	1.0669	-0.1%	0.7%	1.0718	1.0807	0.3%	-0.6%	1.0756	1.1161	-0.1%	-3.9%
1.0588	1.0546					1.05947	-0.1%					1.0607	-0.2%	1.0583		0.1%		1.0558	1.0632	0.3%	-0.4%	1.0595	1.0988	-0.1%	-3.8%
1.0435	1.0438													1.0391	1.0498	0.4%	-0.6%	1.0426	1.0486	0.1%	-0.5%	1.0450	1.0832	-0.1%	-3.8%
1.0286	1.0321	1.02174	0.7%	1.02061	0.8%			1.02061	0.8%	1.02061	0.8%			1.0309	1.0229	-0.2%	0.6%	1.0275	1.0356	0.1%	-0.7%	1.0298	1.0681	-0.1%	-3.8%
1.0141	1.0195					1.01947	-0.5%					1.01609	-0.2%	1.0150		-0.1%		1.0127	1.0195	0.1%	-0.5%	1.0161	1.0522	-0.2%	-3.8%
1.0000	0.9984	0.98449	1.6%	0.96281	3.7%	0.97924	2.1%	0.98449	1.6%	0.96789	3.2%	0.98029	2.0%	0.9984	1.0072	0.2%	-0.7%	0.9984		0.2%		1.0017	1.0367	-0.2%	-3.7%
	Σ		12		10		12		8		10		17			46	28			39	32			44	0
	down to 1‰		1		4		3		4		2		4			12	0			17	0			19	0
	down to 1%		13		14		15		12		12		21			58	29			56	32			63	0

Table 3. EBR resolution increase with data size. Δ-values (in %) here and throughout this study were computed as the difference between an EBR period from cGPS and its EBR counterpart in the leftmost column highlighted blue (here theoretical the EBR periods).

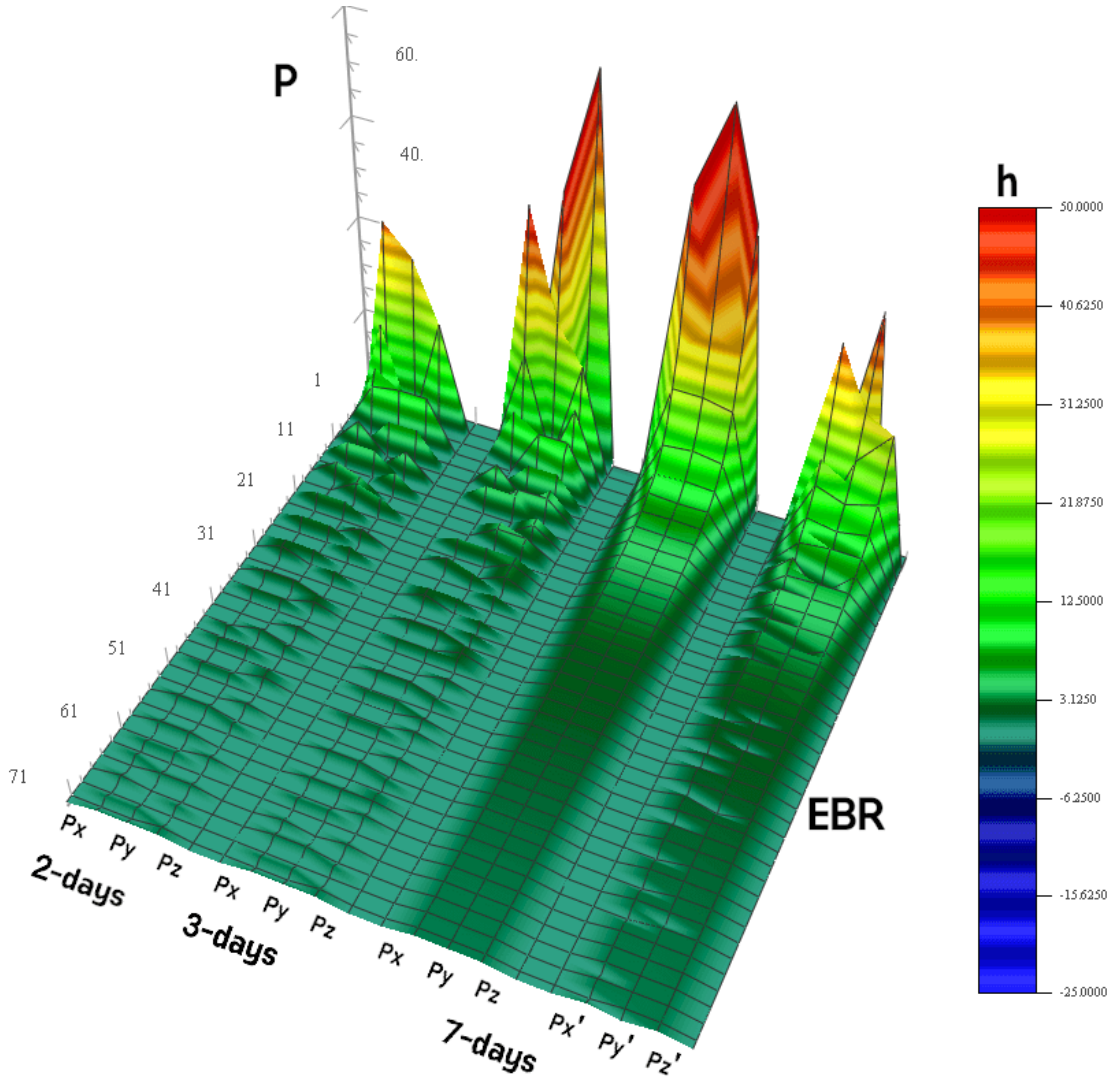

Figure 5. The ability of cGPS to recover EBR, with an increase in data size, example of the ZLA1 station (Los Angeles), Table 3. In the above, the only three periods that were significant at 67%-95% levels were omitted for clarity. The EBR and its undertone series are shown separately.

As seen in Figure 5 & Table 3, the 2-days cGPS records showed no significant improvements from daylong records. However, the 3-days long records did enable a somewhat improved recovery of the 99%-significant EBR periods, most noticeable in the strongest (longest) periods. Finally, expanding data to weeklong has practically raised confidence to the 99%-only level and achieved a complete EBR recovery (of all 72 superharmonic resonance periods). This expansion also enabled the recovery of an undertone series (or overtone, depending on how one looks at it). Undertones are normal (weaker) sympathetic companions of mechanical resonances due to the vibrating body starting re-emitting externally fed resonances in its (modified) modes. When those modes are mostly higher than tones of the lead resonance — we speak of an overtone resonance, and when lower — of an undertone resonance, as in here.

The complete recovery of the theoretical EBR train and its (virtually entire) companion sympathetic resonance from just one week of cGPS data is the most concrete proof of EBR as such, i.e., that the solid Earth does resonate with the EBR periods in the EBR band. Furthermore, EBR recovery errors tend to zero with an increase in data size — and do so even in 99%-significant EBR periods; see Figure 6 & Table 3. For example, the dropping of absolute Δ-values below 1% already after the first (longest) period, for z' in particular, characterized the weeklong data. The same does not appear to hold for the undertone series, whose absolute Δ-values rarely if ever dropped under a few percent of EBR (for z' never below 2.8%), and most of the time kept at a constant level of a few percent.

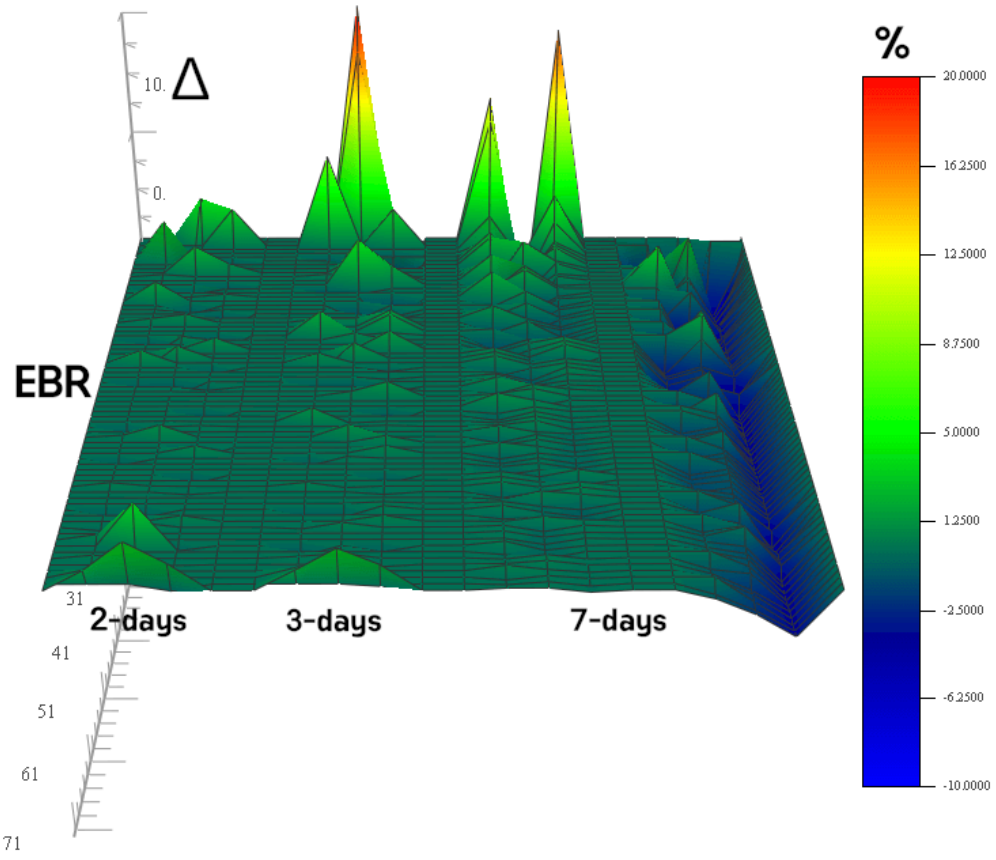

Figure 6. The positive-Δ surface of the cGPS ability to recover EBR at the ZLA1, with an increase in data, Figure 3. The here plotted Δ-values correspond to the Figure-5 values of spectral peaks, Table 3, and are shown separately from the respective undertone series (7-day case).

EBR waves along cGPS profile ZLA1 (Los Angeles County) - MMX1 (Mexico City) - ZOA2 (San Francisco Bay), 01-07 Jan 2020

MMX1

EBR Ptheor	EBR PEQE	Px	Px'	Δx	Δx'	Py	Py'	Δy	Δy'	Pz	Pz'	Δz	Δz'
72.0000	75.0591	63.0978		12.4%		73.1530	49.4919	-1.6%	31.3%	87.0205	49.4919	-20.9%	31.3%
36.0000	33.3241	31.0687	42.6022	13.7%	-18.3%	35.9326		0.2%		35.9326	29.0992	0.2%	19.2%
24.0000	23.2132	23.8154		0.8%		23.2132	29.0992	3.3%	-21.2%	23.2132		3.3%	
18.0000	17.9995	17.8096	19.7225	1.1%	-9.6%	17.4707	19.7225	2.9%	-9.6%	17.4707	19.3077	2.9%	-7.3%
14.4000	14.4466	15.6803		-8.9%		14.2228	15.6803	1.2%	-8.9%	14.2228	15.9528	1.2%	-10.8%
12.0000	12.6545	12.1520		-1.3%		12.3150		-2.6%		12.1520		-1.3%	
10.2857	10.0282	10.3680		-0.8%		10.6076	9.7101	-3.1%	5.6%	10.0282	10.8585	2.5%	-5.6%
9.0000	8.8661	9.8138		-9.0%		8.8661		1.5%		8.7813		2.4%	
8.0000	7.8772	8.0853		-1.1%		7.9454		0.7%		7.8772		1.5%	
7.2000	7.1419	7.1979	7.5532	0.0%	-4.9%	7.1979	7.5532	0.0%	-4.9%	6.9790	7.4309	3.1%	-3.2%
6.5455	6.5321	6.4405	6.8234	1.6%	-4.2%	6.5789	6.9790	-0.5%	-6.6%	6.5789	6.3077	-0.5%	3.6%
6.0000	6.0183	6.0580		-1.0%		5.9404	6.2222	1.0%	-3.7%	5.9404		1.0%	
5.5385	5.6132	5.5457	5.7542	-0.1%	-3.9%	5.6135		-1.4%		5.5794		-0.7%	
5.1429	5.1709	5.1133	5.3517	0.6%	-4.1%	5.2001	5.0018	-1.1%	2.7%	5.1709	4.9747	-0.5%	3.3%
4.8000	4.7434	4.7929	5.0018	0.1%	-4.2%	4.7929		0.1%		4.7929		0.1%	
4.5000	4.6008	4.4449	4.6008	1.2%	-2.2%	4.4449	4.6008	1.2%	-2.2%	4.4234	4.6008	1.7%	-2.2%
4.2353	4.2008	4.2791	4.1439	-1.0%	2.2%	4.1627	4.3194	1.7%	-2.0%	4.1817	4.2992	1.3%	-1.5%
4.0000	3.9650	3.9822		0.4%		3.9650		0.9%		3.9650		0.9%	
3.7895	3.7696	3.7542	3.8648	0.9%	-2.0%	3.8166	3.6938	-0.7%	2.5%	3.8325		-1.1%	
3.6000	3.5236	3.6497	3.5236	-1.4%	2.1%	3.5926		0.2%		3.6643	3.5236	-1.8%	2.1%
3.4286	3.4443	3.4060		0.7%		3.4060	3.5102	0.7%	-2.4%	3.4060		0.7%	
3.2727	3.2842	3.2608	3.3198	0.4%	-1.4%	3.3198		-1.4%		3.2378	3.3198	1.1%	-1.4%
3.1304	3.1275	3.1275	3.1928	0.1%	-2.0%	3.2039		-2.3%		3.1169	3.1707	0.4%	-1.3%
3.0000	2.9949	2.9852	3.0446	0.5%	-1.5%	2.9852		0.5%		3.0146		-0.5%	
2.8800	2.8821	2.8821	2.8288	-0.1%	1.8%	2.8463		1.2%		2.8731		0.2%	
2.7692	2.7691	2.7442		0.9%		2.7944	2.7279	-0.9%	1.5%	2.7279	2.8201	1.5%	-1.8%
2.6667	2.6569	2.6492		0.7%		2.6340		1.2%		2.6646		0.1%	
2.5714	2.5821	2.5606	2.6041	0.4%	-1.3%	2.5534		0.7%		2.5822		-0.4%	
2.4828	2.4911	2.4512	2.5184	1.3%	-1.4%	2.5115	2.4446	-1.2%	1.5%	2.5115	2.4512	-1.2%	1.3%
2.4000	2.4317	2.3999		0.0%		2.3937		0.3%		2.3937		0.3%	
2.3226	2.3269	2.3036	2.3448	0.8%	-1.0%	2.3036	2.3448	0.8%	-1.0%	2.3094	2.3448	0.6%	-1.0%
2.2500	2.2580	2.2147		1.6%		2.2147		1.6%		2.2200		1.3%	
2.1818	2.1524	2.1779		0.2%		2.1727		0.4%		2.1727		0.4%	
2.1176	2.1274	2.1079	2.1373	0.5%	-0.9%	2.1031	2.1324	0.7%	-0.7%	2.1031	2.1324	0.7%	-0.7%
2.0571	2.0514	2.0560	2.0840	0.1%	-1.3%	2.0699	2.0377	-0.6%	0.9%	2.0652		-0.4%	
2.0000	1.9763	1.9891	2.0287	0.5%	-1.4%	1.9978		0.1%		1.9978		0.1%	
1.9459	1.9636	1.9552	1.9265	-0.5%	1.0%	1.9511		-0.3%		1.9511		-0.3%	
1.8947	1.8831	1.9026		-0.4%		1.8792	1.9145	0.8%	-1.0%	1.9026	1.8831	-0.4%	0.6%
1.8462	1.8305	1.8378	1.8792	0.5%	-1.8%	1.8415		0.3%		1.8342		0.7%	
1.8000	1.8160	1.8089	1.7843	-0.5%	0.9%	1.7877	1.8160	0.7%	-0.9%	1.7877	1.8124	0.7%	-0.7%
1.7561	1.7536	1.7637	1.7403	-0.4%	0.9%	1.7536	1.7403	0.1%	0.9%	1.7569	1.7370	0.0%	1.1%
1.7143	1.7016	1.7079		0.4%		1.7143		0.0%		1.7111		0.2%	
1.6744	1.6646	1.6706		0.2%		1.6646	1.6891	0.6%	-0.9%	1.6860		-0.7%	
1.6364	1.6351	1.6349	1.6526	0.1%	-1.0%	1.6526		-1.0%		1.6349	1.6526	0.1%	-1.0%
1.6000	1.5869	1.5951	1.6176	0.3%	-1.1%	1.5951	1.6176	0.3%	-1.1%	1.5924	1.6176	0.5%	-1.1%
1.5652	1.5573	1.5652	1.5494	0.0%	1.0%	1.5573		0.5%		1.5599		0.3%	
1.5319	1.5416	1.5313		0.0%		1.5390		-0.5%		1.5237	1.5416	0.5%	-0.6%
1.5000	1.5062	1.4964		0.2%		1.4939		0.4%		1.4915	1.5111	0.6%	-0.7%
1.4694	1.4676	1.4653	1.4795	0.3%	-0.7%	1.4700		0.0%		1.4724		-0.2%	
1.4400	1.4468	1.4378	1.4514	0.2%	-0.8%	1.4423	1.4266	-0.2%	0.9%	1.4400	1.4537	0.0%	-1.0%
1.4118	1.4091	1.4134		-0.1%		1.4069		0.3%		1.4069	1.4244	0.3%	-0.9%
1.3846	1.3941	1.3692		1.1%		1.3899	1.3774	-0.4%	0.5%	1.3774	1.3920	0.5%	-0.5%
1.3585	1.3590	1.3530		0.4%		1.3530	1.3651	0.4%	-0.5%	1.3651		-0.5%	
1.3333	1.3412	1.3276		0.4%		1.3295	1.3451	0.3%	-0.9%	1.3295	1.3431	0.3%	-0.7%
1.3091	1.2939	1.3180		-0.7%		1.3049	1.3162	0.3%	-0.5%	1.3049	1.3143	0.3%	-0.4%
1.2857	1.2741	1.2795		0.5%		1.2831	1.2957	0.2%	-0.8%	1.2831	1.2939	0.2%	-0.6%
1.2632	1.2636	1.2671		-0.3%		1.2602	1.2724	0.2%	-0.7%	1.2724		-0.7%	
1.2414	1.2381	1.2314		0.8%		1.2482		-0.5%		1.2298		0.9%	
1.2203	1.2103	1.2216	1.2119	-0.1%	0.7%	1.2200		0.0%		1.2183		0.2%	
1.2000	1.2008	1.1993		0.1%		1.1961	1.2071	0.3%	-0.6%	1.1961	1.2087	0.3%	-0.7%
1.1803	1.1762	1.1868		-0.6%		1.1777		0.2%		1.1777	1.1838	0.2%	-0.3%
1.1613	1.1628	1.1628		-0.1%		1.1643		-0.3%		1.1599		0.1%	
1.1429	1.1425	1.1440	1.1526	-0.1%	-0.8%	1.1397	1.1526	0.3%	-0.8%	1.1411		0.2%	
1.1250	1.1299	1.1202		0.4%		1.1285		-0.3%		1.1285	1.1175	-0.3%	0.7%
1.1077	1.1107	1.1041		0.3%		1.1067		0.1%		1.1081		0.0%	
1.0909	1.0909	1.0871		0.4%		1.0884		0.2%		1.0871	1.0988	0.4%	-0.7%
1.0746	1.0693	1.0731		0.1%						1.0769		-0.2%	
1.0588	1.0546	1.0595		-0.1%		1.0644		-0.5%		1.0669		-0.8%	
1.0435	1.0438	1.0403		0.3%		1.0403	1.0498	0.3%	-0.6%	1.0414	1.0510	0.2%	-0.7%
1.0286	1.0321	1.0252	1.0321	0.3%	-0.3%	1.0309		-0.2%					
1.0141	1.0195	1.0127	1.0195	0.1%	-0.5%	1.0127	1.0206	0.1%	-0.6%	1.0127	1.0195	0.1%	-0.5%
1.0000	0.9984	0.9962	1.0050	0.4%	-0.5%	0.9973	1.0061	0.3%	-0.6%	1.0050		-0.5%	
	≤ 1‰		∑	18	0			9	0			10	0
	1‰ - 1%		∑	40	13			45	18			44	19
	≥ 1%		∑	14	22			17	17			17	17
	67%-99%		∑∑	**72**	**35**			**71**	**35**			**71**	**36**

ZLA1

EBR Ptheor	EBR PEQE	Px	Px'	Δx	Δx'	Py	Py'	Δy	Δy'	Pz	Pz'	Δz	Δz'
72.0000	75.0591	63.0978		12.4%		79.4864	49.4919	-10.4%	31.3%	59.0401		18.0%	
36.0000	33.3241	32.1569	42.6022	10.7%	-18.3%	37.3963	30.0517	-3.9%	16.5%	34.5793		3.9%	
24.0000	23.2132	24.4496		-1.9%		24.4496	20.6079	-1.9%	14.1%	23.2132	28.2052	3.3%	-17.5%
18.0000	17.9995	17.4707	20.1555	2.9%	-12.0%	18.1619	16.5272	-0.9%	8.2%	17.1444	19.7225	4.8%	-9.6%
14.4000	14.4466	14.2228	15.6803	1.2%	-8.9%	14.9161	13.3929	-3.6%	7.0%	14.0059	15.4170	2.7%	-7.1%
12.0000	12.6545	11.8386	12.8314	1.3%	-6.9%	12.3150	11.3977	-2.6%	5.0%	11.8386	13.0132	1.3%	-8.4%
10.2857	10.0282	10.0282	10.8585	2.5%	-5.6%	10.4864	9.7101	-2.0%	5.6%	10.1390	10.9885	1.4%	-6.8%
9.0000	8.8661	8.7813	9.4114	2.4%	-4.6%	9.0407		-0.5%		8.8661	9.5089	1.5%	-5.7%
8.0000	7.8772	8.1571	7.6158	-2.0%	4.8%	7.8102	8.4577	2.4%	-5.7%	7.9454	8.3805	0.7%	-4.8%
7.2000	7.1419	7.1419		0.8%		7.3712	6.9790	-2.4%	3.1%	7.1419	7.5532	0.8%	-4.9%
6.5455	6.5321	6.4405	6.7730	1.6%	-3.5%	6.6746		-2.0%		6.5321	6.8234	0.2%	-4.2%
6.0000	6.0183	5.8645	6.1390	2.3%	-2.3%	6.3513		-5.9%		5.9791	6.2647	0.3%	-4.4%
5.5385	5.6132	5.5794	5.3517	-0.7%	3.4%	5.4470	5.6830	1.7%	-2.6%	5.5457	5.7542	-0.1%	-3.9%
5.1429	5.1709	5.1419		0.0%		5.0569	5.2597	1.7%	-2.3%	5.1419	5.3207	0.0%	-3.5%
4.8000	4.7434	4.7680	4.9479	0.7%	-3.1%	4.7190	4.8952	1.7%	-2.0%	4.8181	4.9747	-0.4%	-3.6%
4.5000	4.6008	4.4022	4.6474	2.2%	-3.3%	4.4449	4.5778	1.2%	-1.7%	4.5104	4.6710	-0.2%	-3.8%
4.2353	4.2008	4.2593	4.1253	-0.6%	2.6%	4.2008	4.3194	0.8%	-2.0%	4.2593	4.3812	-0.6%	-3.4%
4.0000	3.9650	3.9995		0.0%		3.9650	4.0886	0.9%	-2.2%	4.0170	4.1253	-0.4%	-3.1%
3.7895	3.7696	3.8166	3.6938	-0.7%	2.5%	3.7696	3.8648	0.5%	-2.0%	3.8166	3.9142	-0.7%	-3.3%
3.6000	3.5236	3.5926		0.2%		3.6643	3.5236	-1.8%	2.1%	3.6209	3.7237	-0.6%	-3.4%
3.4286	3.4443	3.3934	3.4835	1.0%	-1.6%	3.4315		-0.1%		3.4573	3.5372	-0.8%	-3.2%
3.2727	3.2842	3.3078	3.2265	-1.1%	1.4%	3.2725	3.3440	0.0%	-2.2%	3.2960	3.3809	-0.7%	-3.3%
3.1304	3.1275	3.1490	3.0752	-0.6%	1.8%	3.1169	3.1928	0.4%	-2.0%	3.1598	3.2265	-0.9%	-3.1%
3.0000	2.9949	2.9949		0.2%		3.0446	2.9468	-1.5%	1.8%	3.0245	3.0959	-0.8%	-3.2%
2.8800	2.8821	2.8552	2.9187	0.9%	-1.3%	2.8912	2.8288	-0.4%	1.8%	2.9095	2.9659	-1.0%	-3.0%
2.7692	2.7691	2.7442	2.7944	0.9%	-0.9%	2.7691	2.7199	0.0%	1.8%	2.7944	2.8463	-0.9%	-2.8%
2.6667	2.6569	2.6880	2.6416	-0.8%	0.9%	2.6646	2.6190	0.1%	1.8%	2.6492	2.7442	0.7%	-2.9%
2.5714	2.5821	2.5534	2.6041	0.7%	-1.3%	2.5749	2.5323	-0.1%	1.5%	2.5534	2.6959	0.7%	-4.8%
2.4828	2.4911	2.4710	2.5115	0.5%	-1.2%	2.4911	2.4512	-0.3%	1.3%	2.4643	2.5968	0.7%	-4.6%
2.4000	2.4317	2.3874	2.4253	0.5%	-1.1%	2.4062	2.3690	-0.3%	1.3%	2.4253	2.5115	-1.1%	-4.6%
2.3226	2.3269	2.3094	2.3448	0.6%	-1.0%	2.3269	2.2921	-0.2%	1.3%	2.3152	2.3874	0.3%	-2.8%
2.2500	2.2580	2.2694	2.2254	-0.9%	1.1%	2.2527		-0.1%		2.2417	2.3508	0.4%	-4.5%
2.1818	2.1524	2.1831		-0.1%		2.1676	2.1987	0.7%	-0.8%	2.1727	2.2750	0.4%	-4.3%
2.1176	2.1274	2.1127	2.1473	0.2%	-1.4%	2.1324	2.0982	-0.7%	0.9%	2.1127	2.2040	0.2%	-4.1%
2.0571	2.0514	2.0514	2.0792	0.3%	-1.1%	2.0652	2.0377	-0.4%	0.9%	2.0560	2.1423	0.1%	-4.1%
2.0000	1.9763	1.9848	2.0153	0.8%	-0.8%	2.0065		-0.3%		1.9978	2.0840	0.1%	-4.2%
1.9459	1.9636	1.9511	1.9225	-0.3%	1.2%	1.9346	1.9636	0.6%	-0.9%	1.9428	2.0242	0.2%	-4.0%
1.8947	1.8831	1.8908		0.2%		1.8831	1.9065	0.6%	-0.6%	1.8947	1.9720	0.0%	-4.1%
1.8462	1.8305	1.8415	1.8677	0.3%	-1.2%	1.8564	1.8342	-0.6%	0.7%	1.8452	1.9185	0.1%	-3.9%
1.8000	1.8160	1.7808		1.1%		1.7912	1.8124	0.5%	-0.7%	1.8018	1.8715	-0.1%	-4.0%
1.7561	1.7536	1.7603	1.7403	-0.2%	0.9%	1.7502	1.7705	0.3%	-0.8%	1.7569	1.8232	0.0%	-3.8%
1.7143	1.7016	1.7207	1.6984	-0.4%	0.9%	1.7079	1.7304	0.4%	-0.9%	1.7175	1.7808	-0.2%	-3.9%
1.6744	1.6646	1.6767	1.6556	-0.1%	1.1%	1.6676	1.6891	0.4%	-0.9%	1.6767	1.7370	-0.1%	-3.7%
1.6364	1.6351	1.6349		0.1%		1.6291	1.6466	0.4%	-0.6%	1.6408	1.6984	-0.3%	-3.8%
1.6000	1.5869	1.5924	1.6148	0.5%	-0.9%	1.6007		0.0%		1.6035	1.6585	-0.2%	-3.7%
1.5652	1.5573	1.5733	1.5546	-0.5%	0.7%	1.5626	1.5814	0.2%	-1.0%	1.5706	1.6205	-0.3%	-3.5%
1.5319	1.5416	1.5364	1.5186	-0.3%	0.9%	1.5287	1.5468	0.2%	-1.0%	1.5364	1.5869	-0.3%	-3.6%
1.5000	1.5062	1.4939		0.4%		1.4988	1.5136	0.1%	-0.9%	1.5062	1.5546	-0.4%	-3.6%
1.4694	1.4676	1.4771	1.4606	-0.5%	0.6%	1.4700	1.4843	0.0%	-1.0%	1.4747	1.5211	-0.4%	-3.5%
1.4400	1.4468	1.4468	1.4310	-0.5%	0.6%	1.4400	1.4537	0.0%	-1.0%	1.4468	1.4891	-0.5%	-3.4%
1.4118	1.4091	1.4156	1.4026	-0.3%	0.6%	1.4112	1.4244	0.0%	-0.9%	1.4178	1.4606	-0.4%	-3.5%
1.3846	1.3941	1.3794	1.3920	0.4%	-0.5%	1.3857	1.3984	-0.1%	-1.0%	1.3920	1.4310	-0.5%	-3.4%
1.3585	1.3590	1.3550		0.3%		1.3610	1.3733	-0.2%	-1.1%	1.3530	1.4048	0.4%	-3.4%
1.3333	1.3412	1.3295	1.3431	0.3%	-0.7%	1.3353	1.3490	-0.2%	-1.2%	1.3392	1.3774	-0.4%	-3.3%
1.3091	1.2939	1.3049	1.3162	0.3%	-0.5%	1.3105	1.3238	-0.1%	-1.1%	1.3049	1.3651	0.3%	-4.3%
1.2857	1.2741	1.2795	1.2921	0.5%	-0.5%	1.2866	1.2994	-0.1%	-1.1%	1.2813	1.3276	0.3%	-3.3%
1.2632	1.2636	1.2654		-0.2%		1.2567	1.2759	0.5%	-1.0%	1.2602	1.3162	0.2%	-4.2%
1.2414	1.2381	1.2397	1.2516	0.1%	-0.8%	1.2448	1.2347	-0.3%	0.5%	1.2482	1.2939	-0.5%	-4.2%
1.2203	1.2103	1.2167	1.2281	0.3%	-0.6%	1.2232	1.2119	-0.2%	0.7%	1.2281	1.2706	-0.6%	-4.1%
1.2000	1.2008	1.2040	1.1915	-0.3%	0.7%	1.2024		-0.2%		1.2087	1.2381	-0.7%	-3.2%
1.1803	1.1762	1.1807		0.0%		1.1762	1.1853	0.3%	-0.4%	1.1792	1.2183	0.1%	-3.2%
1.1613	1.1628	1.1599	1.1702	0.1%	-0.8%	1.1658	1.1555	-0.4%	0.5%	1.1599	1.1977	0.1%	-3.1%
1.1429	1.1425	1.1411	1.1511	0.2%	-0.7%	1.1468	1.1383	-0.3%	0.4%	1.1425	1.1884	0.0%	-4.0%
1.1250	1.1299	1.1243	1.1327	0.1%	-0.7%	1.1202	1.1299	0.4%	-0.4%	1.1243	1.1687	0.1%	-3.9%
1.1077	1.1107	1.1041	1.1134	0.3%	-0.5%	1.1041	1.1121	0.3%	-0.4%	1.1081	1.1511	0.0%	-3.9%
1.0909	1.0909	1.0935	1.0845	-0.2%	0.6%	1.0884	1.0975	0.2%	-0.6%	1.0909	1.1341	0.0%	-4.0%
1.0746	1.0693	1.0756	1.0669	-0.1%	0.7%	1.0718	1.0807	0.3%	-0.6%	1.0756	1.1161	-0.1%	-3.9%
1.0588	1.0546	1.0583		0.1%		1.0558	1.0632	0.3%	-0.4%	1.0595	1.0988	-0.1%	-3.8%
1.0435	1.0438	1.0391	1.0498	0.4%	-0.6%	1.0426	1.0486	0.1%	-0.5%	1.0450	1.0832	-0.1%	-3.8%
1.0286	1.0321	1.0309	1.0229	-0.2%	0.6%	1.0275	1.0356	0.1%	-0.7%	1.0298	1.0681	-0.1%	-3.8%
1.0141	1.0195	1.0150		-0.1%		1.0127	1.0195	0.1%	-0.5%	1.0161	1.0522	-0.2%	-3.8%
1.0000	0.9984	0.9984	1.0072	0.2%	-0.7%	0.9984		0.2%		1.0017	1.0367	-0.2%	-3.7%
	≤ 1‰			12	0			17	0			19	0
	1‰ - 1%			46	28			39	32			44	0
	≥ 1%			14	27			16	31			9	70
	67%-99%			**72**	**55**			**72**	**63**			**72**	**70**

ZOA2

EBR Ptheor	EBR PEQE	Px	Px'	Δx	Δx'	Py	Py'	Δy	Δy'	Pz	Pz'	Δz	Δz'
72.0000	75.0591	63.0978		12.4%		67.7543		5.9%		63.0978		12.4%	
36.0000	33.3241	35.9326	44.6753	0.2%	-24.1%	35.9326	46.9604	0.2%	-30.4%	35.9326	44.6753	0.2%	-24.1%
24.0000	23.2132	23.8154	30.0517	0.8%	-25.2%	23.8154	29.0992	0.8%	-21.2%	23.8154	29.0992	0.8%	-21.2%
18.0000	17.9995	18.1619	19.7225	-0.9%	-9.6%	16.5272	20.1555	8.2%	-12.0%	17.4707	19.7225	2.9%	-9.6%
14.4000	14.4466	14.6776	16.2349	-1.9%	-12.7%	14.6776	13.2004	-1.9%	8.3%	14.4466	15.9528	-0.3%	-10.8%
12.0000	12.6545	11.8386	13.2004	1.3%	-10.0%	11.8386		1.3%		11.8386	13.0132	1.3%	-8.4%
10.2857	10.0282	10.1390	10.8585	1.4%	-5.6%	10.1390	10.8585	1.4%	-5.6%	10.2522	10.9885	0.3%	-6.8%
9.0000	8.8661	9.0407	9.6084	-0.5%	-6.8%	9.0407	9.6084	-0.5%	-6.8%	9.0407	9.6084	-0.5%	-6.8%
8.0000	7.8772	8.0147	8.5364	-0.2%	-6.7%	8.0147	8.5364	-0.2%	-6.7%	8.0147	8.5364	-0.2%	-6.7%
7.2000	7.1419	7.0867	7.4309	1.6%	-3.2%	7.0324	7.4915	2.3%	-4.0%	7.2547	7.5532	-0.8%	-4.9%
6.5455	6.5321	6.5321	6.8234	0.2%	-4.2%	6.5321	6.7730	0.2%	-3.5%	6.7234	6.9790	-2.7%	-6.6%
6.0000	6.0183	5.9791	6.3077	0.3%	-5.1%	5.9791	6.3077	0.3%	-5.1%	5.9791	6.2647	0.3%	-4.4%
5.5385	5.6132	5.7184		-3.2%		5.5124	5.7184	0.5%	-3.2%	5.4795	5.6830	1.1%	-2.6%
5.1429	5.1709	5.2597		-2.3%		5.2597	4.9747	-2.3%	3.3%	5.2001	5.3517	-1.1%	-4.1%
4.8000	4.7434	4.7680	4.9479	0.7%	-3.1%	4.7680		0.7%		4.7434	5.0569	1.2%	-5.4%
4.5000	4.6008	4.4665	4.6008	0.7%	-2.2%	4.4665	4.6008	0.7%	-2.2%	4.4665	4.9214	0.7%	-9.4%
4.2353	4.2008	4.2396	4.3604	-0.1%	-3.0%	4.2396	4.3604	-0.1%	-3.0%	4.2593	4.6008	-0.6%	-8.6%
4.0000	3.9650	4.0525		-1.3%		4.0347		-0.9%		4.0170	4.3604	-0.4%	-9.0%
3.7895	3.7696	3.8812		-2.4%		3.7696	3.8648	0.5%	-2.0%	3.7851	4.1439	0.1%	-9.4%
3.6000	3.5236	3.5236	3.6790	2.1%	-2.2%	3.6790		-2.2%		3.6790		-2.2%	
3.4286	3.4443	3.4060		0.7%		3.4060	3.4968	0.7%	-2.0%	3.4060	3.4968	0.7%	-2.0%
3.2727	3.2842	3.2493	3.3198	0.7%	-1.4%	3.2493		0.7%		3.2493	3.3198	0.7%	-1.4%
3.1304	3.1275	3.1382	3.0649	-0.2%	2.1%	3.1382	3.1928	-0.2%	-2.0%	3.1382	3.0649	-0.2%	2.1%
3.0000	2.9949	2.9659		1.1%		2.9852	3.0752	0.5%	-2.5%	2.9852		0.5%	
2.8800	2.8821	2.8552		0.9%		2.8641	2.9095	0.6%	-1.0%	2.8641	2.9187	0.6%	-1.3%
2.7692	2.7691	2.7607	2.8029	0.3%	-1.2%	2.7691	2.8115	0.0%	-1.5%	2.7691	2.8115	0.0%	-1.5%
2.6667	2.6569	2.6646	2.7199	0.1%	-2.0%	2.6646	2.7199	0.1%	-2.0%	2.6646	2.7199	0.1%	-2.0%
2.5714	2.5821	2.6041		-1.3%		2.5534	2.5968	0.7%	-1.0%	2.5534	2.6041	0.7%	-1.3%
2.4828	2.4911	2.4710	2.5115	0.5%	-1.2%	2.4843	2.5184	-0.1%	-1.4%	2.4776	2.5047	0.2%	-0.9%
2.4000	2.4317	2.3874	2.4382	0.5%	-1.6%	2.3937	2.4446	0.3%	-1.9%	2.3937	2.4382	0.3%	-1.6%
2.3226	2.3269	2.3094	2.3388	0.6%	-0.7%					2.3094		0.6%	
2.2500	2.2580	2.2527		-0.1%		2.2472	2.2200	0.1%	1.3%	2.2527	2.2864	-0.1%	-1.6%
2.1818	2.1524	2.1727	2.2147	0.4%	-1.5%	2.1779		0.2%		2.1779	2.2200	0.2%	-1.8%
2.1176	2.1274	2.1373		-0.9%		2.1079	2.1373	0.5%	-0.9%	2.1423		-1.2%	
2.0571	2.0514	2.0840		-1.3%		2.0840		-1.3%		2.0468	2.0840	0.5%	-1.3%
2.0000	1.9763	1.9935	2.0287	0.3%	-1.4%	1.9891	2.0332	0.5%	-1.7%	1.9935	2.0287	0.3%	-1.4%
1.9459	1.9636	1.9594		-0.7%		1.9552		-0.5%					
1.8947	1.8831	1.8792	1.9185	0.8%	-1.3%	1.8754	1.9145	1.0%	-1.0%	1.8792	1.9185	0.8%	-1.3%
1.8462	1.8305	1.8489	1.8792	-0.1%	-1.8%	1.8452		0.1%		1.8452		0.1%	
1.8000	1.8160	1.7947		0.3%		1.7947	1.8160	0.3%	-0.9%	1.7947	1.8160	0.3%	-0.9%
1.7561	1.7536	1.7536		0.1%		1.7536	1.7739	0.1%	-1.0%	1.7569	1.7739	0.0%	-1.0%
1.7143	1.7016	1.7079		0.4%		1.7111	1.7337	0.2%	-1.1%	1.7111	1.7370	0.2%	-1.3%
1.6744	1.6646	1.6676	1.6829	0.4%	-0.5%	1.6706	1.6860	0.2%	-0.7%	1.6706	1.6860	0.2%	-0.7%
1.6364	1.6351	1.6349	1.6496	0.1%	-0.8%	1.6205	1.6526	1.0%	-1.0%	1.6320	1.6496	0.3%	-0.8%
1.6000	1.5869	1.5979	1.6176	0.1%	-1.1%	1.5951		0.3%		1.6063		-0.4%	
1.5652	1.5573	1.5573		0.5%		1.5706		-0.3%		1.5841		-1.2%	
1.5319	1.5416	1.5313		0.0%		1.5287	1.5442	0.2%	-0.8%	1.5287	1.5442	0.2%	-0.8%
1.5000	1.5062	1.4964		0.2%		1.4964	1.5161	0.2%	-1.1%	1.4964	1.5136	0.2%	-0.9%
1.4694	1.4676	1.4771		-0.5%		1.4630	1.4771	0.4%	-0.5%	1.4630	1.4771	0.4%	-0.5%
1.4400	1.4468	1.4468		-0.5%		1.4491		-0.6%		1.4378	1.4514	0.2%	-0.8%
1.4118	1.4091	1.4091	1.4244	0.2%	-0.9%	1.4091	1.4244	0.2%	-0.9%	1.4091	1.4244	0.2%	-0.9%
1.3846	1.3941	1.3733	1.4005	0.8%	-1.1%	1.3794	1.3899	0.4%	-0.4%	1.3794	1.3920	0.4%	-0.5%
1.3585	1.3590	1.3471		0.8%		1.3550		0.3%		1.3550	1.3692	0.3%	-0.8%
1.3333	1.3412	1.3314		0.1%		1.3295	1.3451	0.3%	-0.9%	1.3276	1.3451	0.4%	-0.9%
1.3091	1.2939	1.3049		0.3%		1.3143		-0.4%		1.3143		-0.4%	
1.2857	1.2741	1.2939	1.2759	-0.6%	0.8%	1.2813	1.2957	0.3%	-0.8%	1.2831	1.2939	0.2%	-0.6%
1.2632	1.2636	1.2619		0.1%		1.2636		0.0%		1.2584	1.2724	0.4%	-0.7%
1.2414	1.2381	1.2397		0.1%						1.2364	1.2465	0.4%	-0.4%
1.2203	1.2103	1.2087		0.9%						1.2183	1.2265	0.2%	-0.5%
1.2000	1.2008	1.1961		0.3%		1.1977	1.2071	0.2%	-0.6%	1.1977	1.2087	0.2%	-0.7%
1.1803	1.1762	1.1838	1.1762	-0.3%	0.3%	1.1807		0.0%			1.1747		0.5%
1.1613	1.1628	1.1584	1.1672	0.2%	-0.5%	1.1569		0.4%		1.1511		0.9%	
1.1429	1.1425	1.1397	1.1511	0.3%	-0.7%	1.1369		0.5%		1.1397		0.3%	
1.1250	1.1299									1.1216	1.1285	0.3%	-0.3%
1.1077	1.1107	1.0884		1.7%		1.1054		0.2%		1.1054	1.1134	0.2%	-0.5%
1.0909	1.0909	1.0988		-0.7%		1.0884		0.2%		1.0871	1.0975	0.4%	-0.6%
1.0746	1.0693	1.0884		-1.3%		1.0794		-0.4%		1.0718		0.3%	
1.0588	1.0546					1.0656		-0.6%		1.0570	1.0632	0.2%	-0.4%
1.0435	1.0438	1.0403		0.3%		1.0403		0.3%		1.0414		0.2%	
1.0286	1.0321	1.0309	1.0240	-0.2%	0.4%	1.0309	1.0252	-0.2%	0.3%	1.0321		-0.3%	
1.0141	1.0195	1.0127		0.1%		1.0127		0.1%		1.0127		0.1%	
1.0000	0.9984	0.9984	1.0061	0.2%	-0.6%	0.9984		0.2%		0.9973		0.3%	
	≤ 1‰			12	0			10	0			7	0
	1‰ - 1%			43	10			49	16			53	23
	≥ 1%			15	27			9	26			10	32
	67%-99%			**70**	**37**			**68**	**42**			**70**	**55**

Table 4. Post-quiescent EBR between 1-7 January 2020, recovered as alongside a mapping profile that nearly traced a tectonic boundary, Figure 2: stations MMX1 (Mexico City) – ZLA1 (Los Angeles) – ZOA2 (San Francisco Bay). The ZLA1 data are from Table 3. The undertone component periods are listed next to the respective EBR component series for comparison and to get a more natural and complete look at the long-periodic parts of Earth resonances. Δ-values are differences amongst EBR from cGPS and earthquakes (Omerbashich, 2020a). The longest (i.e., strong-seismicity causing) EBR waves of (about five hours or longer) with Δ-values of 1‰ or less (red-framed and green-highlighted) are the most relevant ones for earthquake prediction. Note also that the relationship $|\Delta| < |\Delta'|$ holds generally, as best seen above, as ${}^{ZLA1}|\Delta z| < {}^{ZLA1}|\Delta' z|$; see Figure 9 for a graphical representation. The color scheme (a concept borrowed from genetics) highlights the magnitude-of-order separation in recovering EBR; the scheme is a more natural quantifier of the success of resonance recovery in the longer v. shorter (weaker) parts.

EBR profiles are necessary for mapping the EBR from weeklong and daylong cGPS data sets; see Table 4 & Figures 7-9. Of the three profile stations, ZLA1 has performed the best, as seen in the total recovery of (all 72) EBR periods at the 99% confidence level throughout. The high quality of the ZLA1 data also follows from the complete recovery of the undertone series, which is seen as equiperiodically and negatively offset from the EBR series. The resonance periods recovered at 67%-99% confidence levels are shaded (gray). Possible factors that can affect the performance lie in crust thickness, sea bottom processes, and others. This kind of mapping profiling is an element for creating composite dynamical EBR maps connecting long (strong-seismicity generating) periods between adjacent cGPS stations for hourly-to-daily early warning systems. Then shorter EBR periods would serve as a means for checking data quality and verifying recovered EBR.

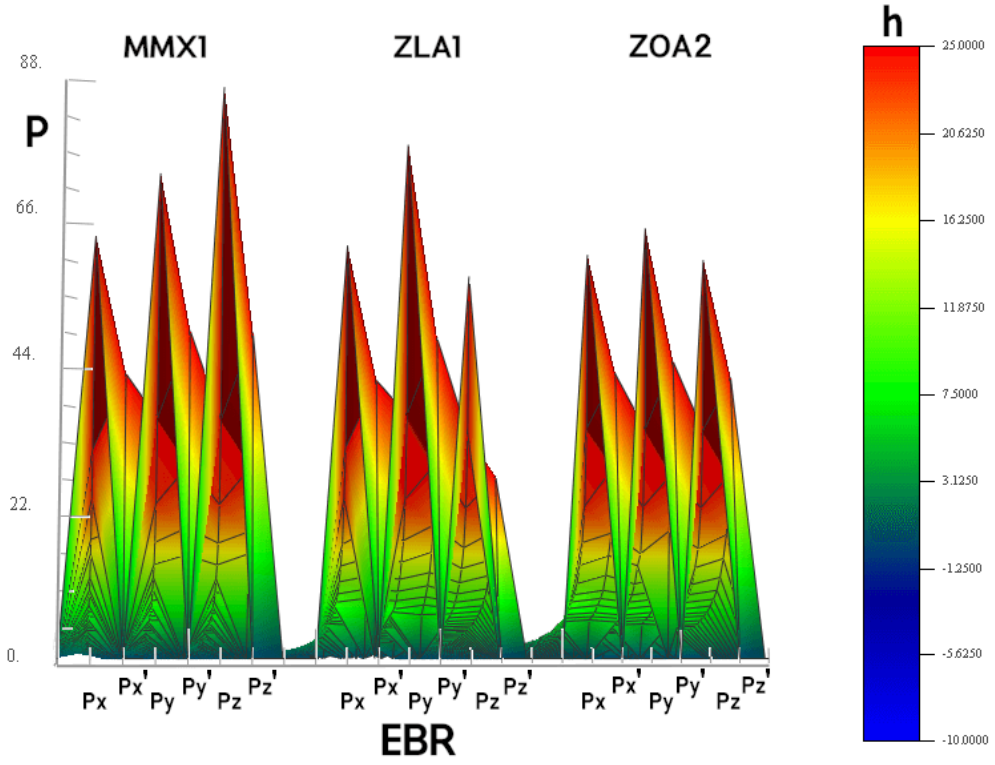

Figure 7. Longest-periodic part (collapsed view) of EBR as recovered alongside the profile, Figure 2. As in Table 4, component-periods of respective undertone series P' appended to component-periods of the corresponding station's EBR for a more natural and complete feel of resonances that affect Earth crust in the seismically most critical parts of EBR spectra.

As seen from Figure 7, noticeable are regular formational features of EBR components in the resonance fingerprint's longest-periodic (strong-seismicity causing) part at each respective station, as well as overall (profile-wise). As seen on Figure 8, while the formation was overall best preserved (least damaged) at the ZLA1 (Los Angeles), the fingerprint that was most responsive in terms of recovery of the longest (strong-seismicity causing) waves was that of the ZOA2 station (San Francisco). Figure 9 depicts the matchings of recovered v. theoretical EBR.

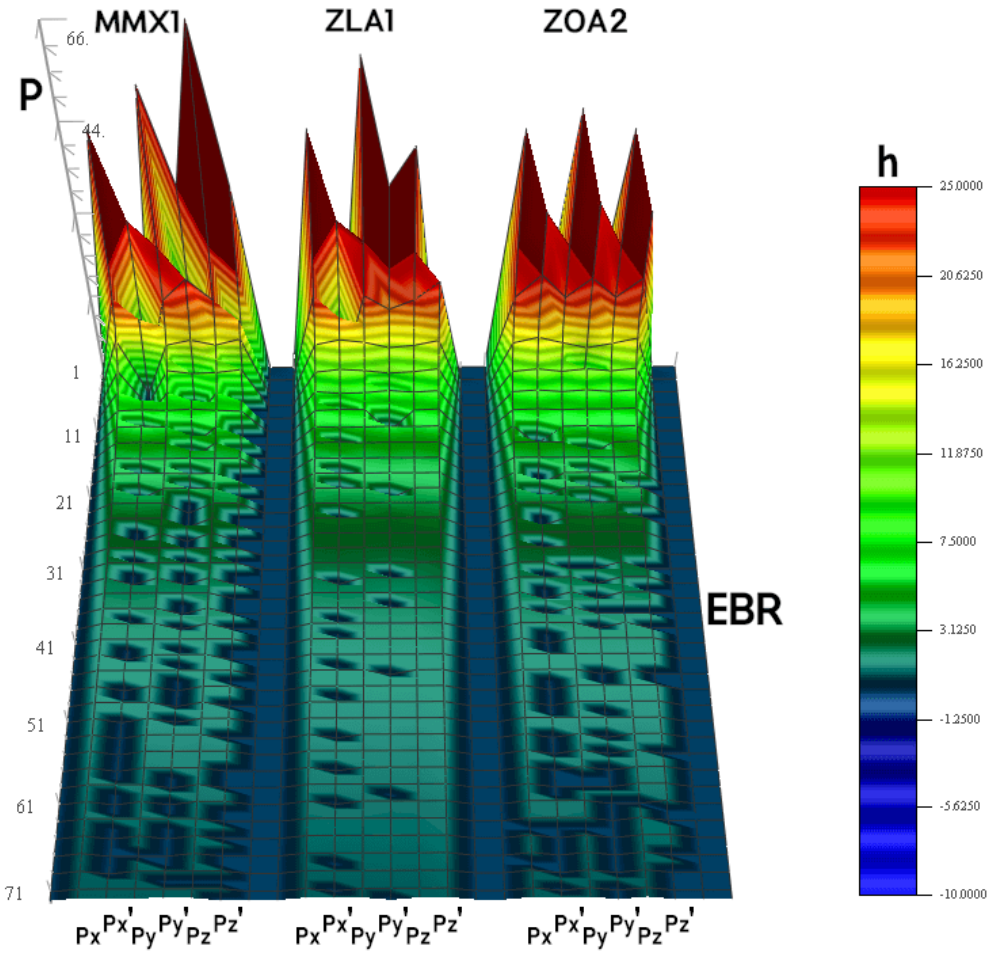

Figure 8. EBR fingerprints from weeklong cGPS recordings from each cGPS station alongside the profile, Figure 2. The valleys represent the respective fingerprint's malformation in terms of damages or destruction of a specific EBR wave, as projected onto a particular cGPS position component. As in Table 4 and Figure 7, for a more natural and complete feel of Earth resonances recovered per station, component periods of respective undertone series P' and the corresponding station's EBR are shown adjoined, exposing the companion as predominantly undertone rather than overtone, i.e., composed of mostly longer waves than their corresponding (nearest) EBR waves.

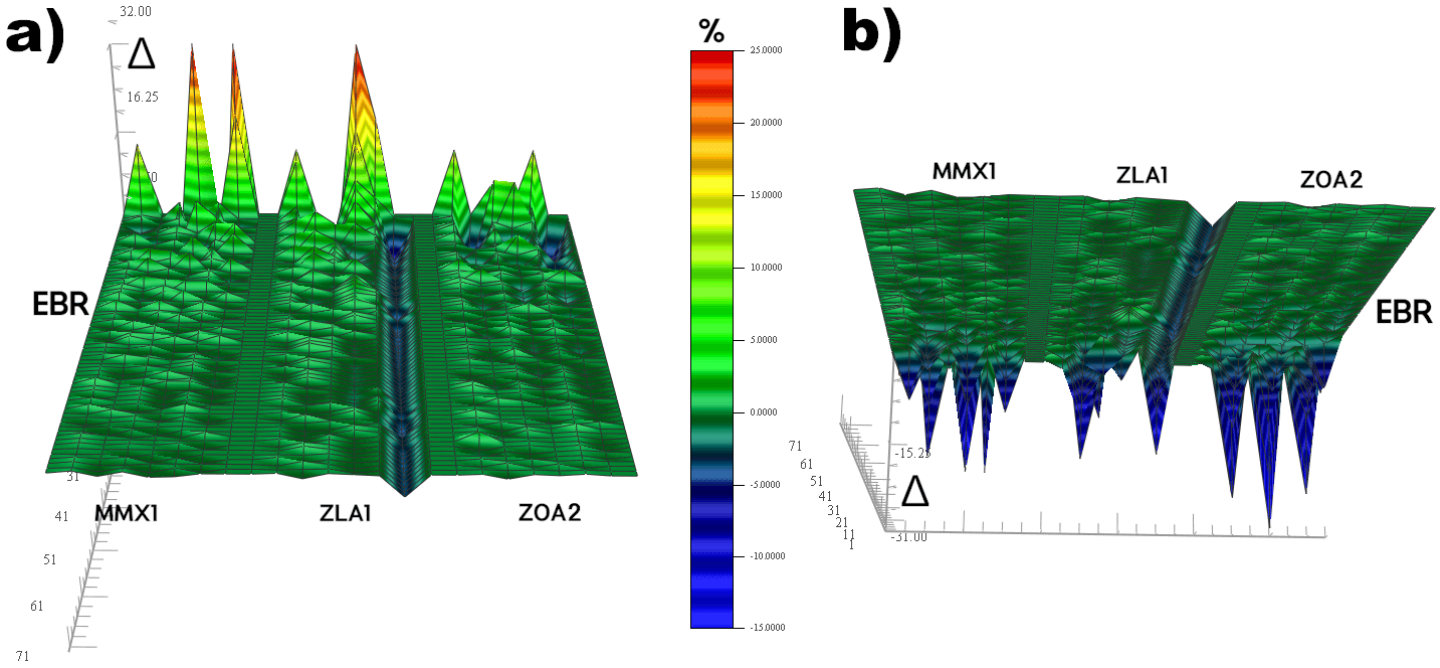

Figure 9. a) The positive-Δ surface of EBR recovery alongside the mapping profile, Figure 2, from weeklong recordings at a quiescent time; b) same negative-Δ-surface (shorter periods towards the viewer). While the ZLA1 (Los Angeles) data were of the highest resolution, enabling total recovery of both EBR and undertone series, the ZOA2 (San Francisco) data performed best in terms of the longest (strong-earthquakes causing) EBR detection. Note that the visually most remarkable feature ${}^{ZLA1}|\Delta_z| < {}^{ZLA1}|\Delta'_z|$, seen on the left panel (a.) above as the dominant blue strait, holds as a rule, i.e., as a general relationship $|\Delta| < |\Delta'|$.

EBR		EBR waves as felt at cGPS station ZLA1 (Los Angeles) around Ridgecrest eartquake of 4 Jul 2019																							
		ZLA1 - pre						27/06 - 03/07						ZLA1 - post						04/07 - 10/07					
Ptheor	PEQE	Px	Px'	Δx	Δx'	Py	Py'	Δy	Δy'	Pz	Pz'	Δz	Δz'	Px	Px'	Δx	Δx'	Py	Py'	Δy	Δy'	Pz	Pz'	Δz	Δz'
72.0000	75.0591		49.4919		31.3%					59.0401	96.1324	18.0%	-33.5%	96.1324		-33.5%						96.1324		-33.5%	
36.0000	33.3241	33.3241		7.4%		46.9604		-30.4%		33.3241	44.6753	7.4%	-24.1%	59.0401		-64.0%		32.1569		10.7%		30.0517		16.5%	
24.0000	23.2132	24.4496		-1.9%		23.8154		0.8%		23.8154		0.8%		25.8251		-7.6%		25.8251	21.5766	-7.6%	10.1%	24.4496		-1.9%	
18.0000	17.9995	18.9101		-5.1%		19.3077		-7.3%		18.9101		-5.1%		21.5766		-19.9%		19.3077		-7.3%		21.5766		-19.9%	
14.4000	14.4466	13.7954	15.6803	4.2%	-8.9%	13.7954	15.9528	4.2%	-10.8%	13.7954	15.9528	4.2%	-10.8%	13.2004		8.3%						13.0132		9.6%	
12.0000	12.6545	11.8386		1.3%		11.9933		0.1%		11.9933		0.1%		11.9933		0.1%		12.1520		-1.3%		11.8386		1.3%	
10.2857	10.0282	9.4114		8.5%		10.6076		-3.1%		10.4864		-2.0%		10.4864		-2.0%		11.2579		-9.5%					
9.0000	8.8661	8.7813		2.4%		8.6981	9.5089	3.4%	-5.7%	8.7813	9.5089	2.4%	-5.7%	8.8661	9.3159	1.5%	-3.5%	8.6165		4.3%					
8.0000	7.8772	7.8772		1.5%		8.0147		-0.2%		8.0147		-0.2%		7.8772	8.3805	1.5%	-4.8%	8.1571	7.6795	-2.0%	4.0%	8.2303		-2.9%	
7.2000	7.1419	7.3125		-1.6%		7.3712		-2.4%		7.3712		-2.4%		7.4309		-3.2%		7.3125		-1.6%		7.7443		-7.6%	
6.5455	6.5321	6.3513	6.8234	3.0%	-4.2%	6.4405	6.8234	1.6%	-4.2%	6.4405	6.8234	1.6%	-4.2%	6.3077		3.6%		6.2222		4.9%		6.2222		4.9%	
6.0000	6.0183	6.0183	5.8645	-0.3%	2.3%	6.0183		-0.3%		6.0183		-0.3%		6.0580		-1.0%		5.9791		0.3%		5.9791		0.3%	
5.5385	5.6132	5.2900		4.5%		5.6135		-1.4%		5.6135		-1.4%		5.7542		-3.9%		5.7184		-3.2%		5.7542		-3.9%	
5.1429	5.1709	5.08494		1.1%		5.0569	5.3207	1.7%	-3.5%	5.0292	5.3207	2.2%	-3.5%	5.1133		0.6%		5.0849		1.1%					
4.8000	4.7434	4.7680		0.7%		4.7680		0.7%		4.7434		1.2%		4.7680	4.9479	0.7%	-3.1%	4.8952		-2.0%		4.8692	4.6710	-1.4%	2.7%
4.5000	4.6008	4.3604		3.1%		4.5551		-1.2%		4.3604		3.1%		4.5551		-1.2%		4.7190		-4.9%		4.5326		-0.7%	
4.2353	4.2008	4.2008		0.8%		4.1627	4.3604	1.7%	-3.0%	4.1627		1.7%		4.2008		0.8%		4.1627		1.7%		4.1439		2.2%	
4.0000	3.9650	3.9822		0.4%		4.0170		-0.4%		3.9995		0.0%		3.9479	4.0704	1.3%	-1.8%	4.0347	3.9142	-0.9%	2.1%	4.0347		-0.9%	
3.7895	3.7696	3.8166	3.6938	-0.7%	2.5%	3.8325		-1.1%		3.8166		-0.7%		3.8325		-1.1%						3.9142		-3.3%	
3.6000	3.5236	3.5647		1.0%		3.5509	3.6790	1.4%	-2.2%	3.5509	3.6790	1.4%	-2.2%	3.5647		1.0%		3.5236		2.1%					
3.4286	3.4443	3.4443		-0.5%		3.4315		-0.1%		3.4187		0.3%		3.4573		-0.8%		3.4443		-0.5%		3.4443	3.3562	-0.5%	2.1%
3.2727	3.2842	3.2960	3.2152	-0.7%	1.8%	3.3078		-1.1%		3.2960		-0.7%		3.2725	3.3440	0.0%	-2.2%	3.3562		-2.6%					
3.1304	3.1275	3.1064		0.8%		3.0959	3.1928	1.1%	-2.0%	3.0959	3.1928	1.1%	-2.0%	3.0649		2.1%									
3.0000	2.9949	3.0047		-0.2%		2.9949		0.2%		2.9949		0.2%		3.0047		-0.2%		2.9949		0.2%		3.0047		-0.2%	
2.8800	2.8821					2.9003		-0.7%		2.9003		-0.7%		2.9280		-1.7%		2.9280		-1.7%		2.9374		-2.0%	
2.7692	2.7691	2.8201		-1.8%		2.8115		-1.5%		2.7361	2.8201	1.2%	-1.8%	2.7038		2.4%		2.6959		2.6%		2.7038		2.4%	
2.6667	2.6569	2.6492		0.7%		2.6569		0.4%		2.6569		0.4%		2.6492		0.7%		2.6416		0.9%		2.6492		0.7%	
2.5714	2.5821					2.5894		-0.7%		2.5822		-0.4%		2.5968		-1.0%		2.5968		-1.0%		2.5968		-1.0%	
2.4828	2.4911	2.5115		-1.2%		2.4577	2.5184	1.0%	-1.4%	2.4577	2.5184	1.0%	-1.4%	2.4382		1.8%		2.4317		2.1%		2.4253		2.3%	
2.4000	2.4317	2.3874		0.5%		2.3874		0.5%		2.3937		0.3%		2.3874		0.5%		2.3874		0.5%		2.3874		0.5%	
2.3226	2.3269	2.3269		-0.2%		2.3328		-0.4%		2.3269		-0.2%													
2.2500	2.2580	2.2694	2.2254	-0.9%	1.1%	2.2254	2.2750	1.1%	-1.1%	2.2254	2.2807	1.1%	-1.4%												
2.1818	2.1524	2.1676		0.7%		2.1779		0.2%		2.1779		0.2%		2.2093		-1.3%		2.2040		-1.0%		2.1935		-0.5%	
2.1176	2.1274	2.1176		0.0%		2.1225		-0.2%		2.1274		-0.5%		2.1625		-2.1%		2.1574		-1.9%		2.1524		-1.6%	
2.0571	2.0514	2.0745		-0.8%		2.0422	2.0792	0.7%	-1.1%	2.0422	2.0840	0.7%	-1.3%												
2.0000	1.9763	1.9848		0.8%		1.9935		0.3%		1.9978		0.1%		2.0153		-0.8%		2.0153		-0.8%		2.0153		-0.8%	
1.9459	1.9636	1.9511		-0.3%		1.9511		-0.3%		1.9552		-0.5%		1.9806		-1.8%		1.9806		-1.8%		1.9763		-1.6%	
1.8947	1.8831	1.9105		-0.8%		1.8792	1.9145	0.8%	-1.0%	1.8792	1.9145	0.8%	-1.0%	1.8869		0.4%		1.8602		1.8%		1.8792		0.8%	
1.8462	1.8305	1.8378		0.5%		1.8415		0.3%		1.8415		0.3%		1.8342	1.8639	0.7%	-1.0%	1.8305		0.9%		1.8564	1.8305	-0.6%	0.9%
1.8000	1.8160	1.8018		-0.1%		1.8053		-0.3%		1.8053		-0.3%		1.8089		-0.5%		1.8089		-0.5%					
1.7561	1.7536	1.7705		-0.8%		1.7436	1.7705	0.7%	-0.8%	1.7403	1.7739	0.9%	-1.0%	1.7436		0.7%		1.7207		2.0%					
1.7143	1.7016	1.7111		0.2%		1.7079		0.4%		1.7079		0.4%		1.7272		-0.8%		1.6984		0.9%		1.7207		-0.4%	
1.6744	1.6646	1.6798		-0.3%		1.6798		-0.3%		1.6767		-0.1%		1.7016		-1.6%						1.6953		-1.2%	
1.6364	1.6351	1.6291	1.6496	0.4%	-0.8%	1.6262	1.6496	0.6%	-0.8%	1.6234	1.6496	0.8%	-0.8%	1.6205		1.0%									
1.6000	1.5869	1.6007		0.0%		1.5979		0.1%		1.5951		0.3%		1.6007		0.0%		1.6007		0.0%		1.6007		0.0%	
1.5652	1.5573	1.5706		-0.3%		1.5679		-0.2%		1.5679		-0.2%		1.5787		-0.9%		1.5814		-1.0%		1.5814		-1.0%	
1.5319	1.5416	1.5237	1.5468	0.5%	-1.0%	1.5442	1.5186	-0.8%	0.9%	1.5211	1.5442	0.7%	-0.8%	1.5494		-1.1%									
1.5000	1.5062	1.5037		-0.2%		1.4964		0.2%		1.4964		0.2%		1.5012		-0.1%		1.4964		0.2%		1.5012		-0.1%	
1.4694	1.4676	1.4771		-0.5%		1.4724		-0.2%		1.4724		-0.2%		1.4795		-0.7%		1.4795		-0.7%					
1.4400	1.4468	1.4583		-1.3%		1.4288	1.4514	0.8%	-0.8%	1.4310	1.4514	0.6%	-0.8%	1.4537		-1.0%									
1.4118	1.4091	1.4222		-0.7%		1.4091		0.2%		1.4091		0.2%		1.4156		-0.3%		1.4134		-0.1%		1.4069		0.3%	
1.3846	1.3941	1.3962		-0.8%		1.3857		-0.1%		1.3878		-0.2%		1.3878	1.3984	-0.2%	-1.0%								
1.3585	1.3590	1.3550		0.3%		1.3671	1.3490	-0.6%	0.7%	1.3490	1.3692	0.7%	-0.8%	1.3471		0.8%									
1.3333	1.3412	1.3295	1.3451	0.3%	-0.9%	1.3295		0.3%		1.3295		0.3%		1.3334		0.0%		1.3334		0.0%		1.3314		0.1%	
1.3091	1.2939	1.3068		0.2%		1.3087		0.0%		1.3105		-0.1%		1.3180		-0.7%									
1.2857	1.2741	1.2903		-0.4%		1.2921	1.2777	-0.5%	0.6%	1.2777	1.2939	0.6%	-0.6%												
1.2632	1.2636	1.2584		0.4%		1.2584		0.4%		1.2602		0.2%		1.2567		0.5%		1.2602		0.2%		1.2654		-0.2%	
1.2414	1.2381	1.2397		0.1%		1.2414		0.0%		1.2431		-0.1%						1.2533		-1.0%		1.2550		-1.1%	
1.2203	1.2103	1.2232		-0.2%		1.2265	1.2135	-0.5%	0.6%	1.2135	1.2281	0.6%	-0.6%	1.2056		1.2%		1.2056		1.2%					
1.2000	1.2008	1.1946		0.5%		1.1961		0.3%		1.1977		0.2%		1.1946		0.5%		1.1946		0.5%		1.1977		0.2%	
1.1803	1.1762	1.1777		0.2%		1.1807		0.0%		1.1823		-0.2%		1.1853		-0.4%									
1.1613	1.1628	1.1658		-0.4%		1.1555	1.1672	0.5%	-0.5%	1.1540	1.1687	0.6%	-0.6%												
1.1429	1.1425	1.1397		0.3%		1.1411		0.2%		1.1397		0.3%		1.1411		0.2%		1.1411		0.2%		1.1468		-0.3%	
1.1250	1.1299	1.1243		0.1%		1.1257		-0.1%		1.1257		-0.1%		1.1313		-0.6%						1.1383		-1.2%	
1.1077	1.1107	1.1121		-0.4%		1.1134	1.1014	-0.5%	0.6%	1.1134	1.1014	-0.5%	0.6%	1.0794		2.6%									
1.0909	1.0909	1.0884		0.2%		1.0884		0.2%		1.0871		0.4%		1.0884		0.2%		1.0871		0.4%		1.0935		-0.2%	
1.0746	1.0693	1.0744		0.0%		1.0756		-0.1%		1.0756		-0.1%		1.0794		-0.4%						1.0845		-0.9%	
1.0588	1.0546	1.0632		-0.4%		1.0644	1.0522	-0.5%	0.6%	1.0644	1.0522	-0.5%	0.6%	1.0522		0.6%									
1.0435	1.0438	1.0438		0.0%		1.0414		0.2%		1.0403		0.3%		1.0450		-0.1%		1.0438		0.0%		1.0438		0.0%	
1.0286	1.0321	1.0298		-0.1%		1.0298		-0.1%		1.0286		0.0%		1.0286	1.0356	0.0%	-0.7%	1.0356		-0.7%		1.0356		-0.7%	
1.0141	1.0195	1.0183		-0.4%		1.0183	1.0083	-0.4%	0.6%	1.0183	1.0083	-0.4%	0.6%					1.0039		1.0%					
1.0000	0.9984	0.9995		0.1%		0.9973		0.3%		0.9973		0.3%		1.0006		-0.1%		0.9962		0.4%		1.0028		-0.3%	
	≤ 1‰		∑	9	0			10	0			9	0			7	0			4	0			4	0
	1‰ - 1%		∑	44	3			44	9			46	12			33	3			23	0			22	0
	≥ 1%		∑	16	7			17	13			17	12			25	5			24	3			21	3
	67%-99%		∑∑	**69**	**10**			**71**	**22**			**72**	**24**			**65**	**8**			**51**	**3**			**47**	**3**

Table 5. Seismic preparation phase (left section) v. seismic destruction (the section on the right) of EBR. The matching was against theoretical EBR.

To verify the here reported EBR detection, I look at the EBR as recorded at ZLA1 during the week preceding the 2019 Ridgecrest, CA, earthquake sequence (Cheng and Ben-Zion, 2020) just north of the station (Harvard Catalog No. 201907041733B) and the week following, Table 5 and Figures 10 & 11. In terms of M6+ strong seismicity, the sequence consisted of an M_w6.4 and an M_w7.1 that had occurred on 03 and 04 July 2019, respectively, exposing a previously unknown seismic fault (or in the mechanical engineering sense: cracking open the shielding of a poorly embedded vibrating engine; see Omerbashich, 2020a). In addition to its apparent mechanical-resonating underlying nature, this event is particularly suitable due to its proximity to ZLA1 and because the 27 June–03 July 2019 was a seismically quiescent week in the sense of M6+ locally and M6.5+ globally. These advantages allow a clear distinction of the earthquake preparation phase v. post-quake destruction phase. Thus an interplay of these exact matches has resonantly affected the Ridgecrest area, causing the initial rupture and probably triggering the release of accumulated stress — resulting in the Ridgecrest sequence instead of just a single earthquake.

The event has then temporarily shut down the ability of the cGPS to recover any undertone series, which made the EBR undertone series vanish virtually entirely compared to the preparation phase, Figure 10. This local event had destroyed about half of the 1%-matched EBR waves (highlighted orange; the green-highlighted 1‰ matches excluded). That the shutdown is temporary is seen from comparison against the post-quiescent EBR obtained at three different stations, Tables 4 & 7.

The exact and regular matching of the longest EBR waves to their theoretical counterparts has revealed some of the characteristic resonant vibration frequencies that cause ~M6+ strong seismicity in the Los Angeles area. Finally, of use for EBR mapping is that virtually all EBR waves aligned with the x-component during the destruction phase, revealing the EBR general orientation at the time of this event, Figure 10. Destruction of EBR waves resulted in a post-event gapped component recovery (right) v. complete component recovery before the event (left). The EBR completeness in all three projections revealed that the preparation phase had commenced. The consistent lagging has revealed composition of EBR wave-trains: a regular formation in the N-E general direction. The longest absolutely-matched EBR waves with their destructive angular deflections then converged resonantly on Ridgecrest, Figure 11.

As seen in Figure 10, seismic waves from the Ridgecrest event had virtually entirely overridden the undertone resonance while severely damaging (the long-periodic) or destroying (the short-periodic) y- and z-component EBR waves. With a common and obvious orientation in the N-S direction (as they are absent from the x component), this reveals that the EBR and companion trains had rolled into California as a *yz* front in a cardinally-northing aligned turbulent (twister) formation. Therefore, the formation post-event is preserved only as a faint signature in the seismically damaged (the longer-wave) and destroyed (the shorter-wave) parts of component trains also. The two resonances then left Ridgecrest and kept rolling N-S back and forth alongside the tectonic plate boundary until its ringing dampened down months later, but not before they caused several more strong events along the way. The matchings amongst cGPS EBR's and seismic EBR's periods (from strong earthquakes; see Omerbashich, 2020a), Figure 12 & Table 6, also show the same as the matchings against theoretical EBR's periods, albeit with waves somewhat impeded by natural Earth processes as those necessarily reflect in a seismic EBR.

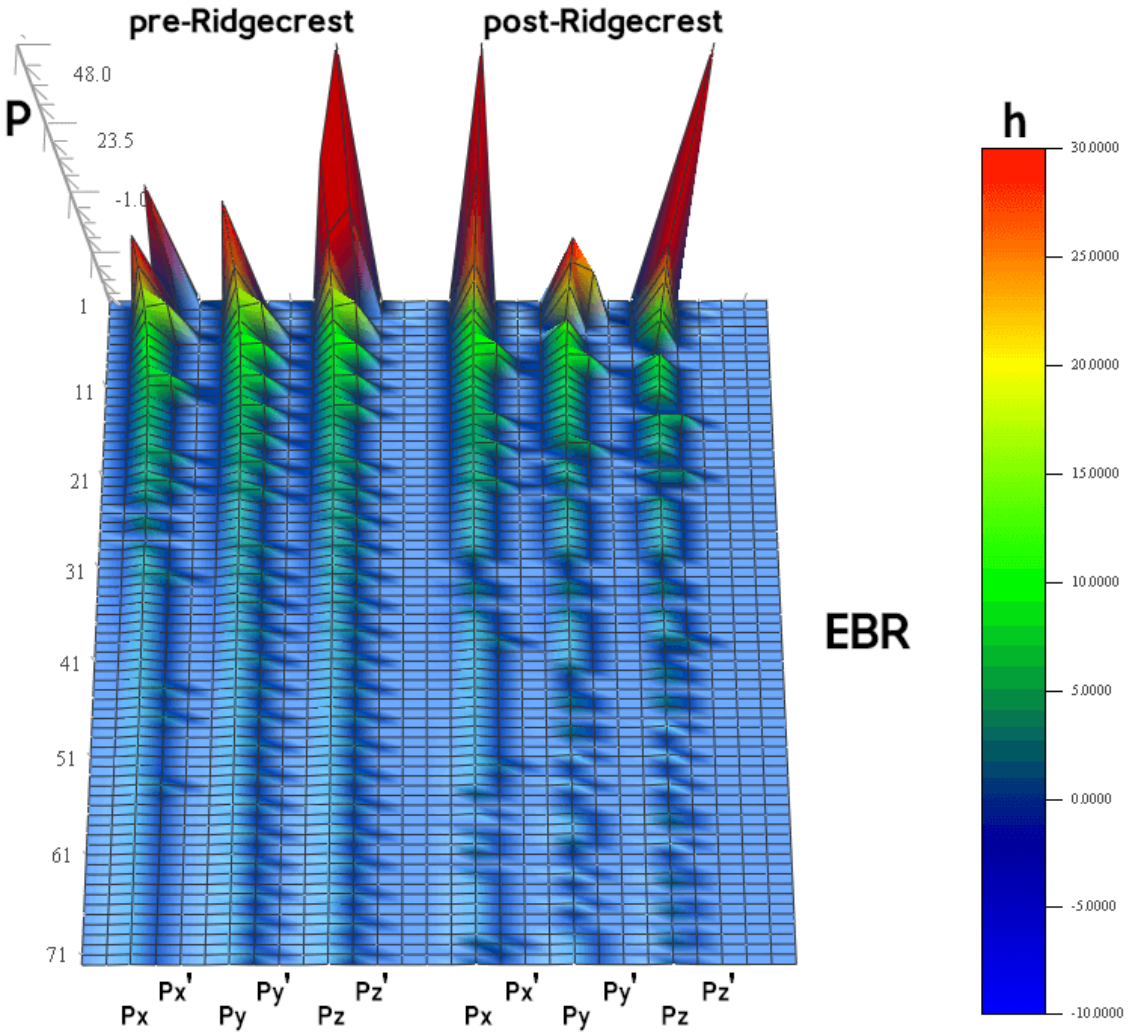

Figure 10. Seismic preparation (on the left) v. seismic destruction (on the right) phases of EBR, Table 5, recorded at the ZLA1 (Los Angeles) station from weeklong cGPS data preceding (left) the Ridgecrest, CA, earthquake series just north of the station, and the weeklong data following (right) the event, respectively. The P' mark component recovery of the accompanying undertone series, Table 5. The matchings are against theoretical EBR.

During the preparation phase (as strong earthquakes initiate), the EBR accuracy mostly stays constant and relatively small across the entire trains and from projection to projection, Figure 11. Seismic waves from the Ridgecrest event have temporarily overridden most of the train (waves) and disturbed the recovery projection-wise. Errors in the matchings of cGPS EBR periods against theoretical EBR periods for all projections became larger in both amplitude and frequency, while the matching in both y- and z-projections has lost uniformity that tells of EBR orientation, Figure 11 (callout).

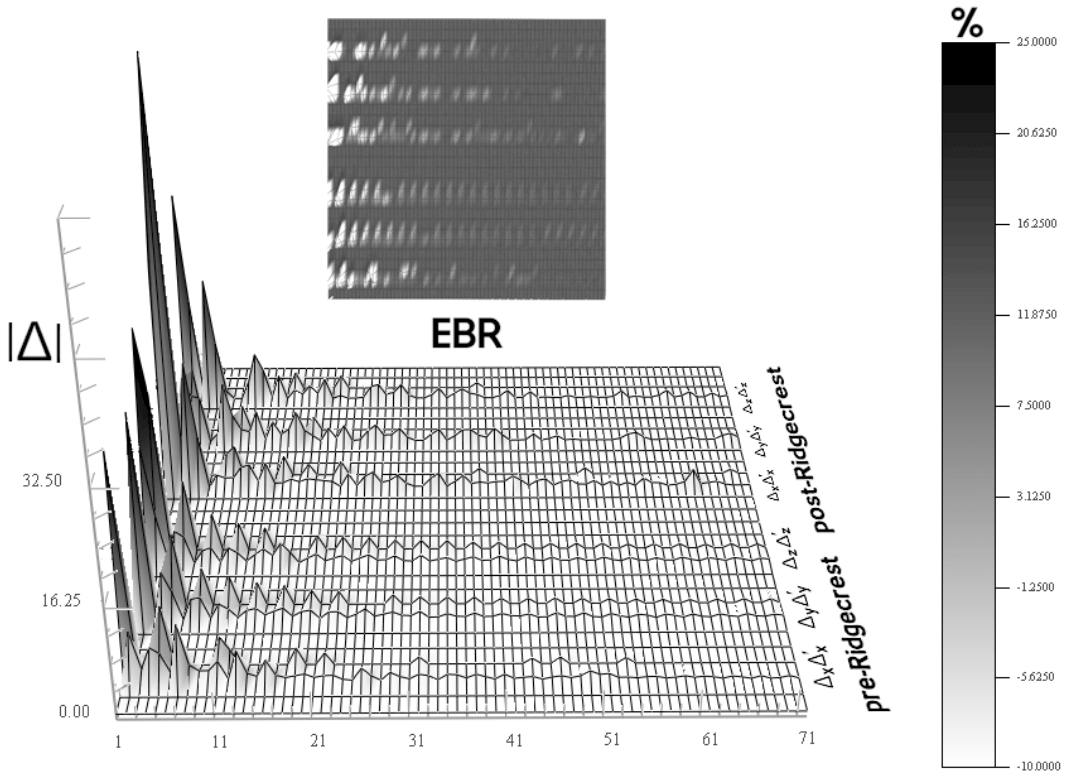

Figure 11. Δ-wireframe of the seismic preparation v. destruction phases at ZLA1, Table 5 & Figure 10. Resonance pairs (EBR waves with their companion undertone waves) here represented as connected train codas, plotted per position component, and then stacked separately for pre-Ridgecrest and post-Ridgecrest phases. Callout: same, but in blind surface representation for easier comparison with Figure 10. Views rotated for better distinction from Figure 10.

EBR		EBR waves as felt at cGPS station ZLA1 (Los Angeles) around Ridgecrest eartquake of 4 Jul 2019																							
		ZLA1 - pre						27/06 - 03/07						ZLA1 - post						04/07 - 10/07					
Ptheor	PEQE	Px	Px'	Δx	Δx'	Py	Py'	Δy	Δy'	Pz	Pz'	Δz	Δz'	Px	Px'	Δx	Δx'	Py	Py'	Δy	Δy'	Pz	Pz'	Δz	Δz'
72.0000	75.0591		49.4919		34.1%					59.0401	96.1324	21.3%	-28.1%	96.1324		-28.1%						96.1324		-28.1%	
36.0000	33.3241	33.3241		0.0%		46.9604		-40.9%		33.3241	44.6753	0.0%	-34.1%	59.0401		-77.2%		32.1569		3.5%		30.0517		9.8%	
24.0000	23.2132	24.4496		-5.3%		23.8154		-2.6%		23.8154		-2.6%		25.8251		-11.3%		21.5766	25.8251	7.1%	-11.3%	24.4496		-5.3%	
18.0000	17.9995	18.9101		-5.1%		19.3077		-7.3%		18.9101		-5.1%		21.5766		-19.9%		19.3077		-7.3%		21.5766		-19.9%	
14.4000	14.4466	13.7954	15.6803	4.5%	-8.5%	13.7954	15.9528	4.5%	-10.4%	13.7954	15.9528	4.5%	-10.4%	13.2004		8.6%						13.0132		9.9%	
12.0000	12.6545	11.8386		6.4%		11.9933		5.2%		11.9933		5.2%		11.9933		5.2%		12.1520		4.0%		11.8386		6.4%	
10.2857	10.0282	9.4114		6.2%		9.5089	10.6076	5.2%	-5.8%	10.4864	9.5089	-4.6%	5.2%	10.4864		-4.6%		11.2579		-12.3%					
9.0000	8.8661	8.7813		1.0%		8.6981		1.9%		8.7813		1.0%		8.8661	9.3159	0.0%	-5.1%	8.6165		2.8%					
8.0000	7.8772	7.8772		0.0%		8.0147		-1.7%		8.0147		-1.7%		7.8772	8.3805	0.0%	-6.4%	7.6795	8.1571	2.5%	-3.6%	8.2303		-4.5%	
7.2000	7.1419	7.3125		-2.4%		7.3712		-3.2%		7.3712		-3.2%		7.4309		-4.0%		7.3125		-2.4%		7.7443		-8.4%	
6.5455	6.5321	6.3513	6.8234	2.8%	-4.5%	6.4405	6.8234	1.4%	-4.5%	6.4405	6.8234	1.4%	-4.5%	6.3077		3.4%		6.2222		4.7%		6.2222		4.7%	
6.0000	6.0183	6.0183		0.0%		6.0183		0.0%		6.0183		0.0%		6.0580		-0.7%		5.9791		0.7%		5.9791		0.7%	
5.5385	5.6132	5.8645		-4.5%		5.6135		0.0%		5.6135		0.0%		5.7542		-2.5%		5.7184		-1.9%		5.7542		-2.5%	
5.1429	5.1709	5.08494	5.2900	1.7%	-2.3%	5.0569	5.3207	2.2%	-2.9%	5.0292	5.3207	2.7%	-2.9%	5.1133		1.1%		5.0849		1.7%					
4.8000	4.7434	4.7680		-0.5%		4.7680		-0.5%		4.7434		0.0%		4.7680	4.9479	-0.5%	-4.3%	4.8952		-3.2%		4.8692		-2.7%	
4.5000	4.6008	4.3604		5.2%		4.5551		1.0%		4.3604		5.2%		4.5551		1.0%		4.7190		-2.6%		4.5326	4.6710	1.5%	-1.5%
4.2353	4.2008	4.2008		0.0%		4.1627	4.3604	0.9%	-3.8%	4.1627		0.9%		4.2008		0.0%		4.1627		0.9%		4.1439		1.4%	
4.0000	3.9650	3.9822		-0.4%		4.0170		-1.3%		3.9995		-0.9%		3.9479	4.0704	0.4%	-2.7%	3.9142	4.0347	1.3%	-1.8%	4.0347		-1.8%	
3.7895	3.7696	3.8166	3.6938	-1.2%	2.0%	3.8325	3.6790	-1.7%	2.4%	3.8166	3.6790	-1.2%	2.4%	3.8325		-1.7%						3.9142		-3.8%	
3.6000	3.5236	3.5647		-1.2%		3.5509		-0.8%		3.5509		-0.8%		3.5647		-1.2%		3.5236		0.0%					
3.4286	3.4443	3.4443	3.5647	0.0%	-3.5%	3.4315		0.4%		3.4187		0.7%		3.4573		-0.4%		3.4443		0.0%		3.4443		0.0%	
3.2727	3.2842	3.2960	3.2152	-0.4%	2.1%	3.3078		-0.7%		3.2960		-0.4%		3.2725	3.3440	0.4%	-1.8%	3.3562		-2.2%			3.3562		-2.2%
3.1304	3.1275	3.1064		0.7%		3.0959	3.1928	1.0%	-2.1%	3.0959	3.1928	1.0%	-2.1%	3.0649		2.0%									
3.0000	2.9949	3.0047		-0.3%		2.9949		0.0%		2.9949		0.0%		3.0047		-0.3%		2.9949		0.0%		3.0047		-0.3%	
2.8800	2.8821					2.9003		-0.6%		2.9003		-0.6%		2.9280		-1.6%		2.9280		-1.6%		2.9374		-1.9%	
2.7692	2.7691	2.8201		-1.8%		2.8115		-1.5%		2.7361	2.8201	1.2%	-1.8%	2.7038		2.4%		2.6959		2.6%		2.7038		2.4%	
2.6667	2.6569	2.6492		0.3%		2.6569		0.0%		2.6569		0.0%		2.6492		0.3%		2.6416		0.6%		2.6492		0.3%	
2.5714	2.5821					2.5894		-0.3%		2.5822		0.0%		2.5968		-0.6%		2.5968		-0.6%		2.5968		-0.6%	
2.4828	2.4911	2.5115		-0.8%		2.5184		-1.1%		2.5184		-1.1%		2.4382		2.1%		2.4317		2.4%		2.4253		2.6%	
2.4000	2.4317	2.3874		1.8%		2.4577	2.3874	-1.1%	1.8%	2.4577	2.3937	-1.1%	1.6%	2.3874		1.8%		2.3874		1.8%		2.3874		1.8%	
2.3226	2.3269	2.3269		0.0%		2.3328		-0.3%		2.3269		0.0%													
2.2500	2.2580	2.2694	2.2254	-0.5%	1.4%	2.2750	2.2254	-0.8%	1.4%	2.2807	2.2254	-1.0%	1.4%												
2.1818	2.1524	2.1676		-0.7%		2.1779		-1.2%		2.1779		-1.2%		2.2093		-2.6%		2.2040		-2.4%		2.1935		-1.9%	
2.1176	2.1274	2.1176		0.5%		2.1225		0.2%		2.1274		0.0%		2.1625		-1.6%		2.1574		-1.4%		2.1524		-1.2%	
2.0571	2.0514	2.0745		-1.1%		2.0422	2.0792	0.4%	-1.4%	2.0422	2.0840	0.4%	-1.6%												
2.0000	1.9763	1.9848		-0.4%		1.9935		-0.9%		1.9978		-1.1%		2.0153		-2.0%		2.0153		-2.0%		2.0153		-2.0%	
1.9459	1.9636	1.9511		0.6%		1.9511		0.6%		1.9552		0.4%		1.9806		-0.9%		1.9806		-0.9%		1.9763		-0.6%	
1.8947	1.8831	1.9105		-1.5%		1.8792	1.9145	0.2%	-1.7%	1.8792	1.9145	0.2%	-1.7%	1.8869	1.8639	-0.2%	1.0%	1.8602		1.2%		1.8792		0.2%	
1.8462	1.8305	1.8378		-0.4%		1.8415		-0.6%		1.8415		-0.6%		1.8342		-0.2%		1.8305		0.0%		1.8305	1.8564	0.0%	-1.4%
1.8000	1.8160	1.8018		0.8%		1.8053		0.6%		1.8053		0.6%		1.8089		0.4%		1.8089		0.4%					
1.7561	1.7536	1.7705		-1.0%		1.7436	1.7705	0.6%	-1.0%	1.7403	1.7739	0.8%	-1.2%	1.7436		0.6%		1.7207		1.9%					
1.7143	1.7016	1.7111		-0.6%		1.7079		-0.4%		1.7079		-0.4%		1.7272		-1.5%		1.6984		0.2%		1.7207		-1.1%	
1.6744	1.6646	1.6798		-0.9%		1.6798		-0.9%		1.6767		-0.7%		1.7016		-2.2%						1.6953		-1.8%	
1.6364	1.6351	1.6291	1.6496	0.4%	-0.9%	1.6262	1.6496	0.5%	-0.9%	1.6234	1.6496	0.7%	-0.9%	1.6205		0.9%									
1.6000	1.5869	1.6007		-0.9%		1.5979		-0.7%		1.5951		-0.5%		1.6007		-0.9%		1.6007		-0.9%		1.6007		-0.9%	
1.5652	1.5573	1.5706		-0.9%		1.5679		-0.7%		1.5679		-0.7%		1.5787		-1.4%		1.5814		-1.5%		1.5814		-1.5%	
1.5319	1.5416	1.5468		-0.3%		1.5442		-0.2%		1.5442		-0.2%		1.5494		-0.5%									
1.5000	1.5062	1.5037	1.5237	0.2%	-1.2%	1.4964	1.5186	0.7%	-0.8%	1.4964	1.5211	0.7%	-1.0%	1.5012		0.3%		1.4964		0.7%		1.5012		0.3%	
1.4694	1.4676	1.4771		-0.6%		1.4724		-0.3%		1.4724		-0.3%		1.4795		-0.8%		1.4795		-0.8%					
1.4400	1.4468	1.4583		-0.8%		1.4514	1.4288	-0.3%	1.2%	1.4514	1.4310	-0.3%	1.1%	1.4537		-0.5%									
1.4118	1.4091	1.4222		-0.9%		1.4091		0.0%		1.4091		0.0%		1.4156		-0.5%		1.4134		-0.3%		1.4069		0.2%	
1.3846	1.3941	1.3962		-0.2%		1.3857		0.6%		1.3878		0.5%		1.3984	1.3878	-0.3%	0.5%								
1.3585	1.3590	1.3550		0.3%		1.3671		-0.6%		1.3490	1.3692	0.7%	-0.7%	1.3471		0.9%									
1.3333	1.3412	1.3451	1.3295	-0.3%	0.9%	1.3490	1.3295	-0.6%	0.9%	1.3295		0.9%		1.3334		0.6%		1.3334		0.6%		1.3314		0.7%	
1.3091	1.2939	1.3068		-1.0%		1.2921	1.3087	0.1%	-1.1%	1.2939	1.3105	0.0%	-1.3%	1.3180		-1.9%									
1.2857	1.2741	1.2903		-1.3%		1.2777		-0.3%		1.2777		-0.3%													
1.2632	1.2636	1.2584		0.4%		1.2584		0.4%		1.2602		0.3%		1.2567		0.5%		1.2602		0.3%		1.2654		-0.1%	
1.2414	1.2381	1.2397		-0.1%		1.2414		-0.3%		1.2431	1.2281	-0.4%	0.8%					1.2533		-1.2%		1.2550		-1.4%	
1.2203	1.2103	1.2232		-1.1%		1.2135	1.2265	-0.3%	-1.3%	1.2135		-0.3%		1.2056		0.4%		1.2056		0.4%					
1.2000	1.2008	1.1946		0.5%		1.1961		0.4%		1.1977		0.3%		1.1946		0.5%		1.1946		0.5%		1.1977		0.3%	
1.1803	1.1762	1.1777		-0.1%		1.1807		-0.4%		1.1823		-0.5%		1.1853		-0.8%									
1.1613	1.1628	1.1658		-0.3%		1.1672	1.1555	-0.4%	0.6%	1.1687	1.1540	-0.5%	0.8%												
1.1429	1.1425	1.1397		0.2%		1.1411		0.1%		1.1397		0.2%		1.1411		0.1%		1.1411		0.1%		1.1468		-0.4%	
1.1250	1.1299	1.1243		0.5%		1.1257		0.4%		1.1257		0.4%		1.1313		-0.1%						1.1383		-0.7%	
1.1077	1.1107	1.1121		-0.1%		1.1134	1.1014	-0.2%	0.8%	1.1134	1.1014	-0.2%	0.8%	1.0794		2.8%									
1.0909	1.0909	1.0884		0.2%		1.0884		0.2%		1.0871		0.4%		1.0884		0.2%		1.0871		0.4%		1.0935		-0.2%	
1.0746	1.0693	1.0744		-0.5%		1.0756		-0.6%		1.0756		-0.6%		1.0794		-0.9%						1.0845		-1.4%	
1.0588	1.0546	1.0632		-0.8%		1.0522	1.0644	0.2%	-0.9%	1.0522	1.0644	0.2%	-0.9%	1.0522		0.2%									
1.0435	1.0438	1.0438		0.0%		1.0414		0.2%		1.0403		0.3%		1.0450		-0.1%		1.0438		0.0%		1.0438		0.0%	
1.0286	1.0321	1.0298		0.2%		1.0298		0.2%		1.0286		0.3%		1.0286	1.0356	0.3%	-0.3%	1.0356		-0.3%		1.0356		-0.3%	
1.0141	1.0195	1.0183		0.1%		1.0183		0.1%		1.0183		0.1%						1.0039		1.5%					
1.0000	0.9984	0.9995		-0.1%		0.9973	1.0083	0.1%	-1.0%	0.9973	1.0083	0.1%	-1.0%	1.0006		-0.2%		0.9962		0.2%		1.0028		-0.4%	
	≤ 1‰		∑	12	0			9	0			13	0			6	0			6	0			4	0
	1‰ - 1%		∑	39	2			45	8			42	6			33	3			18	0			16	0
	≥ 1%		∑	18	9			17	14			17	18			26	5			27	3			27	3
	67%-99%		∑∑	**69**	**11**			**71**	**22**			**72**	**24**			**65**	**8**			**51**	**3**			**47**	**3**

Table 6. The seismic preparation phase (on the left) v. the seismic destruction phase (on the right) of EBR. The matching here was against the seismic EBR, i.e., EBR obtained from time series of global occurrences of large earthquakes (Omerbashich, 2020a).

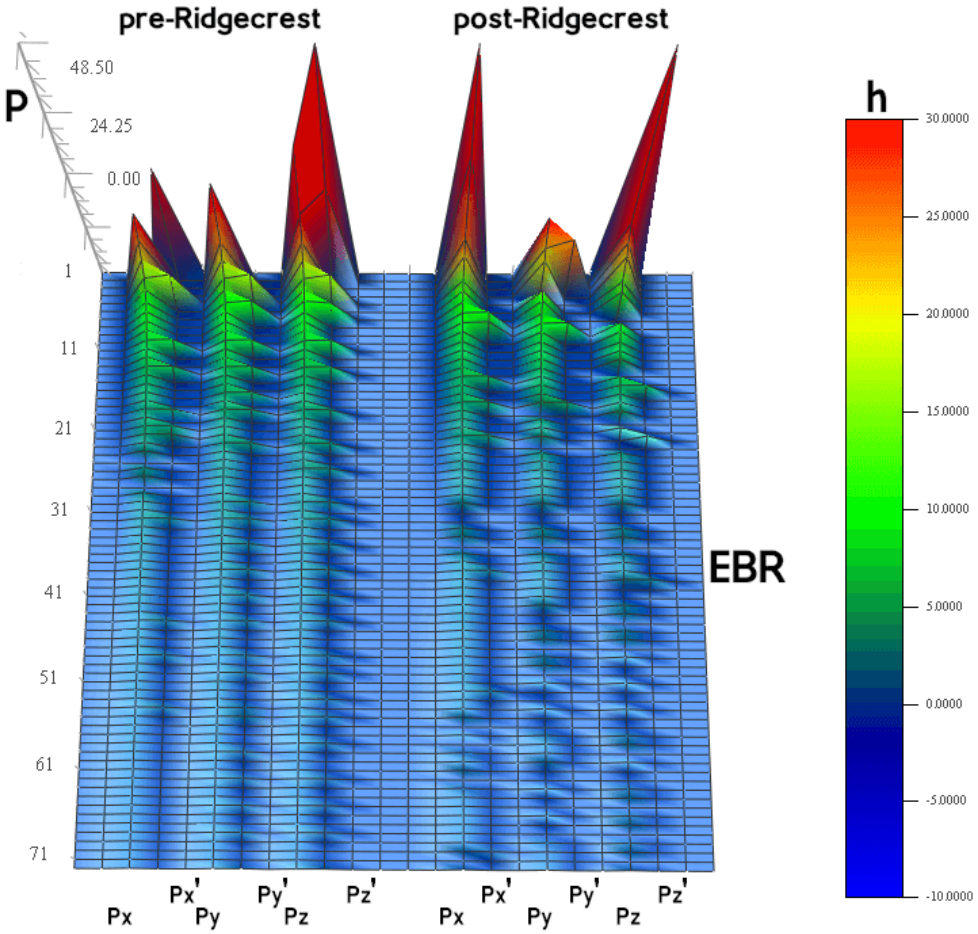

Figure 12. Δ-surface of the seismic preparation v. destruction phases. The matching was against the seismic EBR, i.e., EBR obtained from global seismicity (Omerbashich, 2020a) rather than theoretical EBR; see Table 6.

EBR waves along cGPS profile ZLA1 (Los Angeles County) - MMX1 (Mexico City) - ZOA2 (San Francisco Bay), 01-07 Jan 2020

MMX1

EBR Ptheor	EBR PEQE	Px	Px'	Δx	Δx'	Py	Py'	Δy	Δy'	Pz	Pz'	Δz	Δz'
72.0000	75.0591	63.0978		15.9%		73.1530	49.4919	2.5%	34.1%	87.0205	49.4919	-15.9%	34.1%
36.0000	33.3241	31.0687	42.6022	6.8%	-27.8%	35.9326		-7.8%		35.9326	29.0992	-7.8%	12.7%
24.0000	23.2132	23.8154		-2.6%		23.2132	29.0992	0.0%	-25.4%	23.2132		0.0%	
18.0000	17.9995	17.8096	19.7225	1.1%	-9.6%	17.4707	19.7225	2.9%	-9.6%	17.4707	19.3077	2.9%	-7.3%
14.4000	14.4466	15.6803		-8.5%		14.2228	15.6803	1.5%	-8.5%	14.2228	15.9528	1.5%	-10.4%
12.0000	12.6545	12.1520		4.0%		12.3150		2.7%		12.1520		4.0%	
10.2857	10.0282	10.3680		-3.4%		10.6076	9.7101	-5.8%	3.2%	10.0282	10.8585	0.0%	-8.3%
9.0000	8.8661	9.8138		-10.7%		8.8661		0.0%		8.7813		1.0%	
8.0000	7.8772	8.0853	7.5532	-2.6%	4.1%	7.9454		-0.9%		7.8772		0.0%	
7.2000	7.1419	7.1979		-0.8%		7.1979	7.5532	-0.8%	-5.8%	6.9790	7.4309	2.3%	-4.0%
6.5455	6.5321	6.4405	6.8234	1.4%	-4.5%	6.5789	6.9790	-0.7%	-6.8%	6.5789	6.3077	-0.7%	3.4%
6.0000	6.0183	6.0580		-0.7%		5.9404	6.2222	1.3%	-3.4%	5.9404		1.3%	
5.5385	5.6132	5.5457	5.7542	1.2%	-2.5%	5.6135		0.0%		5.5794		0.6%	
5.1429	5.1709	5.1133	5.3517	1.1%	-3.5%	5.2001	5.0018	-0.6%	3.3%	5.1709	4.9747	0.0%	3.8%
4.8000	4.7434	4.7929	5.0018	-1.0%	-5.4%	4.7929		-1.0%		4.7929		-1.0%	
4.5000	4.6008	4.4449	4.6008	3.4%	0.0%	4.4449	4.6008	3.4%	0.0%	4.4234	4.6008	3.9%	0.0%
4.2353	4.2008	4.2791	4.1439	-1.9%	1.4%	4.1627	4.3194	0.9%	-2.8%	4.1817	4.2992	0.5%	-2.3%
4.0000	3.9650	3.9822		-0.4%		3.9650		0.0%		3.9650		0.0%	
3.7895	3.7696	3.7542	3.8648	0.4%	-2.5%	3.8166	3.6938	-1.2%	2.0%	3.8325		-1.7%	
3.6000	3.5236	3.6497	3.5236	-3.6%	0.0%	3.5926		-2.0%		3.6643	3.5236	-4.0%	0.0%
3.4286	3.4443	3.4060		1.1%		3.4060	3.5102	1.1%	-1.9%	3.4060		1.1%	
3.2727	3.2842	3.2608	3.3198	0.7%	-1.1%	3.3198		-1.1%		3.2378	3.3198	1.4%	-1.1%
3.1304	3.1275	3.1275	3.1928	0.0%	-2.1%	3.2039		-2.4%		3.1169	3.1707	0.3%	-1.4%
3.0000	2.9949	2.9852	3.0446	0.3%	-1.7%	2.9852		0.3%		3.0146		-0.7%	
2.8800	2.8821	2.8821	2.8288	0.0%	1.8%	2.8463		1.2%		2.8731		0.3%	
2.7692	2.7691	2.7442		0.9%		2.7944	2.7279	-0.9%	1.5%	2.7279	2.8201	1.5%	-1.8%
2.6667	2.6569	2.6492		0.3%		2.6340		0.9%		2.6646		-0.3%	
2.5714	2.5821	2.5606	2.6041	0.8%	-0.9%	2.5534		1.1%		2.5822		0.0%	
2.4828	2.4911	2.4512	2.5184	1.6%	-1.1%	2.5115	2.4446	-0.8%	1.9%	2.5115	2.4512	-0.8%	1.6%
2.4000	2.4317	2.3999		1.3%		2.3937		1.6%		2.3937		1.6%	
2.3226	2.3269	2.3036	2.3448	1.0%	-0.8%	2.3036	2.3448	1.0%	-0.8%	2.3094	2.3448	0.8%	-0.8%
2.2500	2.2580	2.2147		1.9%		2.2147		1.9%		2.2200		1.7%	
2.1818	2.1524	2.1779		-1.2%		2.1727		-0.9%		2.1727		-0.9%	
2.1176	2.1274	2.1079	2.1373	0.9%	-0.5%	2.1031	2.1324	1.1%	-0.2%	2.1031	2.1324	1.1%	-0.2%
2.0571	2.0514	2.0560	2.0840	-0.2%	-1.6%	2.0699	2.0377	-0.9%	0.7%	2.0652		-0.7%	
2.0000	1.9763	1.9891	2.0287	-0.6%	-2.7%	1.9978		-1.1%		1.9978		-1.1%	
1.9459	1.9636	1.9552	1.9265	0.4%	1.9%	1.9511		0.6%		1.9511		0.6%	
1.8947	1.8831	1.8792	1.9026	0.2%	-1.0%	1.8792	1.9145	0.2%	-1.7%	1.9026	1.8831	-1.0%	0.0%
1.8462	1.8305	1.8378		-0.4%		1.8415		-0.6%		1.8342		-0.2%	
1.8000	1.8160	1.8089	1.7843	0.4%	1.7%	1.7877	1.8160	1.6%	0.0%	1.7877	1.8124	1.6%	0.2%
1.7561	1.7536	1.7637	1.7403	-0.6%	0.8%	1.7536	1.7403	0.0%	0.8%	1.7569	1.7370	-0.2%	0.9%
1.7143	1.7016	1.7079		-0.4%		1.7143		-0.7%		1.7111		-0.6%	
1.6744	1.6646	1.6706	1.6526	-0.4%	0.7%	1.6646	1.6891	0.0%	-1.5%	1.6860		-1.3%	
1.6364	1.6351	1.6349		0.0%		1.6526		-1.1%		1.6349	1.6526	0.0%	-1.1%
1.6000	1.5869	1.5951	1.6176	-0.5%	-1.9%	1.5951	1.6176	-0.5%	-1.9%	1.5924	1.6176	-0.3%	-1.9%
1.5652	1.5573	1.5652		-0.5%		1.5573		0.0%		1.5599		-0.2%	
1.5319	1.5416	1.5313	1.5494	0.7%	-0.5%	1.5390		0.2%		1.5237	1.5416	1.2%	0.0%
1.5000	1.5062	1.4964		0.7%		1.4939		0.8%		1.4915	1.5111	1.0%	-0.3%
1.4694	1.4676	1.4653	1.4795	0.2%	-0.8%	1.4700		-0.2%		1.4724		-0.3%	
1.4400	1.4468	1.4378	1.4514	0.6%	-0.3%	1.4423	1.4266	0.3%	1.4%	1.4400	1.4537	0.5%	-0.5%
1.4118	1.4091	1.4134		-0.3%		1.4069		0.2%		1.4069	1.4244	0.2%	-1.1%
1.3846	1.3941	1.3692		1.8%		1.3899	1.3774	0.3%	1.2%	1.3774	1.3920	1.2%	0.2%
1.3585	1.3590	1.3530		0.4%		1.3530	1.3651	0.4%	-0.4%	1.3651		-0.4%	
1.3333	1.3412	1.3276		1.0%		1.3295	1.3451	0.9%	-0.3%	1.3295	1.3431	0.9%	-0.1%
1.3091	1.2939	1.3180		-1.9%		1.3049	1.3162	-0.9%	-1.7%	1.3049	1.3143	-0.9%	-1.6%
1.2857	1.2741	1.2795		-0.4%		1.2831	1.2957	-0.7%	-1.7%	1.2831	1.2939	-0.7%	-1.6%
1.2632	1.2636	1.2671		-0.3%		1.2602	1.2724	0.3%	-0.7%	1.2724		-0.7%	
1.2414	1.2381	1.2314		0.5%		1.2482		-0.8%		1.2298		0.7%	
1.2203	1.2103	1.2216	1.2119	-0.9%	-0.1%	1.2200		-0.8%		1.2183		-0.7%	
1.2000	1.2008	1.1993		0.1%		1.1961	1.2071	0.4%	-0.5%	1.1961	1.2087	0.4%	-0.7%
1.1803	1.1762	1.1868		-0.9%		1.1777		-0.1%		1.1777	1.1838	-0.1%	-0.6%
1.1613	1.1628	1.1628		0.0%		1.1643		-0.1%		1.1599		0.3%	
1.1429	1.1425	1.1440	1.1526	-0.1%	-0.9%	1.1397	1.1526	0.2%	-0.9%	1.1411		0.1%	
1.1250	1.1299	1.1202		0.9%		1.1285		0.1%		1.1285	1.1175	0.1%	1.1%
1.1077	1.1107	1.1041		0.6%		1.1067		0.4%		1.1081		0.2%	
1.0909	1.0909	1.0871		0.4%		1.0884		0.2%		1.0871	1.0988	0.4%	-0.7%
1.0746	1.0693	1.0731		-0.4%						1.0769		-0.7%	
1.0588	1.0546	1.0595		-0.5%		1.0644		-0.9%		1.0669		-1.2%	
1.0435	1.0438	1.0403		0.3%		1.0403	1.0498	0.3%	-0.6%	1.0414	1.0510	0.2%	-0.7%
1.0286	1.0321	1.0252	1.0321	0.7%	0.0%	1.0309		0.1%					
1.0141	1.0195	1.0127	1.0195	0.7%	0.0%	1.0127	1.0206	0.7%	-0.1%	1.0127	1.0195	0.7%	0.0%
1.0000	0.9984	0.9962	1.0050	0.2%	-0.7%	0.9973	1.0061	0.1%	-0.8%	1.0050		-0.7%	
	≤ 1‰		∑	6	5			12	3			10	6
	1‰ - 1%		∑	44	11			38	11			39	11
	≥ 1%		∑	22	19			21	21			22	19
	67%-99%		∑∑	72	35			71	35			71	36

ZLA1

EBR Ptheor	EBR PEQE	Px	Px'	Δx	Δx'	Py	Py'	Δy	Δy'	Pz	Pz'	Δz	Δz'
72.0000	75.0591	63.0978		15.9%		79.4864	49.4919	-5.9%	34.1%	59.0401		21.3%	
36.0000	33.3241	32.1569	42.6022	3.5%	-27.8%	37.3963	30.0517	-12.2%	9.8%	34.5793		-3.8%	
24.0000	23.2132	24.4496		-5.3%		24.4496	20.6079	-5.3%	11.2%	23.2132	28.2052	0.0%	-21.5%
18.0000	17.9995	17.4707	20.1555	2.9%	-12.0%	18.1619	16.5272	-0.9%	8.2%	17.1444	19.7225	4.8%	-9.6%
14.4000	14.4466	14.2228	15.6803	1.5%	-8.5%	14.9161	13.3929	-3.2%	7.3%	14.0059	15.4170	3.1%	-6.7%
12.0000	12.6545	11.8386	12.8314	6.4%	-1.4%	12.3150	11.3977	2.7%	9.9%	11.8386	13.0132	6.4%	-2.8%
10.2857	10.0282	10.0282	10.8585	0.0%	-8.3%	10.4864	9.7101	-4.6%	3.2%	10.1390	10.9885	-1.1%	-9.6%
9.0000	8.8661	8.7813	9.4114	1.0%	-6.2%	9.0407		-2.0%		8.8661	9.5089	0.0%	-7.3%
8.0000	7.8772	8.1571	7.6158	-3.6%	3.3%	7.8102	8.4577	0.9%	-7.4%	7.9454	8.3805	-0.9%	-6.4%
7.2000	7.1419	7.1419		0.0%		7.3712	6.9790	-3.2%	2.3%	7.1419	7.5532	0.0%	-5.8%
6.5455	6.5321	6.4405	6.7730	1.4%	-3.7%	6.6746		-2.2%		6.5321	6.8234	0.0%	-4.5%
6.0000	6.0183	5.8645	6.1390	2.6%	-2.0%	6.3513		-5.5%		5.9791	6.2647	0.7%	-4.1%
5.5385	5.6132	5.5794	5.3517	0.6%	4.7%	5.4470	5.6830	3.0%	-1.2%	5.5457	5.7542	1.2%	-2.5%
5.1429	5.1709	5.1419		0.6%		5.0569	5.2597	2.2%	-1.7%	5.1419	5.3207	0.6%	-2.9%
4.8000	4.7434	4.7680	4.9479	-0.5%	-4.3%	4.7190	4.8952	0.5%	-3.2%	4.8181	4.9747	-1.6%	-4.9%
4.5000	4.6008	4.4022	4.6474	4.3%	-1.0%	4.4449	4.5778	3.4%	0.5%	4.5104	4.6710	2.0%	-1.5%
4.2353	4.2008	4.2593	4.1253	-1.4%	1.8%	4.2008	4.3194	0.0%	-2.8%	4.2593	4.3812	-1.4%	-4.3%
4.0000	3.9650	3.9995		-0.9%		3.9650	4.0886	0.0%	-3.1%	4.0170	4.1253	-1.3%	-4.0%
3.7895	3.7696	3.8166	3.6938	-1.2%	2.0%	3.7696	3.8648	0.0%	-2.5%	3.8166	3.9142	-1.2%	-3.8%
3.6000	3.5236	3.5926		-2.0%		3.6643	3.5236	-4.0%	0.0%	3.6209	3.7237	-2.8%	-5.7%
3.4286	3.4443	3.3934	3.4835	1.5%	-1.1%	3.4315		0.4%		3.4573	3.5372	-0.4%	-2.7%
3.2727	3.2842	3.3078	3.2265	-0.7%	1.8%	3.2725	3.3440	0.4%	-1.8%	3.2960	3.3809	-0.4%	-2.9%
3.1304	3.1275	3.1490	3.0752	-0.7%	1.7%	3.1169	3.1928	0.3%	-2.1%	3.1598	3.2265	-1.0%	-3.2%
3.0000	2.9949	2.9949		0.0%		3.0446	2.9468	-1.7%	1.6%	3.0245	3.0959	-1.0%	-3.4%
2.8800	2.8821	2.8552	2.9187	0.9%	-1.3%	2.8912	2.8288	-0.3%	1.8%	2.9095	2.9659	-1.0%	-2.9%
2.7692	2.7691	2.7442	2.7944	0.9%	-0.9%	2.7691	2.7199	0.0%	1.8%	2.7944	2.8463	-0.9%	-2.8%
2.6667	2.6569	2.6880	2.6416	-1.2%	0.6%	2.6646	2.6190	-0.3%	1.4%	2.6492	2.7442	0.3%	-3.3%
2.5714	2.5821	2.5534	2.6041	1.1%	-0.9%	2.5749	2.5323	0.3%	1.9%	2.5534	2.6959	1.1%	-4.4%
2.4828	2.4911	2.4710	2.5115	0.8%	-0.8%	2.4911	2.4512	0.0%	1.6%	2.4643	2.5968	1.1%	-4.2%
2.4000	2.4317	2.3874	2.4253	1.8%	0.3%	2.4062	2.3690	1.0%	2.6%	2.4253	2.5115	0.3%	-3.3%
2.3226	2.3269	2.3094	2.3448	0.8%	-0.8%	2.3269	2.2921	0.0%	1.5%	2.3152	2.3874	0.5%	-2.6%
2.2500	2.2580	2.2694	2.2254	-0.5%	1.4%	2.2527		0.2%		2.2417	2.3508	0.7%	-4.1%
2.1818	2.1524	2.1831		-1.4%		2.1676	2.1987	-0.7%	-2.2%	2.1727	2.2750	-0.9%	-5.7%
2.1176	2.1274	2.1127	2.1473	0.7%	-0.9%	2.1324	2.0982	-0.2%	1.4%	2.1127	2.2040	0.7%	-3.6%
2.0571	2.0514	2.0514	2.0792	0.0%	-1.4%	2.0652	2.0377	-0.7%	0.7%	2.0560	2.1423	-0.2%	-4.4%
2.0000	1.9763	1.9848	2.0153	-0.4%	-2.0%	2.0065		-1.5%		1.9978	2.0840	-1.1%	-5.4%
1.9459	1.9636	1.9511	1.9225	0.6%	2.1%	1.9346	1.9636	1.5%	0.0%	1.9428	2.0242	1.1%	-3.1%
1.8947	1.8831	1.8908		-0.4%		1.8831	1.9065	0.0%	-1.2%	1.8947	1.9720	-0.6%	-4.7%
1.8462	1.8305	1.8415	1.8677	-0.6%	-2.0%	1.8564	1.8342	-1.4%	-0.2%	1.8452	1.9185	-0.8%	-4.8%
1.8000	1.8160	1.7808		1.9%		1.7912	1.8124	1.4%	0.2%	1.8018	1.8715	0.8%	-3.1%
1.7561	1.7536	1.7603	1.7403	-0.4%	0.8%	1.7502	1.7705	0.2%	-1.0%	1.7569	1.8232	-0.2%	-4.0%
1.7143	1.7016	1.7207	1.6984	-1.1%	0.2%	1.7079	1.7304	-0.4%	-1.7%	1.7175	1.7808	-0.9%	-4.7%
1.6744	1.6646	1.6767	1.6556	-0.7%	0.5%	1.6676	1.6891	-0.2%	-1.5%	1.6767	1.7370	-0.7%	-4.3%
1.6364	1.6351	1.6349		0.0%		1.6291	1.6466	0.4%	-0.7%	1.6408	1.6984	-0.3%	-3.9%
1.6000	1.5869	1.5924	1.6148	-0.3%	-1.8%	1.6007		-0.9%		1.6035	1.6585	-1.0%	-4.5%
1.5652	1.5573	1.5733	1.5546	-1.0%	0.2%	1.5626	1.5814	-0.3%	-1.5%	1.5706	1.6205	-0.9%	-4.1%
1.5319	1.5416	1.5364	1.5186	0.3%	1.5%	1.5287	1.5468	0.8%	-0.3%	1.5364	1.5869	0.3%	-2.9%
1.5000	1.5062	1.4939		0.8%		1.4988	1.5136	0.5%	-0.5%	1.5062	1.5546	0.0%	-3.2%
1.4694	1.4676	1.4771	1.4606	-0.6%	0.5%	1.4700	1.4843	-0.2%	-1.1%	1.4747	1.5211	-0.5%	-3.6%
1.4400	1.4468	1.4468	1.4310	0.0%	1.1%	1.4400	1.4537	0.5%	-0.5%	1.4468	1.4891	0.0%	-2.9%
1.4118	1.4091	1.4156	1.4026	-0.5%	0.5%	1.4112	1.4244	-0.2%	-1.1%	1.4178	1.4606	-0.6%	-3.7%
1.3846	1.3941	1.3794	1.3920	1.1%	0.2%	1.3857	1.3984	0.6%	-0.3%	1.3920	1.4310	0.2%	-2.7%
1.3585	1.3590	1.3550		0.3%		1.3610	1.3733	-0.1%	-1.0%	1.3530	1.4048	0.4%	-3.4%
1.3333	1.3412	1.3295	1.3431	0.9%	-0.1%	1.3353	1.3490	0.4%	-0.6%	1.3392	1.3774	0.1%	-2.7%
1.3091	1.2939	1.3049	1.3162	-0.9%	-1.7%	1.3105	1.3238	-1.3%	-2.3%	1.3049	1.3651	-0.9%	-5.5%
1.2857	1.2741	1.2795	1.2921	-0.4%	-1.4%	1.2866	1.2994	-1.0%	-2.0%	1.2813	1.3276	-0.6%	-4.2%
1.2632	1.2636	1.2654		-0.1%		1.2567	1.2759	0.5%	-1.0%	1.2602	1.3162	0.3%	-4.2%
1.2414	1.2381	1.2397	1.2516	-0.1%	-1.1%	1.2448	1.2347	-0.5%	0.3%	1.2482	1.2939	-0.8%	-4.5%
1.2203	1.2103	1.2167	1.2281	-0.5%	-1.5%	1.2232	1.2119	-1.1%	-0.1%	1.2281	1.2706	-1.5%	-5.0%
1.2000	1.2008	1.2040	1.1915	-0.3%	0.8%	1.2024		-0.1%		1.2087	1.2381	-0.7%	-3.1%
1.1803	1.1762	1.1807		-0.4%		1.1762	1.1853	0.0%	-0.8%	1.1792	1.2183	-0.3%	-3.6%
1.1613	1.1628	1.1599	1.1702	0.3%	-0.6%	1.1658	1.1555	-0.3%	0.6%	1.1599	1.1977	0.3%	-3.0%
1.1429	1.1425	1.1411	1.1511	0.1%	-0.8%	1.1468	1.1383	-0.4%	0.4%	1.1425	1.1884	0.0%	-4.0%
1.1250	1.1299	1.1243	1.1327	0.5%	-0.2%	1.1202	1.1299	0.9%	0.0%	1.1243	1.1687	0.5%	-3.4%
1.1077	1.1107	1.1041	1.1134	0.6%	-0.2%	1.1041	1.1121	0.6%	-0.1%	1.1081	1.1511	0.2%	-3.6%
1.0909	1.0909	1.0935	1.0845	-0.2%	0.6%	1.0884	1.0975	0.2%	-0.6%	1.0909	1.1341	0.0%	-4.0%
1.0746	1.0693	1.0756	1.0669	-0.6%	0.2%	1.0718	1.0807	-0.2%	-1.1%	1.0756	1.1161	-0.6%	-4.4%
1.0588	1.0546	1.0583		-0.3%		1.0558	1.0632	-0.1%	-0.8%	1.0595	1.0988	-0.5%	-4.2%
1.0435	1.0438	1.0391	1.0498	0.5%	-0.6%	1.0426	1.0486	0.1%	-0.5%	1.0450	1.0832	-0.1%	-3.8%
1.0286	1.0321	1.0309	1.0229	0.1%	0.9%	1.0275	1.0356	0.4%	-0.3%	1.0298	1.0681	0.2%	-3.5%
1.0141	1.0195	1.0150		0.4%		1.0127	1.0195	0.7%	0.0%	1.0161	1.0522	0.3%	-3.2%
1.0000	0.9984	0.9984	1.0072	0.0%	-0.9%	0.9984		0.0%		1.0017	1.0367	-0.3%	-3.8%
	≤ 1‰			11	1			13	6			10	0
	1‰ - 1%			40	24			38	21			43	0
	≥ 1%			21	30			21	36			19	70
	67%-99%			72	55			72	63			72	70

ZOA2

EBR Ptheor	EBR PEQE	Px	Px'	Δx	Δx'	Py	Py'	Δy	Δy'	Pz	Pz'	Δz	Δz'
72.0000	75.0591	63.0978		15.9%		67.7543		9.7%		63.0978		15.9%	
36.0000	33.3241	35.9326	44.6753	-7.8%	-34.1%	35.9326	46.9604	-7.8%	-40.9%	35.9326	44.6753	-7.8%	-34.1%
24.0000	23.2132	23.8154	30.0517	-2.6%	-29.5%	23.8154	29.0992	-2.6%	-25.4%	23.8154	29.0992	-2.6%	-25.4%
18.0000	17.9995	18.1619	19.7225	-0.9%	-9.6%	16.5272	20.1555	8.2%	-12.0%	17.4707	19.7225	2.9%	-9.6%
14.4000	14.4466	14.6776	16.2349	-1.6%	-12.4%	14.6776	13.2004	-1.6%	8.6%	14.4466	15.9528	0.0%	-10.4%
12.0000	12.6545	11.8386	13.2004	6.4%	-4.3%	11.8386		6.4%		11.8386	13.0132	6.4%	-2.8%
10.2857	10.0282	10.1390	10.8585	-1.1%	-8.3%	10.1390	10.8585	-1.1%	-8.3%	10.2522	10.9885	-2.2%	-9.6%
9.0000	8.8661	9.0407	9.6084	-2.0%	-8.4%	9.0407	9.6084	-2.0%	-8.4%	9.0407	9.6084	-2.0%	-8.4%
8.0000	7.8772	8.0147	8.5364	-1.7%	-8.4%	8.0147	8.5364	-1.7%	-8.4%	8.0147	8.5364	-1.7%	-8.4%
7.2000	7.1419	7.0867	7.4309	0.8%	-4.0%	7.0324	7.4915	1.5%	-4.9%	7.2547	7.5532	-1.6%	-5.8%
6.5455	6.5321	6.5321	6.8234	0.0%	-4.5%	6.5321	6.7730	0.0%	-3.7%	6.7234	6.9790	-2.9%	-6.8%
6.0000	6.0183	5.9791	6.3077	0.7%	-4.8%	5.9791	6.3077	0.7%	-4.8%	5.9791	6.2647	0.7%	-4.1%
5.5385	5.6132	5.7184		-1.9%		5.5124	5.7184	1.8%	-1.9%	5.4795	5.6830	2.4%	-1.2%
5.1429	5.1709	5.2597		-1.7%		5.2597	4.9747	-1.7%	3.8%	5.2001	5.3517	-0.6%	-3.5%
4.8000	4.7434	4.7680	4.9479	-0.5%	-4.3%	4.7680		-0.5%		4.7434	5.0569	0.0%	-6.6%
4.5000	4.6008	4.4665	4.6008	2.9%	0.0%	4.4665	4.6008	2.9%	0.0%	4.4665	4.9214	2.9%	-7.0%
4.2353	4.2008	4.2396	4.3604	-0.9%	-3.8%	4.2396	4.3604	-0.9%	-3.8%	4.2593	4.6008	-1.4%	-9.5%
4.0000	3.9650	4.0525		-2.2%		4.0347		-1.8%		4.0170	4.3604	-1.3%	-10.0%
3.7895	3.7696	3.8812		-3.0%		3.7696	3.8648	0.0%	-2.5%	3.7851	4.1439	-0.4%	-9.9%
3.6000	3.5236	3.5236	3.6790	0.0%	-4.4%	3.6790		-4.4%		3.6790		-4.4%	
3.4286	3.4443	3.4060		1.1%		3.4060	3.4968	1.1%	-1.5%	3.4060	3.4968	1.1%	-1.5%
3.2727	3.2842	3.2493	3.3198	1.1%	-1.1%	3.2493		1.1%		3.2493	3.3198	1.1%	-1.1%
3.1304	3.1275	3.1382	3.0649	-0.3%	2.0%	3.1382	3.1928	-0.3%	-2.1%	3.1382	3.0649	-0.3%	2.0%
3.0000	2.9949	2.9659		1.0%		2.9852	3.0752	0.3%	-2.7%	2.9852		0.3%	
2.8800	2.8821	2.8552		0.9%		2.8641	2.9095	0.6%	-1.0%	2.8641	2.9187	0.6%	-1.3%
2.7692	2.7691	2.7607	2.8029	0.3%	-1.2%	2.7691	2.8115	0.0%	-1.5%	2.7691	2.8115	0.0%	-1.5%
2.6667	2.6569	2.6646	2.7199	-0.3%	-2.4%	2.6646	2.7199	-0.3%	-2.4%	2.6646	2.7199	-0.3%	-2.4%
2.5714	2.5821	2.6041		-0.9%		2.5534	2.5968	1.1%	-0.6%	2.5534	2.6041	1.1%	-0.9%
2.4828	2.4911	2.4710	2.5115	0.8%	-0.8%	2.4843	2.5184	0.3%	-1.1%	2.4776	2.5047	0.5%	-0.5%
2.4000	2.4317	2.3874	2.4382	1.8%	-0.3%	2.3937	2.4446	1.6%	-0.5%	2.3937	2.4382	1.6%	-0.3%
2.3226	2.3269	2.3094	2.3388	0.8%	-0.5%					2.3094		0.8%	
2.2500	2.2580	2.2527		0.2%		2.2472	2.2200	0.5%	1.7%	2.2527	2.2864	0.2%	-1.3%
2.1818	2.1524	2.1727	2.2147	-0.9%	-2.9%	2.1779		-1.2%		2.1779	2.2200	-1.2%	-3.1%
2.1176	2.1274	2.1373		-0.5%		2.1079	2.1373	0.9%	-0.5%	2.1423		-0.7%	
2.0571	2.0514	2.0840		-1.6%		2.0840		-1.6%		2.0468	2.0840	0.2%	-1.6%
2.0000	1.9763	1.9935	2.0287	-0.9%	-2.7%	1.9891	2.0332	-0.6%	-2.9%	1.9935	2.0287	-0.9%	-2.7%
1.9459	1.9636	1.9594		0.2%		1.9552		0.4%					
1.8947	1.8831	1.8792	1.9185	0.2%	-1.9%	1.8754	1.9145	0.4%	-1.7%	1.8792	1.9185	0.2%	-1.9%
1.8462	1.8305	1.8489	1.8792	-1.0%	-2.7%	1.8452		-0.8%		1.8452		-0.8%	
1.8000	1.8160	1.7947		1.2%		1.7947	1.8160	1.2%	0.0%	1.7947	1.8160	1.2%	0.0%
1.7561	1.7536	1.7536		0.0%		1.7536	1.7739	0.0%	-1.2%	1.7569	1.7739	-0.2%	-1.2%
1.7143	1.7016	1.7079		-0.4%		1.7111	1.7337	-0.6%	-1.9%	1.7111	1.7370	-0.6%	-2.1%
1.6744	1.6646	1.6676	1.6829	-0.2%	-1.1%	1.6706	1.6860	-0.4%	-1.3%	1.6706	1.6860	-0.4%	-1.3%
1.6364	1.6351	1.6349	1.6496	0.0%	-0.9%	1.6205	1.6526	0.9%	-1.1%	1.6320	1.6496	0.2%	-0.9%
1.6000	1.5869	1.5979	1.6176	-0.7%	-1.9%	1.5951		-0.5%		1.6063		-1.2%	
1.5652	1.5573	1.5573		0.0%		1.5706		-0.9%		1.5841		-1.7%	
1.5319	1.5416	1.5313		0.7%		1.5287	1.5442	0.8%	-0.2%	1.5287	1.5442	0.8%	-0.2%
1.5000	1.5062	1.4964		0.7%		1.4964	1.5161	0.7%	-0.7%	1.4964	1.5136	0.7%	-0.5%
1.4694	1.4676	1.4771		-0.6%		1.4630	1.4771	0.3%	-0.6%	1.4630	1.4771	0.3%	-0.6%
1.4400	1.4468	1.4468		0.0%		1.4491		-0.2%		1.4378	1.4514	0.6%	-0.3%
1.4118	1.4091	1.4091	1.4244	0.0%	-1.1%	1.4091	1.4244	0.0%	-1.1%	1.4091	1.4244	0.0%	-1.1%
1.3846	1.3941	1.3733	1.4005	1.5%	-0.5%	1.3794	1.3899	1.1%	0.3%	1.3794	1.3920	1.1%	0.2%
1.3585	1.3590	1.3471		0.9%		1.3550		0.3%		1.3550	1.3692	0.3%	-0.7%
1.3333	1.3412	1.3314		0.7%		1.3295	1.3451	0.9%	-0.3%	1.3276	1.3451	1.0%	-0.3%
1.3091	1.2939	1.3049		-0.9%		1.3143		-1.6%		1.3143		-1.6%	
1.2857	1.2741	1.2939	1.2759	-1.6%	-0.1%	1.2813	1.2957	-0.6%	-1.7%	1.2831	1.2939	-0.7%	-1.6%
1.2632	1.2636	1.2619		0.1%		1.2636		0.0%		1.2584	1.2724	0.4%	-0.7%
1.2414	1.2381	1.2397		-0.1%						1.2364	1.2465	0.1%	-0.7%
1.2203	1.2103	1.2087		0.1%						1.2183	1.2265	-0.7%	-1.3%
1.2000	1.2008	1.1961		0.4%		1.1977	1.2071	0.3%	-0.5%	1.1977	1.2087	0.3%	-0.7%
1.1803	1.1762	1.1838	1.1762	-0.6%	0.0%	1.1807		-0.4%			1.1747		0.1%
1.1613	1.1628	1.1584	1.1672	0.4%	-0.4%	1.1569		0.5%		1.1511		1.0%	
1.1429	1.1425	1.1397	1.1511	0.2%	-0.8%	1.1369		0.5%		1.1397		0.2%	
1.1250	1.1299									1.1216	1.1285	0.7%	0.1%
1.1077	1.1107	1.0884		2.0%		1.1054		0.5%		1.1054	1.1134	0.5%	-0.2%
1.0909	1.0909	1.0988		-0.7%		1.0884		0.2%		1.0871	1.0975	0.4%	-0.6%
1.0746	1.0693	1.0884		-1.8%		1.0794		-0.9%		1.0718		-0.2%	
1.0588	1.0546					1.0656		-1.0%		1.0570	1.0632	-0.2%	-0.8%
1.0435	1.0438	1.0403		0.3%		1.0403		0.3%		1.0414		0.2%	
1.0286	1.0321	1.0309	1.0240	0.1%	0.8%	1.0309	1.0252	0.1%	0.7%	1.0321		0.0%	
1.0141	1.0195	1.0127		0.7%		1.0127		0.7%		1.0127		0.7%	
1.0000	0.9984	0.9984	1.0061	0.0%	-0.8%	0.9984		0.0%		0.9973		0.1%	
	≤ 1‰			11	3			8	2			7	3
	1‰ - 1%			37	9			36	11			38	17
	≥ 1%			22	25			24	29			25	35
	67%-99%			70	37			68	42			70	55

Table 7. Same mapping profile as in Table 4, but with matchings of cGPS EBR against seismic EBR (Omerbashich, 2020a). Red-framed values are the absolute such matchings of the long-periodic (~5 h and longer) EBR as most energetic.

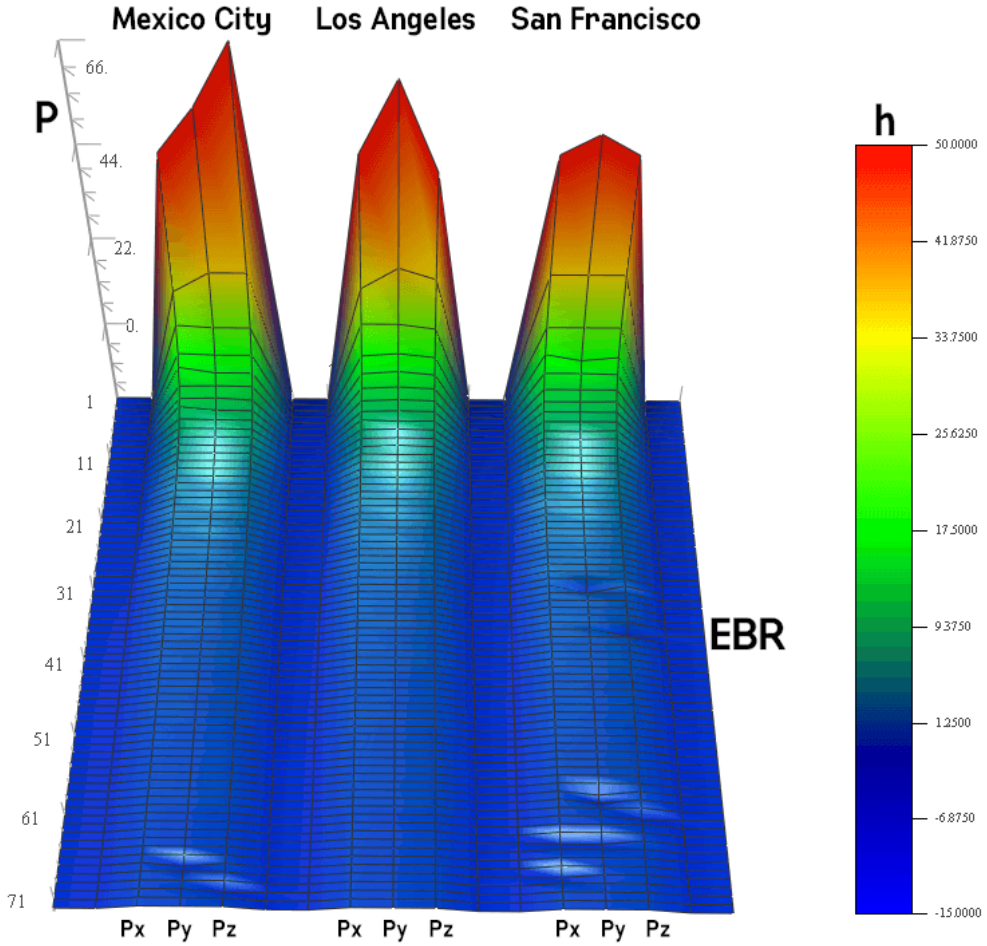

Figure 13. Completely recovered EBR (waves) from weeklong recordings at 1Hz cGPS stations alongside the tectonic plate boundary profile Mexico City (MMX1)–Los Angeles (ZLA1)–San Francisco (ZOA2), Table 7. The matching was against the EBR from global occurrences of large earthquakes (Omerbashich, 2020a) as a more realistic depiction of Earth resonances during the last five years than the theoretical EBR. Undertone series not shown.

As we saw in the above, cGPS stations correctly sensed the EBR during a quiescent week of 01-07 January 2020, Table 4. However, that depiction was at the same time a preparation phase for an M_w6.4 and M_w6.6 Puerto Rico sequence of 2020-01-07 (Harvard Catalog No. 202001070824A) – resulting in many absolute (0.0%; the red-framed green values) matchings among long-periodic cGPS EBR and seismic EBR, Table 7 & Figure 13. That the profile indeed maps the reality well is seen from the gradual drop in the number of (absolute) matches while going away from the (future) Puerto Rico event: 7, 6, and 4, for Mexico City, Los Angeles, and San Francisco, respectively. Note here that, while the long-periodic EBR cutoff is ~five-hour, the drop is maintained even if one starts expending the cutoff to include shorter periods – all the way up to around two-hour (expanding by one adjacent period and including undertones), Figure 14. The same holds without undertones as well. Although somewhat smaller, the same sensitivity of cGPS EBR with distance from a seismic event emerges when matching against theoretical EBR, Table 4: as 6, 3, and 0 long-periodic matches, respectively, also preserved with the cutoff expanded as above.

A remarkable demonstration of the absolute success of EBR detection from cGPS is in Figure 14 that demonstrates the earthquake preparation phase, Figures 10-12, as an entirely Earth resonance phenomenon, and the GVSA as a spectral analysis method of absolute accuracy (down to twice the sampling step). The stations alongside the profile (tectonic plate boundary) always line up in the same way relative to the (future) Puerto Rico strong earthquake that occurred on the 7th day of the weeklong data: as the nearest to the epicenter, Mexico City picks up the most of pre-quake EBR, Los Angeles less, and San Francisco as the farthest away, the least – regardless how big of an EBR train one analyzes. In short, Figure 14 examines the effect of cutoff selection on the sensitivity of cGPS EBR. The same plot then shows that the EBR signal is so strong, pure, and stable that selecting any cutoff is justified by physics; here used is the five-hour cutoff as all matches below are to within 0.0%.

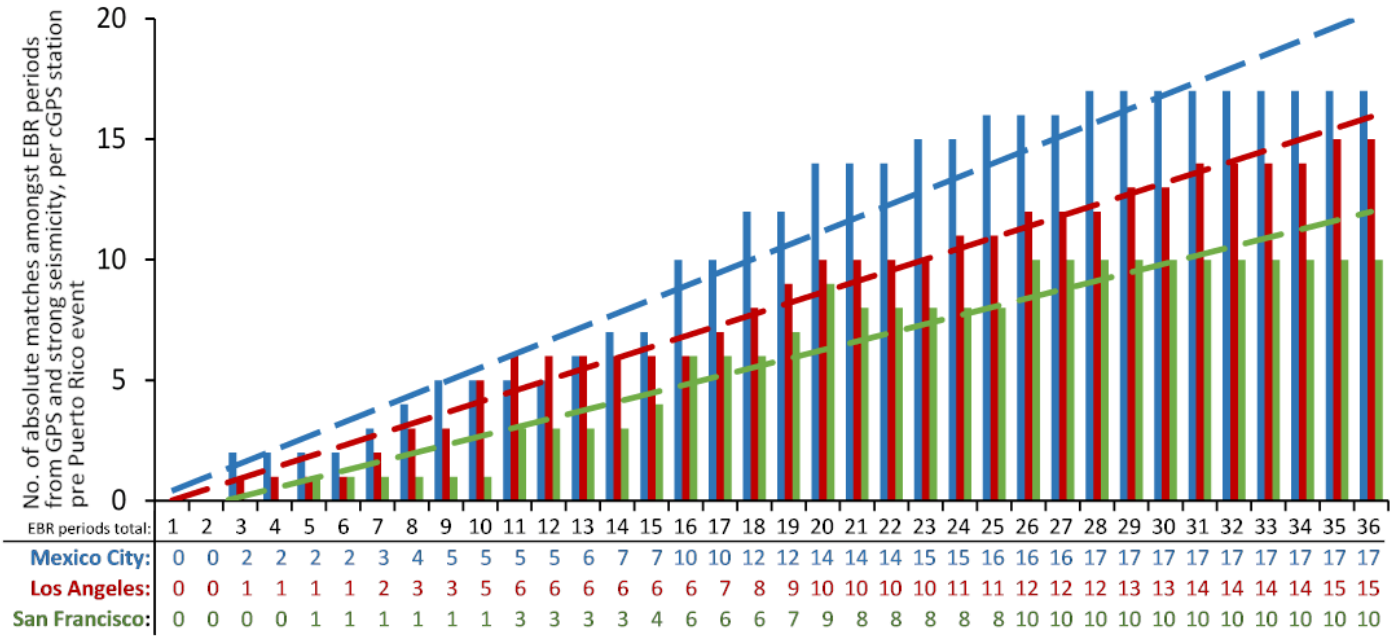

EBR periods total:	1	2	3	4	5	6	7	8	9	10	11	12	13	14	15	16	17	18	19	20	21	22	23	24	25	26	27	28	29	30	31	32	33	34	35	36
Mexico City:	0	0	2	2	2	2	3	4	5	5	5	5	6	7	7	10	10	12	12	14	14	14	15	15	16	16	16	17	17	17	17	17	17	17	17	17
Los Angeles:	0	0	1	1	1	1	2	3	3	5	6	6	6	6	6	6	7	8	9	10	10	10	10	11	11	12	12	12	13	13	14	14	14	14	15	15
San Francisco:	0	0	0	0	1	1	1	1	1	1	3	3	3	3	4	6	6	6	7	9	8	8	8	8	8	10	10	10	10	10	10	10	10	10	10	10

Figure 14. Suitability of weeklong cGPS data for EBR mapping, as an always constant ratio (dashed trend lines) between the number of absolute (to within 1‰) matches of EBR periods (from cGPS v. strong seismicity) and the total number of (longest) periods here considered, per cGPS station. Shown are the first (longest) 36 EBR periods; see Table 7 for their respective values.

Another sign that this study has detected and mapped a broad physical process as picked by the examined cGPS stations lies in the observation that no undertone/overtone periods matched theoretical EBR to within 1‰. Such matchings do occur albeit sporadically in matchings against seismic EBR, Tables 4 v. 7. Also, during the initiation phase (before a strong earthquake in the vicinity of up to several hundred km), long-periodic matches against seismic EBR are absolute-only (0.0%) — never converging even on 1‰. This natural constraint paves the way for real-time earthquake prediction using the cGPS.

EBR		EBR waves at cGPS station PRMI (Puerto Rico), 01-07 Jan 2020																							
		Against theoret. EBR												Against seismic EBR											
Ptheor	PEQE	Px	Px'	Δx	Δx'	Py	Py'	Δy	Δy'	Pz	Pz'	Δz	Δz'	Px	Px'	Δx	Δx'	Py	Py'	Δy	Δy'	Pz	Pz'	Δz	Δz'
72.0000	75.0591	87.0205		-20.9%		55.4728	96.1324	23.0%	-33.5%	79.4864	52.3120	-10.4%	27.3%	87.0205		-15.9%		55.4728	96.1324	26.1%	-28.1%	79.4864	52.3120	-5.9%	30.3%
36.0000	33.3241	37.3963	30.0517	-3.9%	16.5%	31.0687		13.7%		38.9842	30.0517	-8.3%	16.5%	37.3963	30.0517	-12.2%	9.8%	31.0687		6.8%		30.0517	38.9842	9.8%	-17.0%
24.0000	23.2132	25.1185	21.5766	-4.7%	10.1%	23.8154	20.6079	0.8%	14.1%	24.4496	20.6079	-1.9%	14.1%	21.5766	25.1185	7.1%	-8.2%	23.8154	20.6079	-2.6%	11.2%	24.4496	20.6079	-5.3%	11.2%
18.0000	17.9995	17.8096		1.1%		17.8096		1.1%		17.8096		1.1%		17.8096		1.1%		17.8096		1.1%		17.8096		1.1%	
14.4000	14.4466	13.3929		7.0%		13.5912		5.6%		15.4170		-7.1%		13.3929		7.3%		13.5912		5.9%		15.4170		-6.7%	
12.0000	12.6545	11.9933	11.2579	0.1%	6.2%	12.1520	11.1216	-1.3%	7.3%	11.8386	13.0132	1.3%	-8.4%	11.9933	11.2579	5.2%	11.0%	12.1520		4.0%		13.0132	11.8386	-2.8%	6.4%
10.2857	10.0282	10.3680		-0.8%		10.2522		0.3%		10.1390	10.9885	1.4%	-6.8%	10.3680		-3.4%		10.2522	11.1216	-2.2%	-10.9%	10.1390	10.9885	-1.1%	-9.6%
9.0000	8.8661	8.5364	9.5089	5.2%	-5.7%	9.1306		-1.5%		8.8661	9.5089	1.5%	-5.7%	8.5364	9.5089	3.7%	-7.3%	9.1306	8.4577	-3.0%	4.6%	8.8661	9.5089	0.0%	-7.3%
8.0000	7.8772	8.0147		-0.2%		7.9454	8.4577	0.7%	-5.7%	7.8772	8.3805	1.5%	-4.8%	8.0147		-1.7%		7.9454		-0.9%		7.8772	8.3805	0.0%	-6.4%
7.2000	7.1419	7.1979	7.5532	0.0%	-4.9%	7.1979	7.5532	0.0%	-4.9%	7.1979	7.5532	0.0%	-4.9%	7.1979	7.5532	-0.8%	-5.8%	7.1979	7.5532	-0.8%	-5.8%	7.1979	7.5532	-0.8%	-5.8%
6.5455	6.5321	6.6264		-1.2%		6.6264	6.8745	-1.2%	-5.0%	6.5321	6.8745	0.2%	-5.0%	6.6264		-1.4%		6.6264	6.8745	-1.4%	-5.2%	6.5321	6.8745	0.0%	-5.2%
6.0000	6.0183	5.9022	6.1803	1.6%	-3.0%	5.9791	6.3077	0.3%	-5.1%	5.9022	6.2222	1.6%	-3.7%	5.9022	6.1803	1.9%	-2.7%	5.9791	6.3077	0.7%	-4.8%	5.9022	6.2222	1.9%	-3.4%
5.5385	5.6132	5.5457		-0.1%		5.5457		-0.1%		5.4795	5.6480	1.1%	-2.0%	5.5457		1.2%		5.5457		1.2%		5.6480	5.4795	-0.6%	2.4%
5.1429	5.1709	5.1419	5.3207	0.0%	-3.5%	5.1419	5.3207	0.0%	-3.5%	5.0569	5.2900	1.7%	-2.9%	5.1419	5.3207	0.6%	-2.9%	5.1419	5.3207	0.6%	-2.9%	5.0569	5.2900	2.2%	-2.3%
4.8000	4.7434	4.8181	4.9747	-0.4%	-3.6%	4.7190	4.9747	1.7%	-3.6%	4.6710		2.7%		4.8181	4.9747	-1.6%	-4.9%	4.7190	4.9747	0.5%	-4.9%	4.6710		1.5%	
4.5000	4.6008	4.5104	4.6949	-0.2%	-4.3%	4.4883		0.3%		4.4665		0.7%		4.5104	4.6949	2.0%	-2.0%	4.4883		2.4%		4.4665		2.9%	
4.2353	4.2008	4.2201	4.3398	0.4%	-2.5%	4.2201	4.3604	0.4%	-3.0%	4.2008	4.3398	0.8%	-2.5%	4.2201	4.3398	-0.5%	-3.3%	4.2201	4.3604	-0.5%	-3.8%	4.2008	4.3398	0.0%	-3.3%
4.0000	3.9650	3.9995	4.1069	0.0%	-2.7%	3.9822	4.1069	0.4%	-2.7%	3.9142	4.0886	2.1%	-2.2%	3.9995	4.1069	-0.9%	-3.6%	3.9822	4.1069	-0.4%	-3.6%	3.9142	4.0886	1.3%	-3.1%
3.7895	3.7696	3.8166	3.8976	-0.7%	-2.9%	3.7851	3.8976	0.1%	-2.9%	3.7851		0.1%		3.8166	3.8976	-1.2%	-3.4%	3.7851	3.8976	-0.4%	-3.4%	3.7851		-0.4%	
3.6000	3.5236	3.6497		-1.4%		3.6497	3.5372	-1.4%	1.7%	3.6209	3.5236	-0.6%	2.1%	3.6497		-3.6%		3.5372	3.6497	-0.4%	-3.6%	3.5236	3.6209	0.0%	-2.8%
3.4286	3.4443	3.4187	3.4968	0.3%	-2.0%	3.4573	3.3562	-0.8%	2.1%	3.4315		-0.1%		3.4187	3.4968	0.7%	-1.5%	3.4573		-0.4%		3.4315		0.4%	
3.2727	3.2842	3.2265	3.3318	1.4%	-1.8%	3.2265		1.4%		3.2265	3.3440	1.4%	-2.2%	3.3318	3.2265	-1.5%	1.8%	3.2265	3.3562	1.8%	-2.2%	3.2265	3.3440	1.8%	-1.8%
3.1304	3.1275	3.1490	3.0649	-0.6%	2.1%	3.1490	3.0855	-0.6%	1.4%	3.1382	3.0752	-0.2%	1.8%	3.1490	3.0649	-0.7%	2.0%	3.1490	3.0855	-0.7%	1.3%	3.1382	3.0752	-0.3%	1.7%
3.0000	2.9949	2.9755		0.8%		3.0245	2.9659	-0.8%	1.1%	3.0047		-0.2%		2.9755		0.6%		2.9659	3.0245	1.0%	-1.0%	3.0047		-0.3%	
2.8800	2.8821	2.9187	2.8375	-1.3%	1.5%	2.8641		0.6%		2.8821	2.9374	-0.1%	-2.0%	2.9187	2.8375	-1.3%	1.5%	2.8641		0.6%		2.8821	2.9374	0.0%	-1.9%
2.7692	2.7691	2.7361		1.2%		2.7525		0.6%		2.7607	2.8288	0.3%	-2.2%	2.7361		1.2%		2.7525		0.6%		2.7607	2.8288	0.3%	-2.2%
2.6667	2.6569	2.6492		0.7%		2.6492		0.7%		2.6265		1.5%		2.6492		0.3%		2.6492		0.3%		2.6265		1.1%	
2.5714	2.5821	2.5894	2.5323	-0.7%	1.5%	2.5534		0.7%		2.5677		0.1%		2.5894	2.5323	-0.3%	1.9%	2.5534		1.1%		2.5677		0.6%	
2.4828	2.4911	2.4911	2.4446	-0.3%	1.5%	2.5184		-1.4%		2.4776	2.5253	0.2%	-1.7%	2.4911	2.4446	0.0%	1.9%	2.5184		-1.1%		2.4776	2.5253	0.5%	-1.4%
2.4000	2.4317	2.3999		0.0%		2.3874	2.4382	0.5%	-1.6%	2.3874	2.4382	0.5%	-1.6%	2.3999		1.3%		2.4382	2.3874	-0.3%	1.8%	2.4382	2.3874	-0.3%	1.8%
2.3226	2.3269	2.3508		-1.2%		2.3388	2.2978	-0.7%	1.1%	2.3036		0.8%		2.3508		-1.0%		2.3388	2.2978	-0.5%	1.3%	2.3036		1.0%	
2.2500	2.2580	2.2200	2.2864	1.3%	-1.6%	2.2638		-0.6%		2.2417		0.4%		2.2864	2.2200	-1.3%	1.7%	2.2638	2.2147	-0.3%	1.9%	2.2417		0.7%	
2.1818	2.1524	2.1831		-0.1%		2.1727	2.2147	0.4%	-1.5%	2.1935	2.1524	-0.5%	1.3%	2.1831		-1.4%		2.1727		-0.9%		2.1524	2.1935	0.0%	-1.9%
2.1176	2.1274	2.1574		-1.9%		2.0982	2.1373	0.9%	-0.9%	2.1079		0.5%		2.1574		-1.4%		2.1373	2.0982	-0.5%	1.4%	2.1079		0.9%	
2.0571	2.0514	2.0332		1.2%		2.0422		0.7%		2.0468		0.5%		2.0332		0.9%		2.0422		0.4%		2.0468		0.2%	
2.0000	1.9763	1.9891		0.5%		2.0109	1.9806	-0.5%	1.0%	1.9848		0.8%		1.9891		-0.6%		1.9806	2.0109	-0.2%	-1.8%	1.9848		-0.4%	
1.9459	1.9636	1.9346		0.6%		1.9225		1.2%		1.9306		0.8%		1.9346		1.5%		1.9225		2.1%		1.9306		1.7%	
1.8947	1.8831	1.9026	1.8754	-0.4%	1.0%	1.8754		1.0%		1.8831		0.6%		1.8754	1.9026	0.4%	-1.0%	1.8754		0.4%		1.8831		0.0%	
1.8462	1.8305	1.8489	1.8269	-0.1%	1.0%	1.8305		0.9%		1.8527	1.8342	-0.4%	0.7%	1.8269	1.8489	0.2%	-1.0%	1.8305		0.0%		1.8342	1.8527	-0.2%	-1.2%
1.8000	1.8160	1.7843		0.9%		1.8018		-0.1%		1.7808		1.1%		1.7843		1.7%		1.8018		0.8%		1.7808		1.9%	
1.7561	1.7536	1.7569	1.7370	0.0%	1.1%	1.7370	1.7773	1.1%	-1.2%	1.7403		0.9%		1.7569	1.7370	-0.2%	0.9%	1.7370	1.7773	0.9%	-1.4%	1.7403		0.8%	
1.7143	1.7016	1.7111		0.2%		1.7111		0.2%		1.7143		0.0%		1.7111		-0.6%		1.6922	1.7111	0.6%	-0.6%	1.7143		-0.7%	
1.6744	1.6646	1.6737	1.6891	0.0%	-0.9%	1.6646	1.6922	0.6%	-1.1%	1.6798		-0.3%		1.6737	1.6891	-0.5%	-1.5%	1.6646		0.0%		1.6526	1.6798	0.7%	-0.9%
1.6364	1.6351	1.6437	1.6148	-0.4%	1.3%	1.6437		-0.4%		1.6234	1.6526	0.8%	-1.0%	1.6437	1.6148	-0.5%	1.2%	1.6437	1.6176	-0.5%	1.1%	1.6234		0.7%	
1.6000	1.5869	1.5869		0.8%		1.5896	1.6176	0.6%	-1.1%	1.5896	1.6091	0.6%	-0.6%	1.5869		0.0%		1.5896		-0.2%		1.5896	1.6091	-0.2%	-1.4%
1.5652	1.5573	1.5679		-0.2%		1.5679		-0.2%		1.5706		-0.3%		1.5679		-0.7%		1.5679		-0.7%		1.5706		-0.9%	
1.5319	1.5416	1.5262	1.5442	0.4%	-0.8%	1.5390		-0.5%		1.5416		-0.6%		1.5442	1.5262	-0.2%	1.0%	1.5390		0.2%		1.5416		0.0%	
1.5000	1.5062	1.4915		0.6%		1.5037	1.4843	-0.2%	1.0%	1.4891		0.7%		1.4915		1.0%		1.5037	1.4843	0.2%	1.5%	1.4891		1.1%	
1.4694	1.4676	1.4583		0.8%		1.4724		-0.2%		1.4583		0.8%		1.4583		0.6%		1.4724		-0.3%		1.4583		0.6%	
1.4400	1.4468	1.4266		0.9%		1.4266	1.4537	0.9%	-1.0%	1.4266		0.9%		1.4266		1.4%		1.4537		-0.5%		1.4266		1.4%	
1.4118	1.4091	1.4112		0.0%		1.4091		0.2%		1.4091		0.2%		1.4112		-0.2%		1.4091	1.4266	0.0%	-1.2%	1.4091		0.0%	
1.3846	1.3941	1.3794	1.3941	0.4%	-0.7%	1.3815	1.3941	0.2%	-0.7%	1.3794	1.3920	0.4%	-0.5%	1.3941	1.3794	0.0%	1.1%	1.3941	1.3815	0.0%	0.9%	1.3920	1.3794	0.2%	1.1%
1.3585	1.3590	1.3570		0.1%		1.3550	1.3712	0.3%	-0.9%	1.3590		0.0%		1.3570		0.1%		1.3550	1.3712	0.3%	-0.9%	1.3590		0.0%	
1.3333	1.3412	1.3334	1.3451	0.0%	-0.9%	1.3372		-0.3%		1.3392	1.3238	-0.4%	0.7%	1.3451	1.3334	-0.3%	0.6%	1.3372		0.3%		1.3392	1.3238	0.1%	1.3%
1.3091	1.2939	1.3087	1.3218	0.0%	-1.0%	1.3049		0.3%		1.3068	1.2994	0.2%	0.7%	1.3087	1.3218	-1.1%	-2.2%	1.3049		-0.9%		1.2994	1.3068	-0.4%	-1.0%
1.2857	1.2741	1.2848	1.2994	0.1%	-1.1%	1.2939		-0.6%		1.2866		-0.1%		1.2848	1.2994	-0.8%	-2.0%	1.2706	1.2939	0.3%	-1.6%	1.2724	1.2866	0.1%	-1.0%
1.2632	1.2636	1.2619	1.2724	0.1%	-0.7%	1.2550	1.2706	0.6%	-0.6%	1.2584	1.2724	0.4%	-0.7%	1.2619	1.2724	0.1%	-0.7%	1.2550		0.7%		1.2584		0.4%	
1.2414	1.2381	1.2397	1.2499	0.1%	-0.7%	1.2364		0.4%		1.2465	1.2331	-0.4%	0.7%	1.2397	1.2499	-0.1%	-1.0%	1.2364	1.2249	0.1%	1.1%	1.2331	1.2465	0.4%	-0.7%
1.2203	1.2103	1.2281		-0.6%		1.2151	1.2249	0.4%	-0.4%	1.2232	1.2103	-0.2%	0.8%	1.2281		-1.5%		1.2151		-0.4%		1.2103	1.2232	0.0%	-1.1%
1.2000	1.2008	1.2040		-0.3%		1.2040	1.1915	-0.3%	0.7%	1.2040	1.1915	-0.3%	0.7%	1.2040		-0.3%		1.2040	1.1915	-0.3%	0.8%	1.2040	1.1915	-0.3%	0.8%
1.1803	1.1762	1.1915		-0.9%		1.1777		0.2%		1.1792		0.1%		1.1915		-1.3%		1.1777		-0.1%		1.1792		-0.3%	
1.1613	1.1628	1.1526	1.1702	0.8%	-0.8%	1.1643	1.1540	-0.3%	0.6%	1.1628	1.1511	-0.1%	0.9%	1.1702	1.1526	-0.6%	0.9%	1.1643	1.1540	-0.1%	0.8%	1.1628		0.0%	
1.1429	1.1425	1.1425	1.1613	0.0%	-1.6%	1.1383		0.4%		1.1369		0.5%		1.1425	1.1613	0.0%	-1.6%	1.1383		0.4%		1.1369	1.1511	0.5%	-0.8%
1.1250	1.1299	1.1148		0.9%		1.1271		-0.2%		1.1134		1.0%		1.1148		1.3%		1.1271		0.2%		1.1134		1.5%	
1.1077	1.1107	1.1001		0.7%		1.1107	1.1001	-0.3%	0.7%	1.1014		0.6%		1.1001		1.0%		1.1107	1.1001	0.0%	1.0%	1.1014		0.8%	
1.0909	1.0909	1.0909		0.0%		1.0909		0.0%		1.0897		0.1%		1.0909		0.0%		1.0909		0.0%		1.0897		0.1%	
1.0746	1.0693	1.0731	1.0807	0.1%	-0.6%	1.0718	1.0794	0.3%	-0.4%	1.0731	1.0794	0.1%	-0.4%	1.0731	1.0807	-0.4%	-1.1%	1.0718	1.0794	-0.2%	-0.9%	1.0731	1.0794	-0.4%	-0.9%
1.0588	1.0546	1.0558	1.0644	0.3%	-0.5%	1.0619		-0.3%		1.0632		-0.4%		1.0558	1.0644	-0.1%	-0.9%	1.0619		-0.7%		1.0632		-0.8%	
1.0435	1.0438	1.0426	1.0510	0.1%	-0.7%	1.0403		0.3%		1.0522		-0.8%		1.0426	1.0510	0.1%	-0.7%	1.0403		0.3%		1.0522		-0.8%	
1.0286	1.0321	1.0332		-0.5%		1.0321		-0.3%		1.0309		-0.2%		1.0332		-0.1%		1.0321		0.0%		1.0309		0.1%	
1.0141	1.0195	1.0105	1.0183	0.4%	-0.4%	1.0195		-0.5%		1.0127	1.0206	0.1%	-0.6%	1.0183	1.0105	0.1%	0.9%	1.0195		0.0%		1.0206	1.0127	-0.1%	0.7%
1.0000	0.9984	1.0028	1.0105	-0.3%	-1.0%	0.9962	1.0050	0.4%	-0.5%	0.9973	1.0050	0.3%	-0.5%	1.0028	1.0105	-0.4%	-1.2%	0.9962	1.0050	0.2%	-0.7%	0.9973	1.0050	0.1%	-0.7%
	≤ 1‰		∑	21	0			6	0			13	0			12	0			11	0			19	0
	1‰ - 1%		∑	35	15			53	13			42	14			30	13			46	9			34	9
	≥ 1%		∑	16	23			13	22			17	22			30	25			15	26			19	27
	67%-99%		∑∑	**72**	**38**			**72**	**35**			**72**	**36**			**72**	**38**			**72**	**35**			**72**	**36**

Table 8. EBR recovery from PRMI (Puerto Rico) station during the preparation phase for the 07 January 2020 Puerto Rico sequence. Shown is performance of theoretical (left) v. seismic EBR.

To examine if the Mexico City station and that whole profile indeed picked EBR from the 01-07 January 2020 preparation phase of the Puerto Rico 07 January 2020 event, I next processed data from the PRMI (Puerto Rico) station recorded during the same phase. PRMI is a 1Hz cGPS station operated by NGS since 23 March 2006, sits on the Caribbean tectonic plate, and is at the La Parguera Natural Reserve in Puerto Rico. The same as along the EBR profile earlier, one EBR type again is seen performing a magnitude an order better than another EBR type. So not only did the PRMI data from the (future) seismic event's vicinity yield a full EBR recovery (all 72 periods) where 75% of matches on average were within 1% (79% when matching against theoretical EBR), but the preparation phase again is seen too – as eight absolute matchings in long periods (red-framed green-highlighted values), Table 8.

This result is explained by Puerto Rico being an island (a buffer zone in the sense of resonance mechanics) where the surrounding ocean acts as a natural high-pass filter that minimizes damages and destruction of EBR waves (not just those with destructive angular deflection), exposing the physical seismicity-generating mechanism at play as a standalone. Thus, for example, not only was the EBR picked numerically theoretically, but geometrically (formation) theoretically as well – seen as a clustering of the absolute long-period matchings within the xy plane, as expected because the EBR is mainly a horizontal movement. The negation-logic argument is satisfied as well: there are no such (xy) matchings to the seismic EBR, Table 8 (on the right).

Finally, while the analysis of data from ZSU4 (not detailed here) as the only other 1Hz cGPS station in Puerto Rico produced an inconclusive result (half-an-order of magnitude performance difference), ZSU4 yielded a period absolutely (to 0.0%) matched against the theoretical EBR that was in common with PRMI: the 7.55315 h. This period was absolutely (to 0.0%) matched at Mexico City as well, and to 0.8% at both Los Angeles and San Francisco, Table 4, so this period likely was the triggering EBR period of the Puerto Rico sequence, and one of those in the seismogenic assemble for that region.

Discussion

The heat transfer (thermal-chemical convection) geophysical hypothesis fails in the most important aspects, e.g., it explains neither the plate tectonics nor the seismotectonics energy budgets. With its leisurely daffy time scales that are so obviously devoid of our everyday experience and thus fail even a most fundamental reality check, it also contradicts crucial data known for a long time, such as the uppermost mantle's very high velocities, of over 8.5 km/s (Yegorkin and Chernyshov, 1983).

The body (mechanical) resonance is a physical phenomenon in which the natural period of vibration of a physical system coincides with ("resonates to") another system's vibration period or its fractional multiple. The nature of a matched period – i.e., whether it is subharmonic or superharmonic – governs the resonance. Once exposed to a resonance, all solids eventually crumble in a structural failure at the resonance period. To make it worse, Earth resonances arise via magnified (planetary) vibration as due to *frequency demultiplication* — one of the rarest macroscopic phenomena that can magnify the energy injected at the fundamental disturbing frequency by 100s of times (Den Hartog, 1985).

CORS regions have diurnal EBR fingerprints: uniquely arranged sets of 13-18 EBR periods, most clearly formed during M6+ proximal and M6.5+ global quiescence. Seismic waves destroy an original EBR fingerprint, which the Earth then attempts to restore with other EBR waves to resume the undistorted state (energy equilibrium).

As the pretesting revealed, the number of EBR waves in a station's fingerprint from daylong cGPS data drops to ten or less under extremal elevation angle masks like 0º or 30º in cGPS post-processing. Thus daylong cGPS recordings appear suitable to an extent for EBR mapping (but with care taken to find the optimal mask), and their potential for EBR mapping is worth exploring further. On the other hand, EBR recovery from daylong data does not appear to reveal much about the longest of (i.e., strong earthquakes-generating) EBR periods, so longer records are needed for prediction and accurate mapping, i.e., the connecting of the longest of EBR periods characteristic of adjacent cGPS stations during an interval of interest. EBR mapping is most useful for hourly-to-daily early warning systems, with shorter EBR periods used to check the EBR recovery, including consistency and orientation, see Table 4.

Weeklong cGPS data, on the other hand, enable a high enough resolution and require no particular care to finding the optimal mask, as seen in Tables 4 & 7. As a result, EBR maps of resonance variation could be synoptic charts of equiperiodicity contour lines plotted or overlaid on physical maps. Akin to a standard isogon line connecting points of constant magnetic declination, an isodon (*δονώ* for vibrate) would be a line connecting GNSS stations whose positions fluctuate with a same long (strong-earthquakes causing) EBR cycle(s). Then an EBR map would characterize a geographical region of interest in terms of capacity and tendency to become seismically active at a time of externally introduced nonlinearity (Omerbashich, 2020a).

Since an EBR wave is primarily a horizontal movement — forced externally along the Ecliptic and skewed away from geodetic coordinate axes to the maximum due to rotation and obliquity of the Earth and the Moon — cGPS stations reveal us a new and powerful geophysical parameter, the *daily resonance distortion* (DRD). As seen most evidently in the ZLA1 case, the technique presented in this study captures EBR waves mostly while running at angles skewed to the coordinate system (the axes), as projected onto coordinate planes xy, yz, or xz. Only on occasion do they approach the projection axes — as in the ZLA1 case — and take on a geometrically regular formation. This special case (display) of an obvious orientation is then an additional physical demonstration of the EBR (waves) phenomenon, as such.

Thus, DRD measures if EBR waves, characterized by their observed periods P, have lost the original transverse orientation and approached coordinate axes — which would result in independent component spectra, or if they have retained the original orientation — which would result in the formed component spectral pairs P_{XY}, P_{XZ}, or P_{YZ}. Similar to using GPS to map geophysical and physical parameters such as the Total Electron Content, EBR maps now could be produced. Their applications range from estimating the EBR energy budget, seismic forecasting or prediction, to unobscuring (decoupling EBR from) geophysical observables such as stress and strain.

That EBR indeed has caused the initial Ridgecrest rupture, thereby probably triggering the sequence by catalyzing the release of accumulated stresses, is seen from Table 6 and Figure 12. Namely, there is a remarkable match among the long-periodic EBR periods recovered here from cGPS and the seismic EBR periods recovered from global seismicity (Omerbashich, 2020a), as nine absolute (<0.0%) matches (red-framed Δ–values), or a magnitude-of-order increase in seismicity-generating EBR waves, Tables 4 & 7 (disregarding the Puerto Rico event). This jump in sensed physical processes was not a surprise since the latter values reflect real Earth's interior over the last decade far better than theoretical EBR values ever could. This remarkable jump also shows that real-time EBR recovery is verifiable against a seismic EBR as obtained from some reasonably long, immediately preceding interval of time as a physical gauge.

Conclusions

After proving the Earth body resonance (EBR) on global scales from large earthquakes and the Moon body resonance from moonquakes, I now demonstrated the EBR on global-to-local scales from continuous GPS (cGPS) that constantly record actual EBR waves in solid matter. In addition to that main demonstration, I have also shown that cGPS recordings are readily applicable to mapping EBR on scales of choice. Such EBR maps are essential to earthquake prediction and forecasting and as a new and permanently available means of resource exploration.

EBR is a new geophysical force that must be accounted for by decoupling geophysical parameters, such as stress and strain, from EBR. Furthermore, old geophysical hypotheses no longer hold. For instance, the populist thought experiment featuring a kitchen stove with a pot of boiling water, too often used by proponents of the heat transfer hypothesis, now lacks proper context. While the steam does disturb the pot cover, the (unfixed) pot cover is not a reasonable representation of the Earth crust; only the kitchen's ceiling is; steam never scratches, let alone moves kitchen ceilings.

A consequence of the here verified discovery is that the EBR, due to its immense energies and unpredictability as newly discovered and a fundamental force of geophysics, most certainly forbids terrestrial seismic detection of already faint signals emanating from deep space, such as signals of alleged gravitational waves.

References

Bock, Y., Melgar, D. (2016) Physical applications of GPS geodesy: a review. Rep. Prog. Phys. 79:106801 (119pp). DOI: https://doi.org/10.1088/0034-4885/79/10/106801

Cheng, Y., Ben-Zion, Y. (2020) Variations of earthquake properties before, during, and after the 2019 M7.1 Ridgecrest, CA, earthquake. Geophys. Res. Lett. 47:e2020GL089650. DOI: https://doi.org/10.1029/2020GL089650

Den Hartog, J. (1985) *Mechanical Vibrations* (4th ed.) Dover Publications. ISBN 9780486647852

Genrich, J.F., Bock, Y. (2006) Instantaneous geodetic positioning with 10–50 Hz GPS measurements: Noise characteristics and implications for monitoring networks. *J. Geophys. Res.* 111:B03403. DOI: https://doi.org/10.1029/2005JB003617

He, X., Montillet, J.-P., Fernandes, R., Bos, M., Yu, K., Hua, X., Jiang, W. (2017) Review of current GPS methodologies for producing accurate time series and their error sources. *J. Geodyn.* 106:12-29. DOI: https://doi.org/10.1016/j.jog.2017.01.004

Omerbashich, M. (2006) Gauss–Vaníček Spectral Analysis of the Sepkoski Compendium: No New Life Cycles. *Comp. Sci. Eng.* 8(4):26-30. DOI: https://doi.org/10.1109/MCSE.2006.68

Omerbashich, M. (2007a) Erratum due to journal error. *Comp. Sci. Eng.* 9(4):5-6. DOI: https://doi.org/10.1109/MCSE.2007.79; full text: https://arxiv.org/abs/math-ph/0608014

Omerbashich, M. (2007b) Magnification of mantle resonance as a cause of tectonics. *Geod. Acta* 20(6):369-383. DOI: https://doi.org/10.3166/ga.20.369-383

Omerbashich, M. (2020a) Earth body resonance. *J. Geophys.* 63:15-29. ARK: https://n2t.net/ark:/88439/x020219

Omerbashich, M. (2020b) Moon body resonance. *J. Geophys.* 63:30-42. ARK: https://n2t.net/ark:/88439/x034508

Press, W.H., Teukolsky, S.A., Vetterling, W.T., Flannery, B.P. (2007) *Numerical Recipes: The Art of Scientific Computing* (3rd Ed.). Cambridge University Press. ISBN 9780521880688

Vaníček, P. (1969) Approximate Spectral Analysis by Least-Squares Fit. *Astrophys. Space Sci* 4(4):387–391. DOI: https://doi.org/10.1007/BF00651344

Vaníček, P. (1971) Further Development and Properties of the Spectral Analysis by Least-Squares Fit. *Astrophys. Space Sci.* 12(1):10–33. DOI: https://doi.org/10.1007/BF00656134

Vincenty, T. (1975) Direct and inverse solutions of geodesics on the ellipsoid with application of nested equations. *Survey Rev.* 23(176):88–93. DOI: https://doi.org/10.1179/sre.1975.23.176.88

Yegorkin, A.V., Chernyshov, N.M. (1983) Peculiarities of Mantle Waves from Long-Range Profiles. *J. Geophys.* 54(1):30-34. ARK: https://n2t.net/ark:/88439/y090547

Young, L.E., Neilan, R.E., Bletzacker, F.R. (1985) GPS Satellite Multipath: An Experimental Investigation. *Proceedings of the First International Symposium on Precise Positioning with the Global Positioning System*, pp.423–432.